POLITECNICO DI TORINO

Master's Degree in Biomedical Engineering

Master's Thesis

Development of a Paper-Based Enzymatic Microfluidic Biosensor to Detect Organophosphate Pesticides

Supervisors

Prof. Gianluca CIARDELLI
Prof. Chiara TONDA TURO
Prof. Peter ERTL
Tutor
Dr. Mario ROTHBAUER

Candidate

Noemi PARATO

Academic Year 2022/2023
March 2023

Table of Contents

Table of Figures

Abstract

Food safety is a critical issue, and the detection of food pollutants is of paramount importance. The development of rapid, reliable, and effective tools for the identification of food contamination is crucial to meet the growing demand for high-quality food. This thesis presents the development of a colorimetric microfluidic paper-based biosensor for the detection of organophosphate pesticides (OPs) by measuring the quantity of the enzyme acetylcholine esterase (AChE). The biosensor uses a colorimetric assay to detect the presence of OPs in sample solutions based on the principle of enzyme inhibition. The AChE substrate chromogen indoxyl acetate (IDA) is used to identify these toxic substances. The activity of the enzyme is hindered when OPs are present in the sample being tested, resulting in a less intense color change. The biosensor assay uses simple sensitive visual screening carts in which the enzyme is immobilized by physical absorption directly on the paper support. Different concentrations of the organophosphate pesticides (chlorpyrifos, dichlorvos, and malathion) were used to validate the biosensor, and the inhibition color change and IC_{50} value were compared with those obtained using colorimetric biosensors for OPs in the literature. A proof-of-concept an optical biosensor was developed using these paper tests, combining seven microfluidic channels with paper-based sensing platforms. The optical biosensor showed medium-low sensitivity and accuracy for the detection of organophosphate pesticides. However, optimization of the biosensor has the potential to offer an accurate and affordable method for field-based monitoring and detection. This biosensor could have various applications, including agricultural, food safety, and environmental monitoring, offering a promising platform for numerous applications. Improved performance and reliability of the optimized biosensor could make it a valuable tool for the detection of organophosphate pesticides in various environments.

Chapter 1: Introduction

1.1 Pesticides: what they are, how they are used and their health effect

As the world's population has expanded in recent decades, there has been an increase in the demand for and production of food, particularly fruit and vegetables, which has resulted in an increase in the usage of pesticides to prevent insects and pests from contaminating crops[1]. Pesticides are a class of thousands of chemical molecules with various structural variations (in Figure 1 some of the most used one). Pests can cause harm during the processing, manufacture, storage, transport, and marketing of wood, wood products, food, or feed. They are also transmitters of diseases that affect both humans and animals. The term "pesticides" can also refer to substances with a range of additional purposes, such as agents to stop fruit from falling off the tree too early, chemicals applied to crops before or after harvest to avoid rotting during transport or storage, defoliants, plant growth regulators, etc[1–5]. The rapid increase in pesticide use is also observed in non-agricultural applications, such as in industrial vegetation control (roads, railways), public health or grass management. This occurs in both developed and developing countries, including Thailand that is the agricultural country where the utilization of organophosphates (OPs) and carbamates (CMs) accounts for the major usage of pesticides[6–8]. Similar chemical substances have also been synthesised for military use as Chemical Warfare Agents (CWAs)[9] for example, because they are very toxic to humans[10]. It is evident from the foregoing that pesticides are dual chemicals, having both negative and positive effects. Even though they have drawbacks, pests are nonetheless used because of how useful they are given that losses from pests to crops run from 40 to 70 percent[11]. This is supported by the argument that the loss of potential global food production would be twice if current pesticides were abandoned[6]. Between the adverse impacts and prolonged use of these chemical hazards in all of their applications, grain, vegetables, and some other agricultural goods are becoming severely contaminated, which harms ecosystems and harms people[2]. The concentration of

these toxic substances in the environment is growing exponentially day by day.

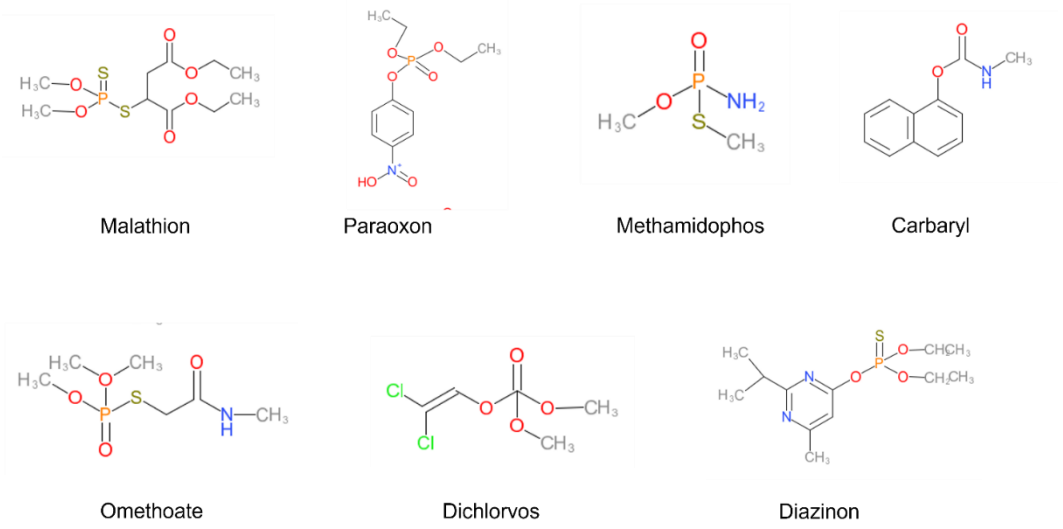

Figure 1. Structures of some of the most used pesticides used as target in AChE biosensors[12]

Over the past 30 years, the usage of OPs and carbamates among the numerous agrochemicals has increased due to their great efficacy in the eradication of insects and pests and shorter environmental half-lives than organochlorine pesticides (DDT, aldrin, lindane, etc.)[1,2,13]. Because of their excellent effectiveness as insecticides (chlorpyrifos, methyl parathion), nematicides (carbaryl, carbofuran), fungicides (thiabendazole, imazalil), and herbicides (imazalil), they have been widely used in agricultural pest control (diuron, glyphosate)[14]. They must be used and consumed in moderation because they are considered to be neurotoxic chemicals. Some experts assert that acetylcholinesterase (AChE) inhibitor pesticides like carbamates and organophosphates cause more acute poisoning deaths than any other category of pharmacological medicines[15]. Particularly in underdeveloped nations, where hundreds of thousands of people are said to use very dangerous pesticides every year because they are easily accessible[16]. Fortunately, the death rate is estimated to be between 10% and 20%, and the number of suicide attempts involving these chemicals that result in fatalities is lower than efforts involving ingestion[17,18]. However, the incidence of OP and CM-related intoxication is substantially lower in more developed nations. While there were 25,288 suicides in India in 2010, the American Association of Poison Control Centers only got 4,150 complaints of

exposure to the two chemicals there in 2012, resulting in a total of 3 fatalities[19]. The prevalence of (unintentional) poisonings in agriculture is another issue that, despite being less serious, needs to be under control[20,21]. These substances have been associated to respiratory and immunological issues, cancer, bone marrow diseases, infertility issues, cytogenetic impacts, and neurological diseases[10,22]. Their toxicity is determined by the pesticides' chemical structure (Figure 1)[23,24]

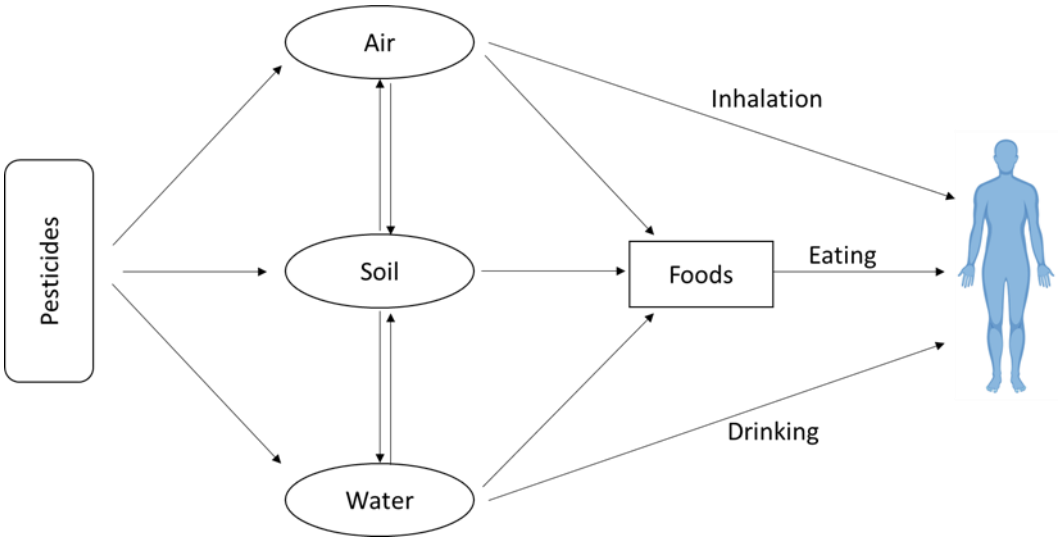

Figure 2. Proposed pesticide exposure paths for humans and the environment[25]

1.1.1 Organophosphates as pesticides

Of all types of pesticides, the organophosphate pesticides (Figure 3, Figure 4) are the most widely used in a variety of settings (Table 1) due to their fast response, low cost, wide availability, and high potency[1,14].Although these pesticides are used to protect crops from pests and potential diseases or to safeguard residential and commercial settings, the residues left behind after their application result in serious issues. According to certain findings, barely 10% of liquid pesticides and no more than 30% of powder pesticides that are sprayed on crops manage to attach to the plants after contact. OPs not only remain on the surface of fruit and vegetables, but through the food chain can also accumulate in livestock, fish, and shrimp[26]. If there are humans at the end of this chain, they could be poisoned by the various residual OPs. It is significant to note that the Environmental Protection Agency has prohibited or intends to remove several OPs from the US, which will

reduce their use for many of these applications[27]. One of the phosphorus-based substances employed is used to treat glaucoma (diisopropyl phosphorofluorodate)[28,29]. Then there are the nerve agents, militarized OPs that are considered to be actual chemical weapons and destructive weapons[30]. Numerous thousands of these compounds were developed throughout the 20th century. In fact, there are nerve agents such as soman, sarin, VX, tabun or cyclosarin, which, besides being used as potent organophosphorus inhibitors for military purposes, can be misused in terrorist activities [31–33]. Fortunately, only a tiny portion of these were employed in clandestine operations. The 1995 terrorist attack in Tokyo, which left over 5,000 people injured and 11 dead, was one of the incidents in which nerve agents were used[34]. Following this, it was also employed covertly in the Iran-Iraq War, Iran's attack on the Kurds, and the 2013 Syrian Civil War, which resulted in more than 14 deaths[19].

Table 1. Different application of organophosphorus pesticides [35]

Sources of organophosphorus pesticides	
Domestic	Garden sheds
	Surface and room sprays
	Baits for cockroaches and other insects (e.g., chlorpyrifos)
	Shampoos against head lice (e.g., malathion)
	Pet preparations (e.g., pet washes, collars)
Industrial or occupational	Crop protection and livestock dipping
	Large scale internal control, including fumigation
Terrorism or warfare (nerve agents)	e.g., sarin (used in Tokyo subway attack), tabun and sarin (used during the Iraq-Iran conflict

The main common negative effects that they can cause to humans are drowsiness, headache, confusion, irritability, depression, disorientation, impaired concentration and memory, speech difficulties, abdominal pain, eye pain, respiratory failure, convulsions, dyspnea, arrhythmia, muscle twitching, hypoxia, and various neurological disorders. Even low levels of these substances can be enough to cause intoxication that can lead to damage to the heart, kidneys, lungs, and other organs[26,36–40].

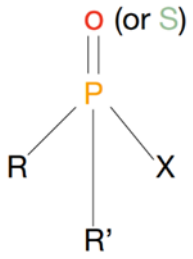

Figure 3. General formula for OP compounds

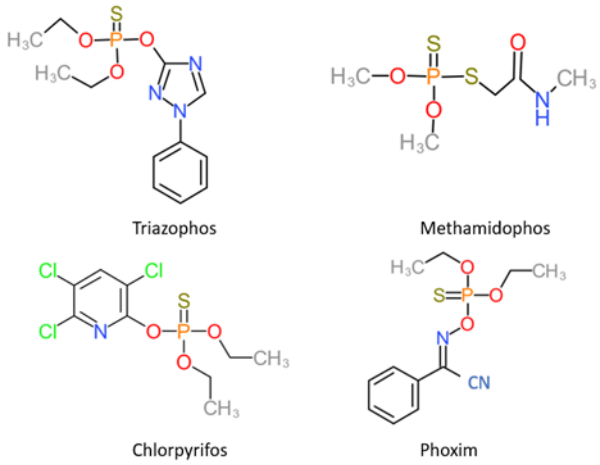

Figure 4. Some of the Organophosphates structures

It is therefore easy to understand why according to Environmental Protection Agency (EPA), OPs are highly toxic to humans, wildlife and bees and are classified as the most toxic 'Class 1' compounds[14,41]. Even a very small dose, repeated exposure to OPs[14] leads to acute toxicity to human health, according to the World Health Organisation, 1.5 billion cases of diarrhoea in children (with over 3 million deaths) are caused by contaminated food every year [40,42]. Even in the United States, although one of the world's best food safety systems has been

established, according to the Centers for Disease Control and Prevention's estimations, about 48 million people get foodborne illnesses per year, causing 128,000 hospitalizations and 3000 deaths[43].

1.1.2 Effects of pesticides on enzyme activity: Acetylcholinesterase

Pesticide OPs are one of a group of chemical compounds that are cholinesterase inhibitors. The two known cholinesterases are acetylcholinesterase (AChE) and butyrylcholinesterase (BChE). The two enzymes are present in the body under certain physiological conditions. Pseudocholinestarese (BChE) is more quickly than AChE. It is synthesised by the liver and is secreted into the blood plasma, where it performs its main function: it tests the proper functioning of the liver[29,44]. AChE is part of the cholinergic nervous system, where it terminates excitation through hydrolysis of the neurotransmitter acetylcholine in the blood, neuromuscular junctions, nerve junctions and elsewhere[29,45,46]. Due to the well-known role of AChE, pharmacologists developing new drugs are more interested in this enzyme than in BChE, as the biological function of the latter is not well understood[44,45,47]. Both the enzymes can be inhibited by chemical compounds that can interact with them in certain crucial structures, responsible for hydrolysis or substrate distribution. The two enzymes are very similar to each other but have some minor structural dissimilarities. As a result, many of their inhibitors have affinity for either one or the other, while some have affinity for just one. The quaternary structure of AChE and BChE, for instance, may be the same, yet their molecular weights may be different. In general, three sites of the cholinesterase are responsible for its enzymatic activity: β anionic site (also known as the peripheral anionic site), aromatic gorge and the active site. If we imagine a substrate, as shown in

Figure 6, the compound encounters the cholinesterase on the peripheral anionic site, which is located on the surface of the molecule. This part is another detail that differentiates the two enzymes: that of AChE is highly developed by the presence of aromatic amino acids, that of BChE is not. Due to the presence of aromatic amino acids, through the chemical interaction cation-π or π-π interaction with both the substrate acetylcholine and inhibitors is possible. The aromatic gorge, which is the second section of the passage through the active site,

resembles the peripheral anionic site in terms of its characteristics. Because it is made up of aromatic amino acids, it can attach to substances through cation-π and π-π interactions. Again, AChE has the gorge covered by many more aromatic amino acids than BChE[48]. When the compound has finally passed both the β anionic site and the aromatic gorge, it arrives at the active site. In this zone, in the case of AChE, acetylcholine, being its natural substrate, is cleaved into acetic acid and choline. The active site has the esteratic subsite (also called ester or esteric) and the α anionic subsite. As can be seen in the Figure 7 below, the α anionic subsite has the role of properly orienting the acetylcholine (fixing it by cation-π interaction) while the esteratic subsite is capable of cleaving the ester bond by a nucleophilic substitution mechanism. Both AChE and BChE can be inhibited by various chemical compounds.

Among the inhibitors of cholinesterases, there are two groups in particular, organophosphates and carbamates, which covalently modify the two enzymes. Carbamates create unstable esters with cholinesterases; when the carbamate moiety leaves the cholinesterase by spontaneous hydrolysis, enzyme activity is restored. This is why the mechanism of cholinesterase inhibition by a carbamate is called pseudo-irreversible. Organophosphates, on the other hand, produce stable esters and have an inhibition mechanism that is irreversible[49]. The inhibition process has already been explained in *chapter 1.1.2*. This difference between the two pesticides also leads to different applications. Carbamates, due to their pseudoreversible mechanism, are widespread in the pharmacological field. They are widely used in therapies for Alzheimer's or myasthenia gravis. Rivastigmine, for example, is a cholinesterase inhibitor, used as a drug for Alzheimer's, and is able to cross the blood-brain barrier. Pyridostigmine and neostigmine, on the other hand, which are used for the treatment of myasthenia gravis and for anaesthesia, only inhibit cholinesterases in the blood and peripheral nerves, as they are not able to reach the brain or only to a limited extent[33,46] . Organophosphates have also been used for the former Alzheimer's disease drug and a metrifonate anthelmintic (trichlorfon). The oxide forms of the organophosphates malaoxon, paraoxon and chlorpyrifos-oxon are used as the final form of cholinesterases inhibition[33,50].

In the following lines, attention will be focused on the inhibition process on which the detection principle of the biosensor realised is based: that of the AChE enzyme caused by the presence of OPs. What makes OPs so toxic is their ability to bind the esteratic active site of AChE because of their molecular shape (which imitates the substrate acetylcholine),inhibiting its activity. This concept was first used only in the late 1980s, when the presence of such pesticides was determined electrically, but using butyrylthiocholine[6,51].

Irreversibly inhibition of AChE enzyme activity in the central and peripheral nervous system results in malfunction of the affected areas[52–54] because a neurotransmitter operating at cholinergic synapses, called acetylcholine (ACh), is not hydrolysed in time[1]. The presence of ACh in the blood plasma is not only an important indicator of liver disease, but as ACh accumulates in the body, it also causes serious damage to the nervous system, respiratory tract, and cardiovascular system, which can lead to organ failure and ultimately to death[2]. The hydrolysis of acetylcholine in the presence of AChE is shown in reaction on the Figure 5:

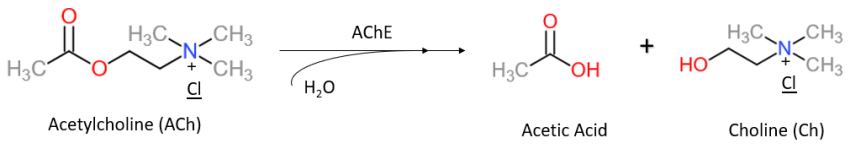

Figure 5. Acetylcholinesterase hydrolyses acetylcholine into acetic acid and choline

In the absence of inhibitors, AChE has a very high catalytic activity: each AChE molecule is able to degrade approximately 25,000 ACh molecules every second; choline and acetic acid are obtained as products. The choline produced returns to the nerve terminals to be reused in the synthesis of new ACh molecules. AChE belongs to the hydrolase family, whose active site is characterised by a coordinated catalytic triad of three essential amino acids: aspartic acid, histidine and serine. Catalysis of the triad occurs when the positively charged quaternary ammonium group of AChE is attracted to the anionic binding site of the triad. The hydroxyl group of the serine, after being deprotonated by the neighbouring histidine group in the traide, attacks and cleaves the ester[12] . For public safety and

environmental protection, therefore, the selective detection and quantitative determination of OPs in food is desirable[3,4,27–29].

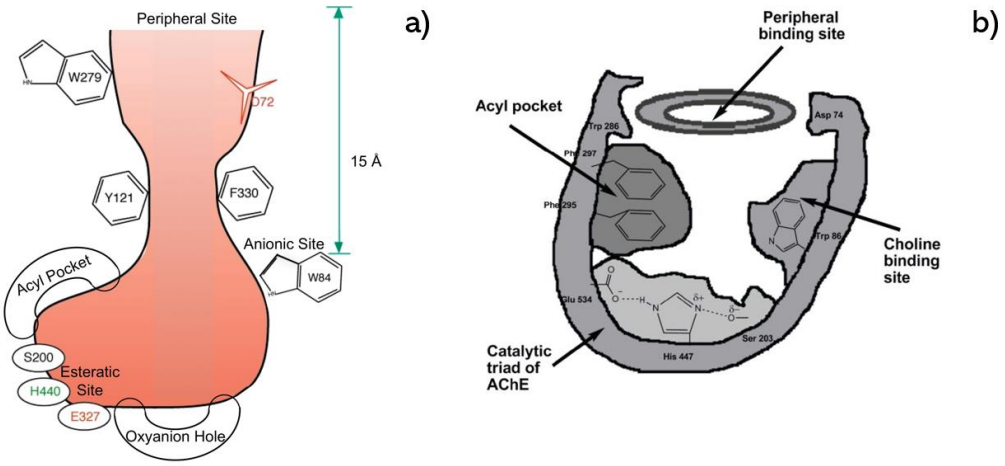

Figure 6. a) Schematic view of the active-site gorge of TcAChE. The esteratic site, which contains the three residues of the catalytic triad; the oxyanion hole, and the acyl pocket, which confers substrate specificity[51] b) Schematic representation of AChE binding site[55]

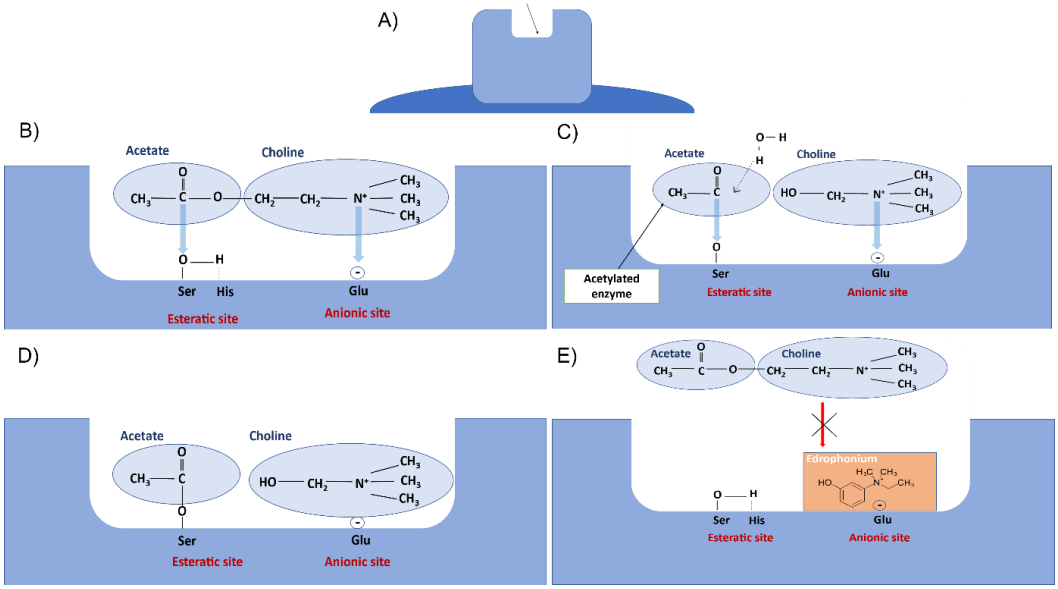

Figure 7. Mechanism of action of irreversible anticholinest A) A simplified model of an enzyme. This enzyme's active core is located 20 Å below the surface of the gorch. B) The AChE enzyme's structure Serine (Ser) and histidine's esteratic sites are on the left, whereas glutamate's anionic site is on the right. The acetylcholine molecule is on top. The process begins with the positively charged nitrogen being electrostatically drawn to the anionic site (shown by the right narrow) and the carbon being drawn to the oxygen (indicated by the left narrow). Acetylcholine is brought even closer to the active site, resulting in the development of an enzyme substrate complex C) Following the rupture of the ester bond, free choline and acetylated enzyme are produced, which will be quickly hydrolyzed. Acetate and free enzyme are created upon hydrolysis. Acetate and choline

then diffuse away at the conclusion of the procedure. This entire process is completed in less than 150 μseconds. D) Drugs having quick acting times, such as certain Ops, only bind to the anionic site of the acetylcholinesterase active site. The enzyme needed to hydrolyze acetylcholine is not available as long as the medication is bound in this location. The covalent bond of the other medications is stronger than the electrostatic and hydrogen bonding that occurs with this type of drug. Due to this, the duration of these medications is brief—between 2 and 10 min. If the medication ultimately dissipates and the enzyme is prepared to hydrolyze acetylcholine.

1.2 Tradition analytical methods used to detect pesticides

With the foregoing ideas in mind, it is simple to see why worry over pesticide residues in food and water contamination brought on by agricultural practises have increased so considerably in recent years[6]. The risk associated with widely used chemicals and the acute toxicity endangering human health through residues in agricultural products and water contamination is an issue to be considered when deciding to use them[3,56].

Limits for pesticides in drinking water were introduced by the European Union through the Drinking water directive (98/84/EC), which sets the maximum residue level (MRL) of permitted pesticides in the range of 0.01-0.02 mg-L^{-1} for many fruits limit[5758]. The maximum recommended level in drinking water in the UK for example ranges from 0.3 to 400 μL^{-1}, depending on the type of pesticide[6]. To comply with these limits, and more generally to detect the presence of pesticides in products in which they may be contained, it is essential to develop and use reliable, sensitive, and rapid analytical detection systems. To comply with these limits and more generally for reliable quantification of OPs at low concentrations in food and drinking water, it is increasingly necessary to develop reliable, sensitive, inexpensive, and rapid analytical detection systems[58]. As things stand at present, conventional analysis kits for OPs can detect various OPs but their sensitivity is limited, and they are incapable of detecting total concentrations of mixed OPs. Expensive instruments such as gas chromatography (GC)[59], gas/liquid chromatography/liquid mass spectrometry (GC/LC-MS)[60–63],or high-performance liquid chromatography (HPLC)[60] are used[64]. Of all the methods to detect the existing (supra-electrochemical) presence of pesticides in various matrices, gas chromatography is undoubtedly the most common, especially when coupled with FTIR or mass spectrometer as they have the unique ability to 'fingerprint'

pesticides. The problem is due to not only to the time-consuming sample pre-treatment, expensive reagents related to them, but even to the thermal lability, low volatility, and high polarity that some pesticides have, which can lead to unsupervised analysis using this method[22]. The overcome of these limitations related to the polar and thermolabile compounds leads to the need of using sophisticated extraction systems, like electrophoresis or liquid chromatography, that are not amenable to field analytical procedures[226]. More in general, all these conventional methods are time-consuming, expensive instruments and complex operations, even though they are sensitive and reliable. Consequently, they are not suitable for real-time measurements, on-site applications, or domestic use[65].

Since the reactivator can induce reactivation of the inhibited AChE, in addition to inhibitors, its control is also important. For organophosphate pesticides, detection methods are mainly based on the principle of cholinesterase inhibition[66–68]. Of the various methods for AChE assay that have already been developed, including chemiluminescence method[69,70], fluorescence method[71–73], chromatographtbioautographic[74,75], capillary electrophoresis[76], electrochemical method[66,67] and colorimetric method[68,77], the last two are the ones on which attention will be focused in this text. The two methods are based on the electrical current and colour signal between the system before and after the enzymatic reaction of acetylcholinesterase, respectively.

In general, each analytical device should be designed according to the use for which it is made. In the case of pesticides, an ideal analytical device should be simple, portable and easy to use as pesticide residues are concentrated in rivers and ponds, through rainwater or irrigation runoff, but also near places where pesticides are widely used, giving rise to water pollution[57].

A few decades ago, many immunoassay techniques were developed to trace many pesticides, such as chlorpyrifos, pyrimiphos, and fenitrothion[22]. The characteristic feature of these methods is that they use antibodies specific to the analyte to be examined. The limitation of these methods is that they have a very high specificity towards a single analyte, so they are not able to determine the general toxicity of a given sample due to a family of products. Later, in 1983, it was discovered and

demonstrated that microorganisms can be used for the non-specific detection of pesticides. Among the most widely used methods in recent years is enzyme inhibition. These are an excellent alternative to the sophisticated equipment used in tradition detection methods. In the *chapter 1.1.2 Effects of pesticides on enzyme activity: Acetylcholinesterase*, there is an example that shows how pesticides inhibit a large number of enzymes (cholinesterase, tyrosinase, per-oxidase, glucose oxidase, etc)[22].

Thanks to this approach, it is possible to obtain a wide range of procedures for the quantification of pesticides. The choice of a certain enzyme for the detection of its destructive activity is based on the mechanism of toxicity to living beings. For organophosphate and carbamate pesticides, insect cholinesterases are considered to be the suitable enzymes[78]. This simple way of tracing the presence of various toxic substances through enzyme inhibition has encouraged the adoption of new analytical methodologies that are not only simpler, but also less expensive and with lower detection limits than the capillary electrophoresis[76], gas chromatography (GC)[59], gas/liquid chromatography/liquid mass spectrometry (GC/LC-MS)[60–63], high-performance liquid chromatography (HPLC)[60] or electrochemical [79–81] analysis methods[64].

1.3 Altenative to traditional analytical methods: what is a biosensor?

Through the use of bionsensors, it is feasible to combine the unique functional properties of biological molecules with those of measuring devices[22]. Biosensor technology and research have seen a considerable increase in interest during the last three decades[82]. A biosensor is described as "*an independently integrated receptor transducer device, which is capable of providing selective quantitative or semi-quantitative analytical information using a biological recognition element*" by the International Union of Pure and Applied Chemistry (IUPAC)[83]. Biosensors have been widely used as cost-effective, in situ, fast and real-time analytical techniques. In response to the need to overcome the limitations of traditional analytical techniques, and thus the need for portable, fast, intelligent biosensor devices, biosensors with new functional technological features have been developed in recent years[84]. The ability to detect biological or chemical molecules utilizing electrical[85], optical[86] or mass change readout techniques[87] is provided by

this, making biosensing technology a potent analytical tool. A schematic of a biosensor's component pieces is shown in Figure 8. The type of biological recognition sensing element and the transducers are the two key features that set biosensors apart[88]. To enhance the functionality of biosensors, new transduction materials derived from nanotechnology and multiplexed pollutant detection, involving multidisciplinary specialists,
have been created[84].

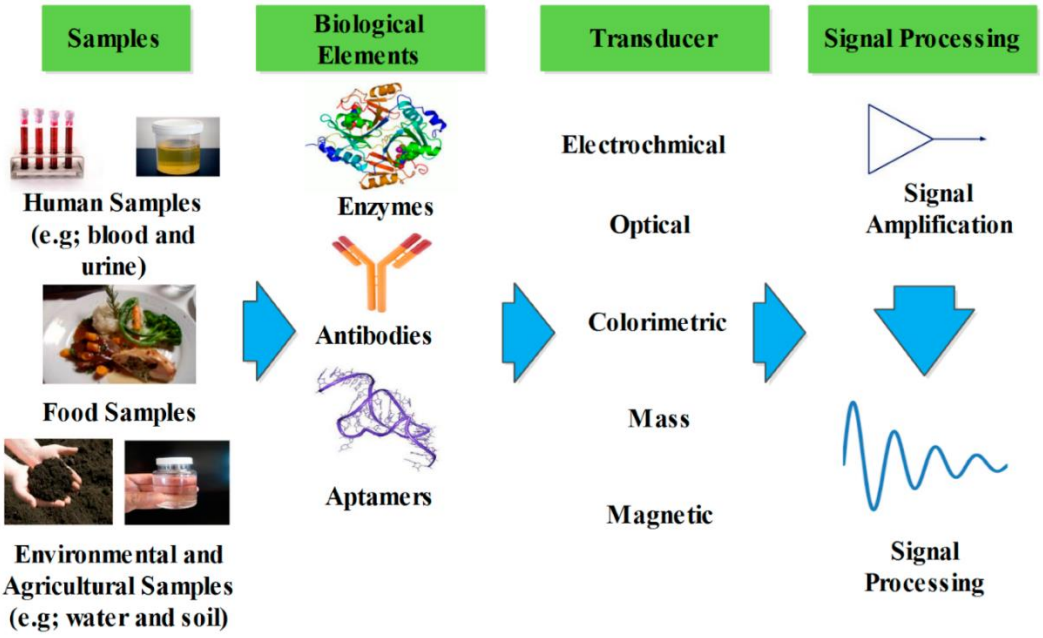

Figure 8. Diagram shows the many components of a biosensor, including the transducers, detectors, and biological identification components [88].

1.3.1 Biosensors characteristics

It is possible to classify into several different kind a biosensor according to its transduction principle, according to the kind of transducer used. The transducer transforms the biomolecule-analyte interaction into a measurable electrical[89] or optical signal[90]. The selection of the transducer depends on the nature of the physicochemical change of the reaction that takes place at the sensing layer generated[91]. A wide range of transducers has been developed and employed; however, the most popular methods are: electrochemical biosensors (including amperometric and impedance biosensors), optical biosensors (including colorimetric,fibre-optic biosensors and surface plasmonic resonance

biosensors),piezoelectric biosensors (including quartz crystal microbalance biosensors) and magnetic[84,88] . Another classification that can be utilized is one based on the recognition component that sensors possess when aptamers, nucleic acids, anti-bodies, and enzymes are used; this would result in aptasensors, genosensors, immunosensors, and enzyme biosensors, respectively. Since device creation in this thesis focuses on the development of enzyme biosensors, these have been highlighted thus far because they are the ones that are most frequently used for environmental monitoring. But more recent research indicates that aptamer development has accelerated lately as well. The thermal stability, in vitro production, and simplicity of modification of aptamers are only a few of their many beneficial characteristics. The possibility of designing their structure and distinguishing targets with different functional groups and re-hybridisation are other features that make these devices very attractive, which overcomes the immunoassays' shortcomings of non-specificity[92]. Enhancing the sensitivity and detection limit of the biosensor requires both transducers and biological recognition components[93].

The selectivity and specificity required by the biosensor to respond to a particular target or class of analytes are determined by the biological recognition sensing element, which also reduces the likelihood of interference from unwanted chemicals[94]. The target of interest determines which biological recognition element should be used (e.g., antibodies and aptamers are more suitable for the detection of bacteria or pathogens, whereas enzymes are more suitable for catalytic reactions). In general, a variety of techniques, including adsorption, covalent binding, entrapment, and membrane confinement, are used to immobilize the biological recognition elements.

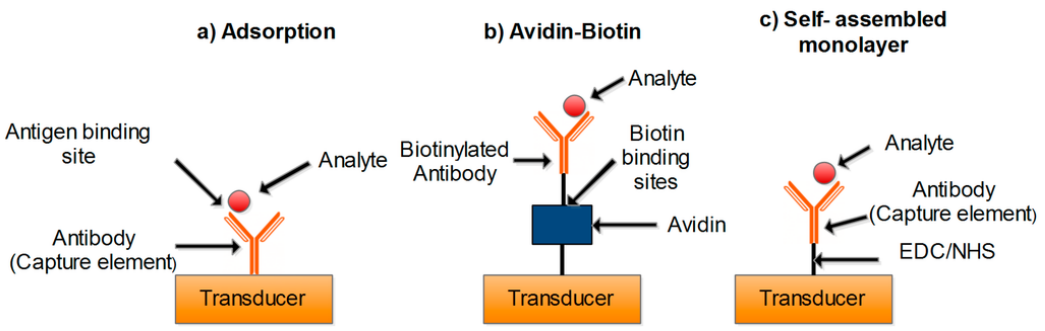

Figure 9. Schematic illustrating the primary and most popular immobilization techniques.[88]

The schematic for several of the most popular immobilization techniques is shown in Figure 9. The most popular and effective form of immobilization is covalent bonding because it is stable and irreversible, preventing the leaking of biological components from the support surface[95,96].

1.3.2 Nanotechnology advances in biosensing

The role of nanotechnology has been crucial in addressing the issues that traditional analytical methods have with in situ measurements, such as in the case of accidental pesticide release or acute poisoning, for which not only rapid but also miniaturized and portable equipment, such as biosensors for environmental monitoring, is necessary[97–99]. Indeed, the development of quick, sophisticated biosensing devices that are ideal for the detection of environmental toxins, such as pesticides, is made possible by nanotechnology. It is advantageous to incorporate nanoparticles and nanocomposites into the biosensor system, particularly in terms of the analytical performance of the devices in which they are integrated[100].

Gold nanostructures are an illustration of how the inherent contribution of nanotechnology and bionanotechnology can enhance the analytical performance, such as sensitivity or detection limit, of sensing systems. They may be a promising and adaptable platform for enzyme immobilization matrix due to their high surface area and good electron-mediating capacity to enable enzyme through electrostatic interactions[101,102]. As Zhao *et al.*[101] revealed in their investigations, gold nanoparticles also shown great biocompatibility and minimal cytotoxicity in vivo, which was another benefit.

1.3.3 Colorimetric strategies for AChE assay

Of all the modern analytical techniques for monitoring the presence of organophosphorus pesticides (see *chapter 1.2*), the colorimetric method is one of the most widespread today. The main advantages of colorimetric sensor arrays are their potential speed of analysis, their low cost, their convenience and their observation with the naked eye. Another advantage is that they are not only capable of detecting pesticides but also inhibitors and reactivators screening and OP nerve agents and heavy metals detection; as already discussed in *chapter 1.2*,

these features are preferable for a better device. Among the early innovative work on colorimetric sensor arrays by Suslick's group[103], chemo-responsive dyes and metalloporphyrin were used and studied as detection elements for convenient detection with the naked eye. Basically, the interaction between the analytes of interest and the sensing elements is based on hydrogen bonds, acid-base interactions, π-π molecular complexation, van der Waals interaction and dipolar and multipolar interactions. Therefore, the strategy of indicator displacement assays (IDA) is used extensively to build colourimetric sensor arrays. One of the limiting factors of most of these systems is that they only respond to gases or volatile organic compounds (VOCs). On the other hand, the analysis of biomolecules and complex biological samples using these sensor arrays is a major challenge. Another, more practical limitation concerns the cost of certain reagents and their stability [104].

The main categories into which the currently established colorimetric methods for the assay of AChE based on changes in the UV-Vis absorption intensity caused by AChE catalysis are subdivided into: Ellman's method, TMB-based colorimetric method (oxidase-like activity catalyst, peroxidase-like activity catalyst, ChOx coupled with peroxidase-like activity catalyst, oxidising agent, pH indicator-based colorimetric method), noble metal nanomaterial-based colorimetric method and substrate-based colorimetric method[105].

The conventional colorimetric approach is the Ellman's method. It has been used extensively for AChE testing for many years. Ellman *et al.* [39] provided the initial description of it in 1961. Since then, the AChE assay protocol has been standardized. The hydrolysate of acetylcholine, 5,5-dithiobis-(2-nitrobenzoic acid) (DTNB), is utilized as a thiocholine-sensitive indicator (TCh) in Ellman's method for the AChE assay. It is predicated on the creation of TNB, or 5-thio-2-nitrobenzoic acid, which is produced when TCh reacts with DTNB[39]. The end result can be seen with the unaided eye, but it can also be quantified in a spectrometer at a wavelength of 412 nm[106], read from a computer image[107,108], or recognized using a paper biosensor[109,110]. In Ellman's approach, spectrophotometric detection is typically used, and 96-well microplates have been employed for high-throughput assays[106,111–113]. Computer image analysis for high-

throughput dosing, which was developed more recently[107,108], makes use of an office scanner to capture the colourimetric reaction in real-time and professional picture editing software to determine the yellow intensity of the captured photos. The in situ colorimetry reaction required the development of a paper-based AChE reactor[109]. Following incubation with the substrate acetylthiocholine iodide (ATCl), TCh is interacting with DTNB to form the yellow-colored TNB in method's drawbacks include the false target detections and inadequately high sensitivity for target detection. This method's drawbacks include the possibility of false positive results and its insufficiently high sensitivity for target recognition. Thiol-containing compounds interacting with DTNB to obstruct the measurement of TNB is the likely reason of this.

The pH indicator-base colorimetric method is another detection method. Acetic acid is utilized in this method as a pH indicator. This substance is released from ACh and has the capacity to make the solvent more acidic[114–117]. It can also be utilized as a chromogenic reagent for the colorimetric analysis of AChE (in Figure 10 the reaction mechanism is shown). Wong *et al.*[115] developed an optical biosensor using a sol-gel sheet immobilized with lipophilic chromophores and AChE. Since it is sensitive to the pH change brought on by the enzymatic synthesis of acetic acid, the lipophilic chromionephore (9-(diethyl-lamino)-5-(octadecanoylimino)-5Hbenzo [a]phenoxazine(ETH 5294), a byproduct of the Nile, is utilized in this work as a pH indicator. The study by Xin *et al.* [117], in which amino-terminated polyadiacetylene (PDA) was utilized as a pH indicator for the colorimetric detection of AChE, serves as another illustration of this approach. PDA, which is amino-terminated and blue when the pH is neutral, changes red if the pH drops because of the acetic acid created by the enzymatic activity of Ache. The pH indicator has drawbacks despite being sensitive to pH shift and working well with colorimetric test. In effect, a false-positive reaction could be brought on by the acid component.

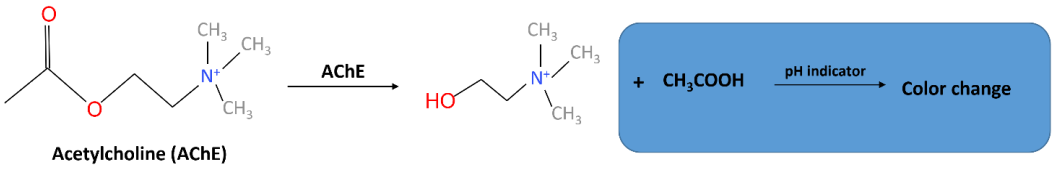

Figure 10. Principle of pH indicator-based colorimetric technique illustrated schematically [118].

There are also techniques that make use of TMB, a typical chromogenic reagent. When converted to oxTMB from its colorless natural structure, it turns blue[119,120]. The following categories can be used to categorize existing research for AChE assays, which ways to oxidize TMB to oxTMB: peroxidase-like activity catalyst[121,122], oxidase-like activity catalyst[89,123], choline oxidase (ChOx) paired with peroxidase-like activity catalyst[124,125], or oxidizing agent[126]. This technology, along with the AuNPs-based colorimetric method, is very well-liked by researchers since it is sensitive to targets but necessitates time-consuming sample-handling procedures[118].

Noble metal nanomaterial-based colorimetric detection methods can also be utilized to test for AChE. For the creation of colorimetric tests, gold nanoparticles, or AuNPs, have been frequently used as chromogenic reagents. They are excellent for this kind of application due to their distinct size-dependent optical characteristics and strong extinction coefficients. The use of AuNPs as chromogenic reagents for the AChE test can be divided into four separate categories: the catalytic synthesis/growth of AuNPs[127,128], etching of gold nanorods (AuNRs)[129], aggregation of AuNPs[130,131], and dissolution of AuNPs[132]. Other nanoparticles, such as silver nanoparticles (AgNPs) and AgNPs-based nanocomposites, have also been reported as chromogenic reagents for colorimetric experiments. However, because of their biological toxicity, AgNPs are not generally regarded as being extremely valuable by researchers. The disadvantage of noble metal nanomaterial-based colorimetric methods more generally is that they are not stable enough because even a small change in the environment could lead to the aggregation of AuNPs[118].

Finally, there is a method that, unlike all the others thus far described, does not depend on the inclusion of an additional chromogen. One of two requirements

must be met in order to quantify the enzyme dose using the colorimetric method: either the sub-layer must exhibit UV-Vis absorption at a certain wavelength or the enzyme product must exhibit UV-Vis absorption at a specific wavelength that is unaffected by the substrate. Wearyl derivatives such as indophenyl acetate[133] , indoxyl acetate[134,135], N-methylindoxyl acetate[136] , and 2,6-dichloroindophenyl acetate are examples of chromogenic substrates that have been found and exploited. The second substance listed, indophenyl acetate, is the one used in this project's device because it is the most prevalent and is converted to hydroxylindole by AChE. After catalysing, the resultant hydroxylindole is converted to blue indigo by oxygen oxidation. Due to the sluggish enzymatic conversion of acetate, this method's main drawback is that it takes longer than other ones now in use. The benefit of this procedure is that it saves money because it doesn't need any additional chromogenic chemicals.

At the state of art, the colorimetric AChE tests are currently employed in reactivators screening, inhibitor screening, heavy metals detection, and pesticide detectors. A speed test card for pesticide residue is one of the commercially available gadgets. The method relies on the colorimetric reaction between AChE and indofelnil acetate to detect OP pesticides or carbamates. High dosages of pesticide residues are required, false positives are a possibility, and background color interference in detection are some of its drawbacks. Additionally, Ellman's approach, which is not only insensitive but can also result in false positives, is the basis for the sole commercially available color AChE assay kit for clinical use. Therefore, it is absolutely essential to strive to create new kinds of AChE color assay kits for the clinical detection of AChE [118]

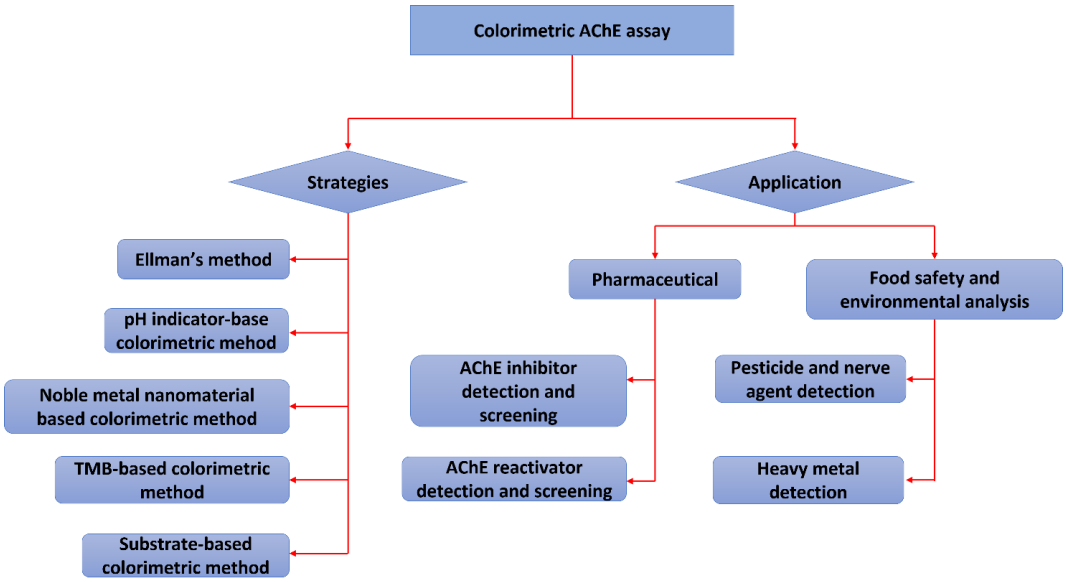

Figure 11. Summary diagram of different strategies and application of the AChE colorimetric assay. [118]

1.3.4 Microfluidic devices as point of care (POC)

One of the most important systems to be merged with biosensor technology is microfluidics[88]. For various biological and chemical applications, a variety of microfluidic devices have been developed[137]. Microfluidic systems were categorized by Haeberle and Zengerle into droplet-based microfluidics, centrifugal microfluidics, electro-kinetic platforms, large-scale integrated microfluidic techniques (pressure-guided devices), and free-scale non-contact dispensing systems[138]. Three categories of microfluidic devices have been established more recently: continuous flow, droplet-based, and digital microfluidic systems (Figure 12 A-C)[88]. Traditional microfluidic systems work by establishing continuous flow regimes in etched microchannels that are linked to micropumps and valves that encourage flow throughout the apparatus. Soft lithography techniques are typically used to create these microchannels[139]. Droplet-based microfluidic systems have been designed to create isolated reaction sites and decrease sample consumption[140]. The current widespread usage of droplet-based microfluidics as a novel platform for a variety of applications pertinent to the subject matter of this thesis, such as biomedical, environmental, security, and defence applications, makes it even more intriguing. With this kind of technology, portability may be improved and power usage reduced. Digital

microfluidic systems control the flow of droplets using electrostatically driven electrode arrays, negating the need for pumps, valves, and channels, in contrast to droplet-based microfluidic devices, which use immiscible fluids to create droplets in microchannels.

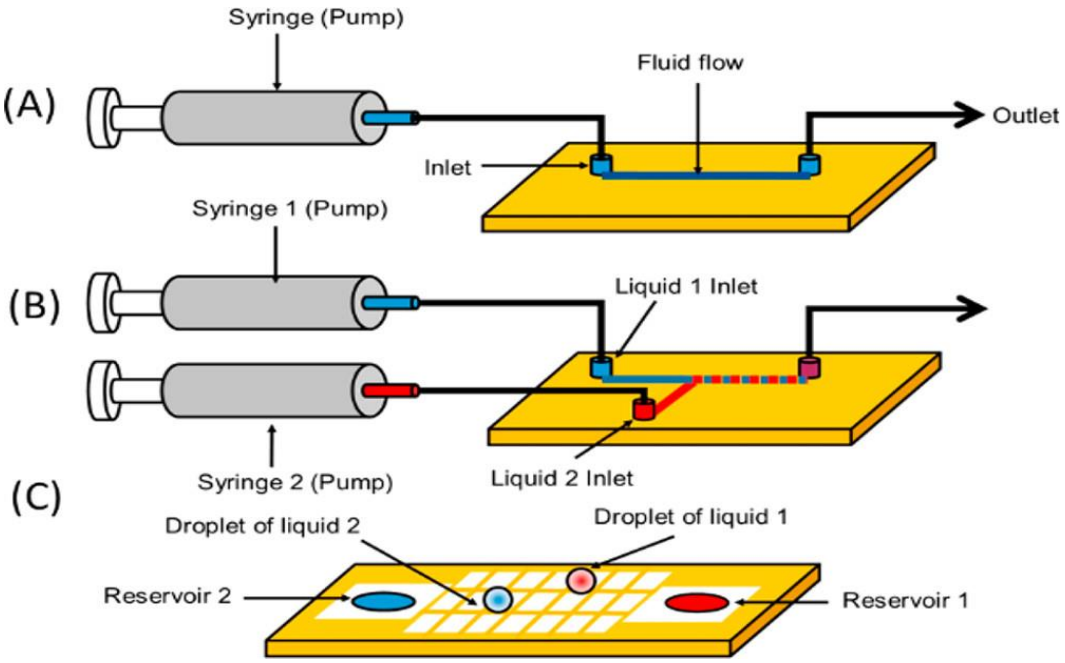

Figure 12. Schematic of the three types of microfluidic systems: (A) continuous, (B) droplet-based, and (C) digital microfluidics. Reproduced from ref ([88]).

The mobility, accessibility, and in-situ analytical capabilities of biosensors can be increased by combining microfluidic devices and biosensors to mix biological and chemical components on a single platform. This is especially true when wireless technology is added[88,141]. Microfluidic systems have been demonstrated to be in high demand and to be used in conjunction with biosensors to create lab-on-a-chip (LOC) technology, which adds many benefits to biosensor technology[142]. LOCs are analytical measurement devices that can complete small-scale laboratory operations such sample preparation, separation, and detection on a single platform. They are also frequently referred to as "micro total analysis systems" (μTAS). Samples and reagents can be transferred between various on-chip fluidic components using LOC devices' microfluidic channels[143,144]. LOC devices offer enormous surface-to-volume ratios (which speed up reaction times), low sample and reagent volume needs (sometimes nano to attolitre), and highly controlled sample handling[88,145,146]. A single microfluidic biosensor may execute an entire

analysis[147], including continuous sampling, sample separation and mixing[148], pre-concentration and processing[149], thanks to the tiny size of microsystems. This qualifies them for quick in loco analysis applications such process control, medical diagnostics, and environmental monitoring[88,145,146]. Additionally, point-of-care (POC) applications can use these microfluidic biosensors because of their portability, high throughput, real-time detection, and better analytical performance[150,151]. Overall, the combination of biosensors and microfluidic devices yields a potent analytical tool that moves testing closer to the house, helping both developed and developing nations.

Silicon, glass, as well as polymers including polydimethylsiloxane (PMDS), polyethylene terephthalate (PET), and poly(methyl methacrylate) (PMMA), cyclic olefin copolymers (COC), polycarbonates, and paper are among the materials used to create LOCs. The design, the materials, and the intended application all influence the fabrication method[143]. By reaching a high degree of precision, photo-lithography and etching processes are used to create glass- and silica-based devices, but they have the drawback of taking a long time and being expensive[152]. Most frequently, soft lithography, hot embossing, injection molding, laser ablation, lamination, nanofabrication, and three-dimensional printing are used to create polymer-based devices[58]. Microfluidic paper-based analytical devices (μPADs), which are another type of microfluidic device, are a good screening method for pollutants in food. They overcame the issues by relying on the numerous detection techniques that have been created up until this point. Even while the conventional analytical procedures had good performance, as explained in the *chapter 1.2* they relied on expensive and large equipment, required experienced operators, frequent equipment maintenance, and took a lot of time. Applications in underdeveloped nations and isolated villages are significantly limited by the method' relative inefficiency and cost[153–156]. Microfluidic technology continues to mature, which makes its rapid development clear to everyone and gives it an unrivalled position in the detection sector[157]. The objective of μPADs, a portable chip technology, is to archive simple, efficient, and low sample consumption detection that is appropriate for on-site detection quickly and accelerates the technological transition from the lab into the

field[158,159]. Because they are affordable, nontoxic, and simple to adapt, µPADs have emerged as one of the greatest tools for analysis and detection studies[160–162]. The development and use of µPADs in food analysis has increased significantly during the past ten years. In order to quickly analyse complex biochemical samples, these new groupings of analytical tools often use paper-based devices with a two-dimensional (2D) or three-dimensional (3D) structure made (see Figure 13) of tiny pieces of patterned paper[163].

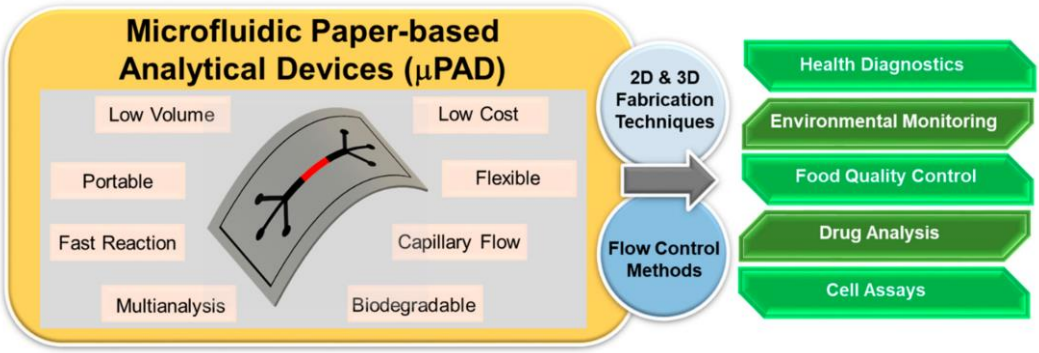

Figure 13. Benefits and possible uses of 2D and 3D microfluidic paper-based analytical devices are shown schematically in the diagram. Reproduced from ref ([164]).

Different detection technologies can be linked to the paper on such a robust analysis platform to obtain sensitive identification of food risks. The ability to evaluate complicated biological and chemical specimens, such as macromolecules, proteins, nucleic acids, cells, pathogens, dangerous compounds, and others, is provided by µPADs for analytical chemists[165]. Drug testing, mental health surveillance, and other factors[166]. The robust µPADs still need to overcome a number of real-world obstacles before they can be commercialised. The World Health Organization (WHO) established the "ASSURED" criteria, which should be met by analytical devices used in resource-limited settings. These criteria are: affordable (A), sensitive (S), specific (S), user-friendly (U), quick and reliable (R), equipment-free (E), and delivered to those in need (D)[162]. The majority of µPADs now under development focus primarily on the characteristics that are affordable, sensitive, specific, fast, and robust to implement ("ASSR"), but it is frequently simple to overlook "U," which is the fundamental barrier preventing the commercialization of devices[167]. Additionally, some detection techniques that depend on tools like colorimeters, fluorometers, and electrochemical workstations

to interpret detection findings are unable to successfully meet the "E" and "D" criteria, making them challenging to adopt by non-expert u. The user-friendliness ("U") component of PADs, particularly the development of intelligent detection results analysis programmes, can be successfully improved by the development of a variety of portable and tiny detection tools, such as smartphone-based detection methods[168]. Micro devices can be used to conduct experiments on a micro scale because to the miniaturisation of PADs. As a result, μPADs can complete a number of experimental steps, including sample mixing, separation, incubation, elution, and detection, in a single analysis process[169]. The operation of the users for sample preparation to detection will be drastically reduced by these automated stages, producing an adequate degree of "UED" experimental results.

Since the Whitesides group brought μPADs to the scientific community, fabrication methods have improved in accuracy and simplicity[170]. The cellulose paper is hydrophobically treated to create a hydrophobic barrier and act as a liquid flow channel, forcing the liquid to flow in a specific direction. This is the core production principle of μPADs[171,172]. Photolithography[173], wax printing[174], inkjet printing[175–177], laser printing[178], screen printing[179], plasma treatment[180], plotting[181,182], stamping[183,184], vapour deposition[185], wet etching[186], spraying[187], corona treatment[188], cutting[189–191], embossing[192], and laser etching[193] are some of the frequently used channel pattern processes. The manufacture of μPADs should satisfy reasonable standards regarding high batch stability, budget, and timeliness in light of the necessities of commercialization[159]

The development of easier and more affordable detecting techniques is just as important to the advancement of μPAD technology as the need for better materials. Most μPADs over the last ten years have used optical and electrochemical sensing methods. The most straightforward, useful, and common analytical technique is optical detection, which primarily uses colorimetry[194,195], fluorescence[196], chemiluminescence[197], and surface-enhanced Raman spectroscopy (SERS)[198]. The well-established and frequently used colorimetric assay, which is the reaction of an analyte solution with a loaded reagent to cause visual changes, has been investigated in this thesis[199]. A colour reader or mobile phone can be used to take a photo of the visual findings of the μPAD detecting

area to be used in semiquantitative analysis. Additionally, the multichannel nature of µPADs enables flexible colorimetric single-component analysis as well as simultaneous study of many targets. The main drawbacks of colorimetry, however, are its low sensitivity and interference from the food sample matrix[200].

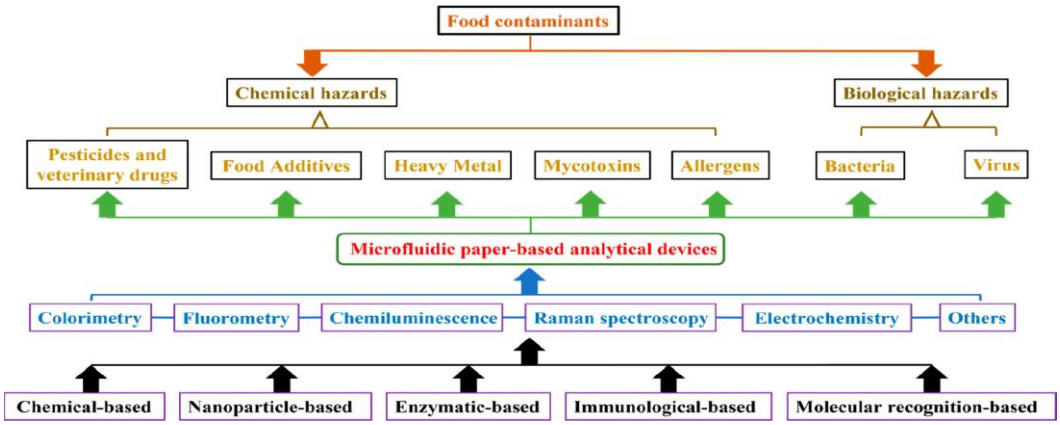

Figure 14. Conceptual framework based on µPADs for food contamination analysis. Reproduced from ref ([159])

1.4 Colorimetric microfluidic paper-based biosensors: state of art

Since in this thesis the colorimetric microfluidic paper-based biosensor as the aim to detected organophosphate pesticide, a brief resume of the one already existing will follow.

To identify organophosphate and carbamate pesticides, No *et al.* [136] used paper-based dipsticks made of various cellulosic derivatives for the first time in 2007. Depending on the concentration of the target pesticide, the acetylcholine esterase (AChE) enzyme activity is inhibited in the working principle.

Later, Hossain *et al.* [201,202] created paper-based dipsticks with great success using sol-gel silica as an entrapment material, which can improve the enzyme stability and provide an alternative to traditional lateral flow-based methods. It was discovered that the devices could detect paraoxon pesticides at a limit of detection (LOD) of 27.5 µg/L for 60 days at 4°C. These techniques nevertheless call for the user to carry out numerous steps of operation, such as turning the device around at a certain moment to generate a signal or adding outside reagents.

Jahanshahi-Anbuhi *et al.*[203] have created a paper-based device with two flow channels to get around these problems. Before the colorimetric substrate indophenyl acetate (IPA) is introduced to the reaction zone by a second, slower flow channel, a fast flow channel allows the interaction of the pesticide in the sample with the AChE enzyme. A manually operated paper ON-OFF valve regulates the pesticide-AChE interaction time resulting to target concentration-dependent enzyme inhibition. The length of the "slow" flow channel limits the sample-enzyme interaction time prior to the arrival of the colorimetric substrate in addition to the requirement to manually switch a paper flap at a precise point in the experiment.

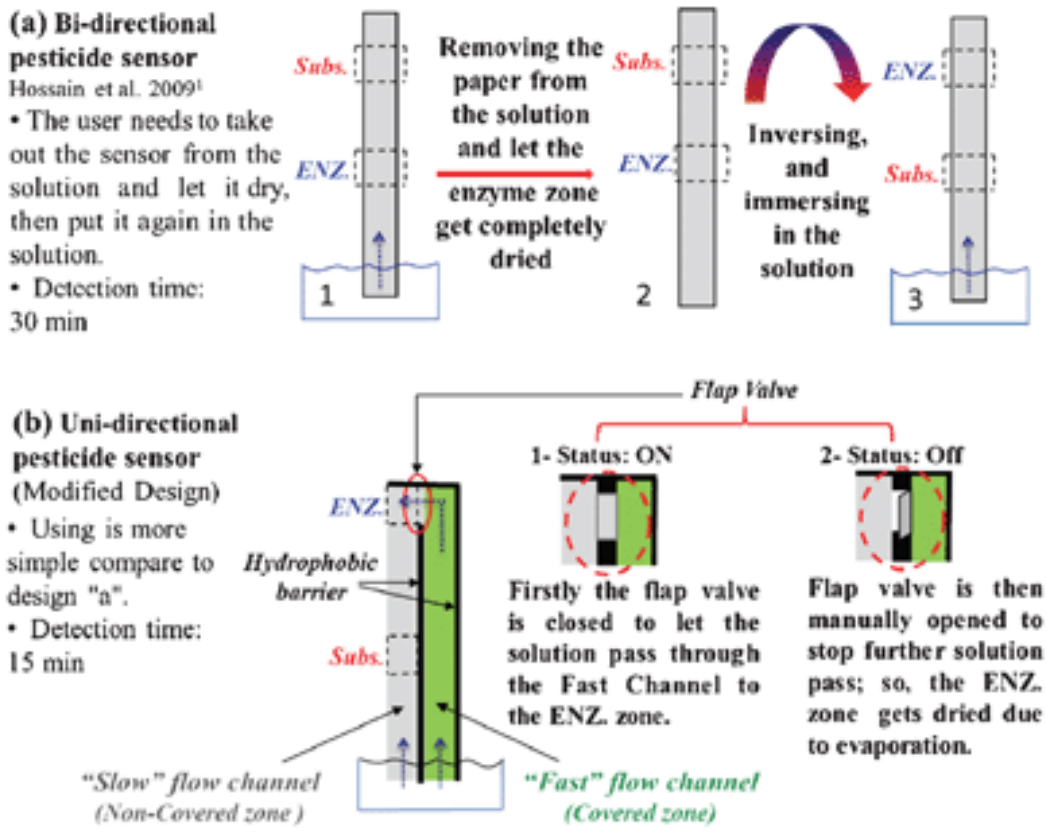

Figure 15. Adapting bioactive paper to detect pesticides by Jahanshahi-Anbuhi *et al.* [203] (a) A sensor for bidirectional pesticide detection[202]. (b) A modified sensor for unidirectional pesticide detection. PET cover slips are used to create a faster-flowing zone over the green zone. The top of the paper strip is designed with a manual valve. This change makes it possible to use a simpler unidirectional pesticide sensor [203].

Sicard *et al.* (2015) [204] used a smartphone for signal readout to demonstrate the usefulness of μPADs for on-site pesticide analysis. However, that system also needs to be tested in two steps: first, a sample solution must be added, and then

the device must be submerged in distilled water until the liquid level reaches a predetermined level.

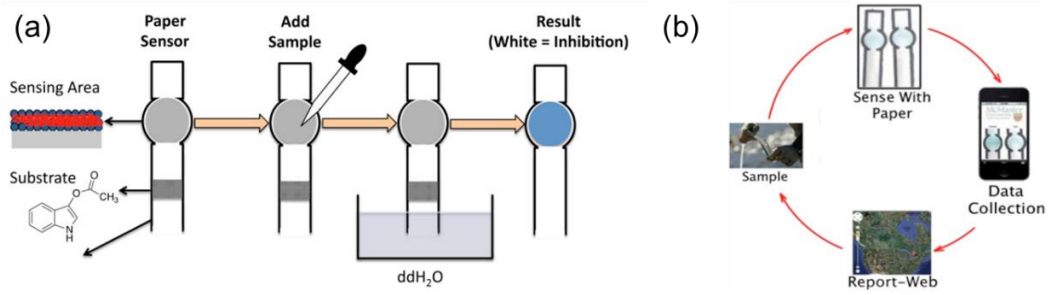

Figure 16. Representation of Sicard *et al*. [204] device a) Paper-based sensors have the potential to revolutionise how the world tests and monitors water quality. Data gathering and data pushing from mobile devices to websites that display data on maps are both possible. Areas of pollution become visible and can prompt the need for extra monitoring. b) To stabilise the enzyme, AChE is immobilised between two layers of silica sol-gel. To catch indigo as it forms, a cationic polymer (poly-arginine) is put to the paper's surface; (C) The procedure for analysing water samples using a paper sensor. (The reader is directed to the web version of this article for clarification on the meaning of the colour references in this figure legend).

The same enzymatic reaction method has recently been used to create a test strip that is extremely sensitive[134] .Based on the relatively lengthy pesticide-AChE interaction period (20 min), a very low LOD (0.01 µg/L) has been achieved, leading to a significant level of enzyme inhibition. Once more, the indoxyl acetate (IDA) colorimetric substrate is an external reagent that users must add, which makes this device less suitable for actual applications.

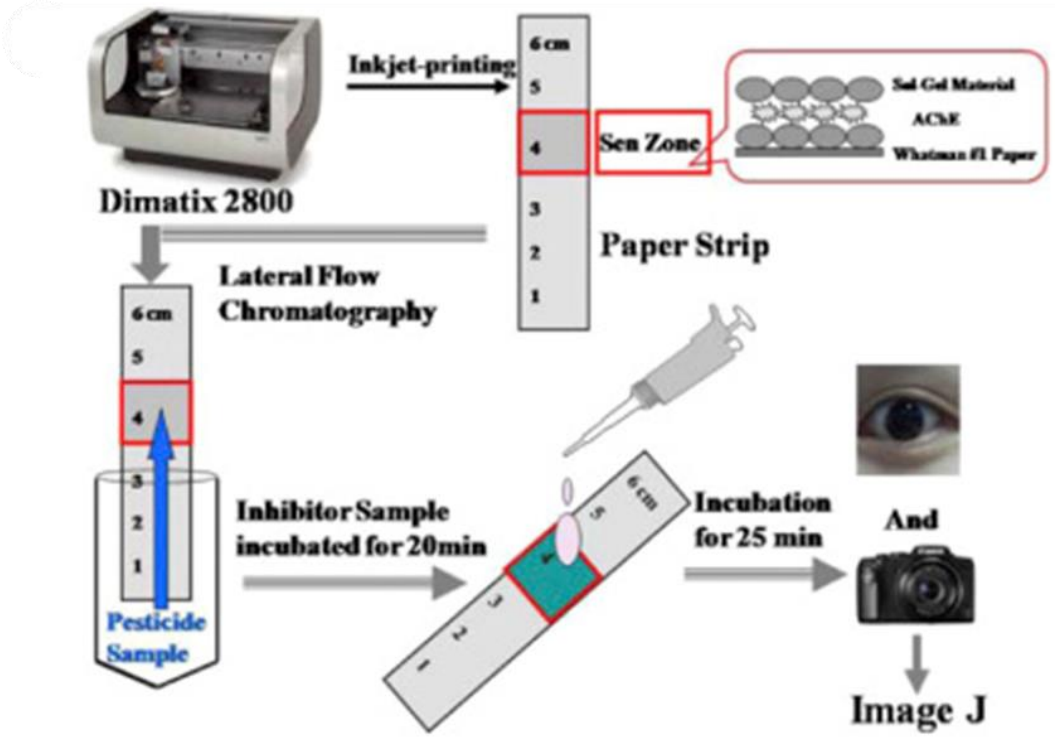

Figure 17. The paper-based strip's basic idea by Xiao *et al.*[134]. The AChE biomolecules are trapped between two layers of biocompatible silica generated from sol-gels in the sensing zone, which is manufactured using inkjet printing technology and has a "sandwich" shape.

In conclusion, numerous paper-based devices for colorimetric pesticide analysis have been reported in the literature; however, to the best of our knowledge, they do not permit straightforward assays involving the addition of samples. Instead, they typically require additional operational steps, frequently at a specific timing, as described above. Therefore, there is still room for the creation of more straightforward paper-based devices to get over this restriction. Many researchers have studied the issue of how to regulate and modify fluid flow in µPADs, for instance, in order to regulate reaction time[205]. In order to autonomously adjust liquid flow rates and produce temporal delays, Lutz *et al.*[206] deposited varying concentrations of sucrose inside flow tubes.

Wax-printing, which results in differences in paper permeability for aqueous solutions, is another method for precise flow control on µPADs[207]. However, these flow control techniques are rarely used in actual assays; instead, dye solutions are typically used in research as proof-of-concept. The utilisation of pressed regions in wax-printed channels by Park *et al.* [208] allowed for the

modification of liquid permeability across the pressed region as a result of changes in pressing force. This method's limitation of only achieving delay times of up to 200 s prevents it from being used in the current situation, where an enzyme inhibition reaction is necessary for the purpose of realising a "walk-away" µPAD for the user-free analysis of organophosphate pesticides.

To trace the presence of organophosphates using µPAD technology, Ua *et al.* [209] realised a device—one of the most complex identified in the literature— that uses the phrase "walk-away". The use of this word refers to the fact that their equipment simply needs a sample solution to be added, skipping other procedures and allowing lengthy incubation periods before scanning the images for signal capture. For flow control, their approach introduces wax-printed channels built within a 3D µPADs device (Figure 18).

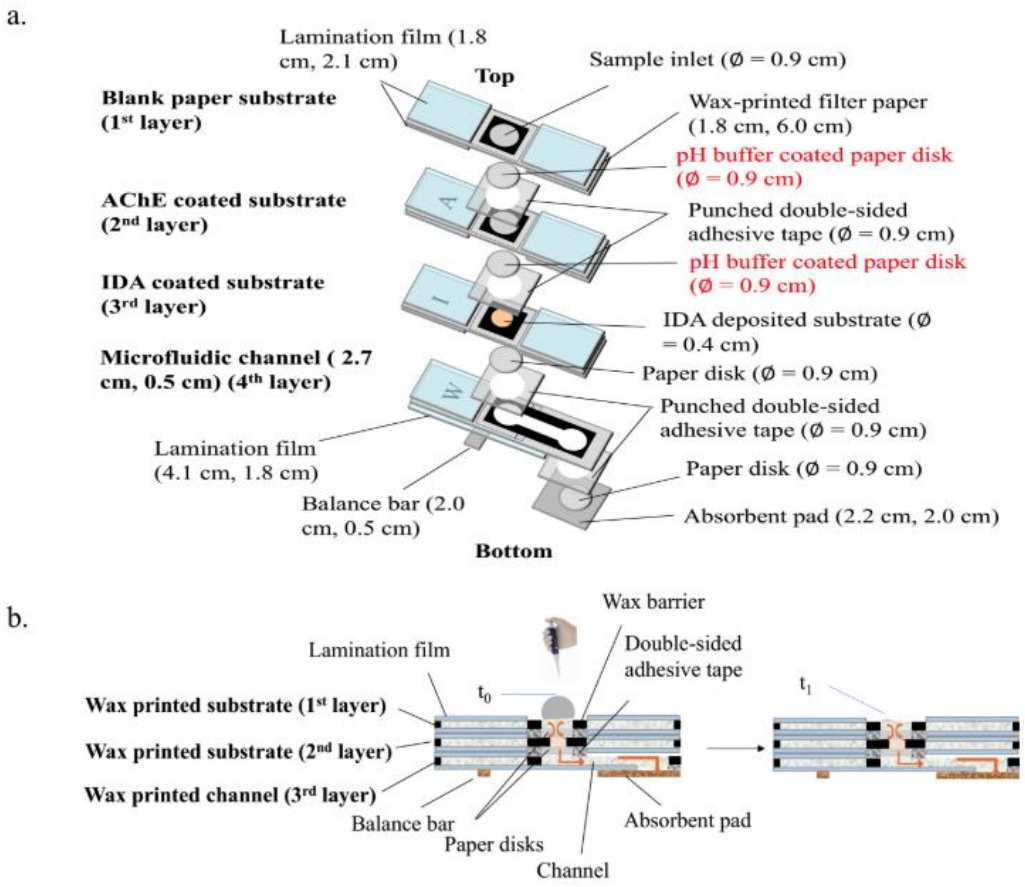

Figure 18. a) Schematic illustration of a 3D µPAD developed by Ua et al. [209] showing the arrangement and layout of individual paper layers, double-sided tape and paper disks with integrated buffer components for reagentless operation b) Cross-section of a 3D µPAD

and schematic illustration of the experimental method for evaluating the delay time (t1–t0) in 3D μPADs. Reproduced with permission from Springer Nature.

The enzymatic reaction between the non-inhibited AChE enzyme and the IDA substrate as well as the inhibition reaction between the enzyme and pesticide have both been delayed using liquid flow control. Additionally, all relevant assay reagents were put on separate paper layers, eliminating the need for additional reagents. As far as we are aware, their paper is the first to address the incorporation of wax-printed channels into 3D μPADs for flow rate control, which can reduce the requirement for human intervention.

Chapter 2: Aim of the thesis

The objective of this thesis is to reproduce and optimize a paper-based colorimetric assay for the detection of organophosphate compounds, a specific group of acetylcholinesterase (AChE) inhibitors commonly used in pesticides. This approach utilizes indoxyl acetate (IDA) as a chromogenic substrate, which is catalysed by the AChE enzyme to produce indoxyl, a blue molecule visible to the naked eye. The presence of organophosphate compounds inhibits the hydrolysis of IDA by the AChE enzyme, resulting in a decrease in color intensity. The goal of this study is to optimize the sensitivity, specificity, and reliability of the assay, making it suitable for detecting organophosphate compounds in various environmental samples. To achieve this goal, the first step was to conduct a literature review to identify previous research on paper-based colorimetric assays and to determine the most effective methods and materials. Then, a simple visual screening card was created to establish a proof of concept before being integrated into a microfluidic platform to create a μPAD. The performance of the assay was evaluated by assessing various parameters, such as stability, linearity, precision, limit of detection, accuracy, sensitivity, selectivity, and robustness. Additionally, the device was evaluated based on the "ASSURED" criteria established by the World Health Organisation (WHO) for analytical devices used in resource-limited settings, including accessibility, sensitivity, specificity, ease of use, rapid and reliable results, equipment-free operation, and provision to those in need. To test the generalizing capacity of the sensor, three different organophosphate pesticides were used: Chlorpyrifos, Dichlorvos, and Malathion. The selectivity of the device against both organophosphate pesticide and AChE inhibitors is achieved through the use of organophosphate compounds in all three components. This study aims to provide a comprehensive understanding of the strengths and limitations of the paper-based colorimetric assay for detecting organophosphate compounds, and to provide a foundation for the development of future devices with similar capabilities. The results of this research may have broad implications for environmental monitoring, agriculture, and public health. Ultimately, the aim of

this thesis is to contribute to the growing body of knowledge in the field of colorimetric assays for pesticide detection and promote the development of low-cost, portable, and user-friendly detection devices for organophosphate compounds.

Chapter 3: Experimental section

3.1 Chemicals and materials

The pesticides used were Chlorpyrifos (45395), Dichlorvos (45441) and Malathion (36143). The chromogens were 5,5′-Dithio-bis-(2-nitrobenzoesäure) (DTNB) (10250003) and Indoxyl Acetate (IDA) (I3500). The substrate and the enzyme ordered were respectively Acetylcholine chloride (A6625) and Acetylcholinesterase from Electrophorus electricus (electric eel) (Type V-S) (C2888). All of them were obtained from Sigma-Aldrich. Other products ordered for general improvements of the solution/final device were: Bovine Serum Albumin (BSA), 0.1 M TRIS-HCl pH 8-10% (07066), Potassium chloride, Sodium Chloride and Triton X-100 were also obtained from Sigma-Aldrich. Di-sodium hydrogen phosphate (106585) and Potassium dihydrogen phosphate (104871) were obtained from Merck. 25 mm Syringe filter (w/ 0.2 µm polyethersulfone membrane) was obtained from VWR international while Syringe from TERUMO. Nylon (NY) membrane (disk diam. 25 mm, pore size 0.45 µm) (1213768) was purchased from GVS. Whatman #4 (diameter 125mm) and Whatman #1 filter papers (diameter 150 mm) were from Cytiva. Microcope slides by Marienfeld, Methanol, Chloridic acid, Sodium hydroxide and distilled water were provided by Technischen Universität Wien.

3.2 Solutions

To reduce the possibility of deterioration, stock solutions of indoxyl acetate, malathion, chlorpyrifos, and dichlorvos were prepared every day and utilised for no more than 3 hours following production.

AChE working solution: AChE (1000 U/mL) was diluted with DPBS (pH 6.5) to a final solution 500 U/mL.

The blocking solution was a 20 mM phosphate buffered saline solution (PBS, pH 7.24: 25mM Na_2HPO_4, 4.4 mM KH_2PO_4, 6.7 mM KCl, 342 mM dissolved in

distilled water, stirred and filtered 0.2 μm) with 0.5% (w/v) BSA, and the washing solution was 20 mM PBS with 0.01 % Triton X-100.

0.1 M Tris-HCl was diluted with distilled water to obtain a final concentration of 10mM (pH 7.4).

Indoxyl acetate (IDA) working solution: IDA was dissolved in This-HCl (10 mM, pH 7.4) with 5% (v/v) of methanol (v/v) to obtain a concentration of 6.6 mM.

Malathion, Chlorpyrifos and Dichlorvos were prepared by diluting an appropriate volume of each stock of the pesticide sample with Tris-HCl with 50% (v/v) methanol.

Tris-HCl with 50% methanol (v/v) not only aided in dissolution of the AChE inhibitors but also enhanced the affinity of pesticides for binding to AChE[210–212].

3.3 Equipment and software to analyse data results

For a qualitative investigation, the color signal produced by the reaction of AChE with the indoxyl acetate substrate can be assessed visually. For quantitative analysis, spectrometer EnSpire 2300 Multilabel Plate Reader was used to measure the absorbance of solution in 96-well plates. The data obtained were analysed with the GraphPad Prism software (version 8.4.3) or Excel. For the results obtained on assay paper, only a semi-quantitative analysis could be performed: a digital image device (Nikon D3100 digital camera carried out in automatic mode with no flash) captured the images and transferred to ImageJ software. Each test zone's intensity value was estimated by subtracting firsr its intensity from the background's (the area above the test zone) and then white color intensity. The pH meter Mettler Toledo FiveEasy to measure the pH of the solutions. VWR INCU-line IL-10 was used to incubate the solutions or the paper where enzyme was immobilised at high temperatures. Janke & Kunkel IKA IKAMAG RH was used to stir the solutions.

3.4 Calibration and correction of the use of the spectrometer

Before starting to use the substances required for the experiments, simple tests were conducted to test the correct functioning and calibration of the spectrometer.

Only two substances were used for this type of test: sodium fluorescein and distilled water (dH_2O). Sodium fluorescein was used for its properties: it is very easy to process as it is an active dye at very high levels. It is sodium salt and an organic fluorescent yellow-red, synthetic dye. For the use of this salt in the experiments conducted it was important to know that its molecular weight is 376.67 g/mol and it has a peak excitation at 494 nm and a peak emission at 512 nm[213]. Several serial and simple dilution methods were performed to test pipetting skills after a bit of practice and to see if the optical instrument was working properly.

The best circumstances for collecting and analysing chromogen data with the spectrometer were subsequently determined by three more trials using indoxyl acetate at different concentration, obtaining a curve to compare. The first to determine which of the various wavelengths (605[134], 620[214], and 650[215] nm) discovered in the literature was the most suitable one for this apparatus to measure the product's absorbance. The second was to determine the best volume to deposit in the 96-well plate, which ranged between 50, 75, and 100 µL. The limit of detection (LOD), a bioanalytical performance metric that is defined as the lowest concentration of an analyte in a sample that can be reliably identified with a stated probability (usually at 95% certainty), was used in the previous experiment [216] . LOD has been calculated with the following equation(1):

$$LOD = 3.3\frac{\sigma}{S} \qquad (1)$$

where σ is the S.D. intercept and S is the Slop. All three experiments were conducted by pipetting different concentrations of IDA (6.6, 3.3, 1.65, 0.825, 0.412 and 0.206 mM) diluted in Tris-HCl with (10 mM, pH 10) 96-well plate containing AChE. In this case, there was no need to add the enzyme to obtain a color change, but it was sufficient to adjust the pH of the solvent by adding HCl.

3.5 Characterization and optimization of the chromogen substrate

For the optimization process, pH and temperature effects on indoxyl acetate stability, the substrate's hydrolysis time of reaction when catalysed by AChE and its concentration on signal output were investigated.

3.5.1 pH influence on indoxyl acetate stability

An initial solution was prepared with a concentration of 10 mM IDA in Tris-HCl (10 Mm). The pH meter was first used to measure the initial solution, that was 7.4. Subsequently, a certain amount of this solution was divided into seven further vials to which Chloric acid (HCl) or sodium hydroxide (NaOH) was added to reduce or increase the pH respectively. To avoid drastic changes in acidity, measurements were made after each addition of 50 µL HCl to reach pH of 3, 4 and 6 or NaOH to reach values of pH of 8, 10, 11 and 12. Three samples of each solution having different pH were pipetted in 96-well plate. After 5 min from the correction of pH, absorbance values were measured with the spectrometer.

3.5.2 External temperature influence on indoxyl acetate stability

The second experiment conducted to test whether the chromogen changed its properties due to external agents was carried out by controlling the temperature. Since the enzyme can be influenced by the external temperature during the reaction, it was tested whether the chromogen only changes when subjected to three different temperatures during his change of color: room temperature (24°), body temperature (37°) e temperature at which the chromogen is stored (-4°). The solution to taste the color change of the IDA were obtained by adding 150 µL of NaOH were added to 1mL of indoxyl acetate solution (10 mM), in this way the pH of the initial solution changed from 7.4 to 10. After that samples of 100 µL of this solution were pipetted in 3 different 96 well plate and were putted at the 3 different temperatures. After 20 min, the absorbance at 650 nM was measured with the spectrometer.

3.5.3 Time of reaction of the hydrolysis mechanism

Before proceeding with the optimisation of the concentrations used for the solutions of the reagents used (AChE and IDA), an experiment was carried out to check what the absorbance values were during the AChE-catalysed IDA

hydrolysis reaction and after how many minutes the results were reliable. For this experiment, 80 µL of IDA (10 mM) prepared methanol (knowing that methanol inhibits the enzyme's activity, the solution was prepared using only methanol to put itself in the worst possible condition) and 20 µL of AChE (1000 U/mL) diluted in DPBS (final concentration 800 U/mL) were pipetted into the 96-well plate. The absorbance change was measured at 650nm every 60s for 60 min after the begging of the reaction.

3.5.4 Optimization of reagent solutions for the assays using 96-well plate

Three tests were conducted to examine the impact the drug has on the solution it is being prepared for. First, the IDA was prepared in Tris-HCl (10 mM, pH 7.4, with a final concentration close to 6.6 mM. The second IDA was prepared in Tris-HCl with 90% (v/v) of methanol and the same final contraception as the first. The third experiment used the same solvent as the first, but with IDA concentrations around 100 mM. Then, based on the findings of these three experiments, an additional two were conducted to maximise the concentrations of chromogen substrate and enzyme. The first of the two procedures called for using a fixed concentration of IDA (10 Mm) prepared in Tris-HCl with 5% (v/v) methanol (pH 6.5) and a range of AChE concentrations (1,000, 800, 500, 250, 100, 50, 20, 5, and 0 U/mL diluted in DBPS. After determining the optimal AChE concentration, several IDA concentrations were tested (10, 6.6, 3.3, 1.6 and 0.412 mM).

3.6 Conceptual design of the visual screening cards

The first device is a sensitive visual screening card that is constructed from many NY membranes, each of which has been divided into a disk (Ø= 6mm), and affixed to a polymer surface. It was possible to obtain numerous test cards in this way. By physical absorption, the enzyme was immobilised on paper disks. AChE solution (500 U/mL) in the amount of 5 µL was pipetted onto the paper. Paper disks were placed in the refrigerator for 30 min at 4° and left there for another 2 h to enable the immobilisation of the enzyme. The test cards were stored at -20° C. in a sealed zip-lock bag.

3.7 Optimization of the visual screening cards

3.7.1 Immobilization methods

In this initial experiment, test cards were created using the same assembly procedure as described in *chapter 3.6 Conceptual design of the visual screening cards.* The immobilisation of the enzyme involved the use of physical adsorptive techniques. Following that, several immobilisation conditions have been demonstrated, including the amount of enzyme to be immobilised, the immobilisation temperature, drying modes, and treatment of the paper with blocking and washing solution. Five different enzyme volumes (1,000 U/mL) were pipetted onto various sheets (1-5 µL) and were tested at four different immobilisation temperatures: -20°, 4, and 25. (room temperature). The test cards were left at these temperatures for a total of 30 min. In summary, there were two drying modes: the first required that the enzyme be heated to 4° for at least 2 h (sometimes the paper discs weren't fully steamed, so they were left in for an additional 10 or 20 min), and the second required that the enzyme be heated to 40° for 10 min. Finally, the efficiency and usefulness of using a blocking and washing solution after immobilising the enzyme (using the temperature defined in the previous step), before drying the enzyme (using time and temperature chosen after previous steps), was evaluated. A drop of AChE was applied to the ready paper, and it was given 30 min to dry. By dipping the paper for 20 min at room temperature in the blocking solution, the paper was protected against non-specific binding. Then, after immersion in the washing solution for 30 min at room temperature, the blocked paper was dried for two hours. For all the experiments, to see color change the volume of IDA (10 mM) addicted after the immobilization was 4 times the volume of the enzyme pipetted. Photos to analyse the results were taken after 30 min from IDA deposition.

3.7.2 Estimation of the immobilized enzyme on paper support

To roughly estimate the percentage amount of enzyme immobilised (EI%) to the substrate, an indirect method was devised to study the activity of the enzyme before and after immobilisation. To estimate the activity of the enzyme after immobilisation, using a 96-well plate, the following steps were followed:

1. 30 µL of 500 U/mL AChE were pipetted in 96-well plate (for 3 times in three different wells).
2. (4 different) paper disks (Ø=6mm) were immersed in each of the three wells for two min.
3. Paper disks were removed from the solution and left at 4° for 2 h and 30 min.
4. In the meantime, 3 rows of the 96wellplate were prepared with 120 µL of 4 different concentrations of indoxyl acetate (10, 6.6, 3.3 and 1.65 mM) in Tris-HCl with 5% (v/v) of methanol.
5. After 2 h and 30 min, the paper disks were immerged in the well plate for 25 min.
6. 100 µL were retrieved (making sure to do not touch the paper disk) and pipetted into another well.

In the last step, it was essential not to touch the disk paper as the same experiment had been performed by taking the paper instead of the volume. The results obtained in that case were poor as the amount of fluid was highly operator-dependent (the sheet was squeezed differently and uncontrollably).

The values acquired were compared with those obtained with free enzyme. In this case, the amount of volume pipetted was less as there was no paper to absorb the liquid, but still in a 1:4 ratio between the volume of the enzyme solution and that of the chromogen (20 µL of AChE and 80 µL of IDA).

The EI(%) was calculated by subtracting the absorbance values measured with the free enzyme (A_1) from those with the immobilised enzyme (A_2):

$$EI(\%) = \frac{\Delta A_{12}}{A_1} \times 100 \qquad (2)$$

3.7.3 Optimization of reagent concentrations used for testing pesticides on paper

Fixed concentration in 20 µL of IDA (10 mM) was deposited on paper disks have different values of AChE concentrations from 1,000 to 250 U/mL immobilized on

paper. After determining the optimal AChE concentration, IDA concentrations from 10 to 1.6 mM were tested.

3.8 Performance of the visual screening cards

3.8.1 First test of pesticide inhibition on paper-based assay

Test papers were prepared as explained in *chapter 3.6 Conceptual design of the visual screening cards*, on each paper 10 µL of different concentrations of malathion (from 100 µM to 1 nM) were pipetted. After 20 min for inhibition, IDA (6.6 mM) was added to have color change. Photos for analysing the results were taken 30 min after the addiction of chromogen (Figure 19).

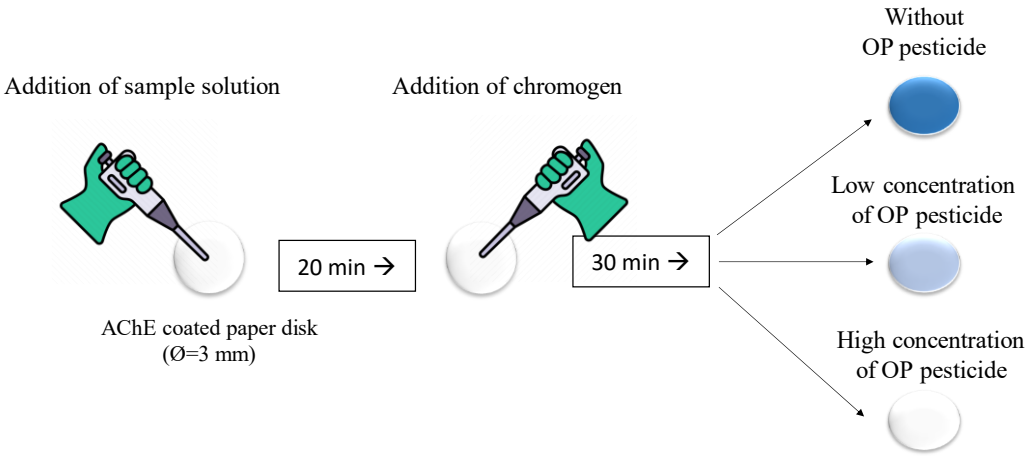

Figure 19. Conceptual design and mechanism of visual screening cards

3.8.2 Optimization for enhancement of pesticide inhibition

To help the enhancement of the inhibition of pesticides, various factors that could influence on it, including inhibition time, volume of pesticide added, concentration, methanol % (v/v) of the solvent used.

1) Inhibition time and volume pipetted → On each paper disk 10 µL (or 20 µL) of a relative high concentration of malathion (1 mM) were addicted. 5 inhibition time were tried (0, 5, 10, 15, 20, 30 and 40 min).

2) Methanol % (v/v) → On each paper disk 10 µL of malathion (1mM) prepared in Tris-HCl (10 mM, pH 7.4) in different % of methanol from 10% to 90% were tried.

Following the respective inhibition times, 20 µL of IDA (6.6 mM) was added.

3.8.3 Multiple visual screening cards validation test with pesticides

To investigate the inhibition of enzyme activity by pesticides, a study was conducted under optimized conditions using multiple visual screening cards. To assess the effectiveness of these cards in detecting the inhibition of enzyme activity, standard commercial products of malathion, dichlorvos, and chlorpyrifos were measured as representative species of OP pesticides. For the purposes of comparison with previous studies, the same concentrations (0-45 mM for dichlorvors[215] , 0-265 µM for chlorpyrifos [215] and 0-100µM for malathion[202]) of these pesticides were used as in other studies that employed more sophisticated instruments. To determine the limit of detection (LOD) for each pesticide, the concentration of the pesticide that inhibits 50% of the activity of the enzyme acetylcholinesterase (AChE), which is called the IC_{50} concentration, was measured. The IC_{50} value is commonly used to assess the potency of an inhibitor and compare the effectiveness of different pesticides. By measuring the IC_{50} concentration for each pesticide, it is possible to assess the potency of each pesticide and compare their inhibitory effects on AChE activity. The IC_{50} values (50% inhibition) were calculated by fitting the dose response curves to the Hill equation, using a modified MATLAB function[1].

3.9 Design of the µPADs

The paper-based visual screening card enzyme developed was integrated in a microfluidic platform for fully reagentless operation. The design and schematic fabrication procedure for the primitive µPAD (**Device I**) are shown in Figure 20. **Device I** is composed of two reagent-coated paper disks separated by an unmodified paper microfluidics channel for liquid flow. Microfluidic pattern or disks were designed, cut and assembled manually. The disk on the right was the

[1] View Appendix A and Appendix B

visual screening card tested (*chapter 3.6*). To form the right disk, 20 µL of IDA working solution were pipetted and left to dry for 15 min.

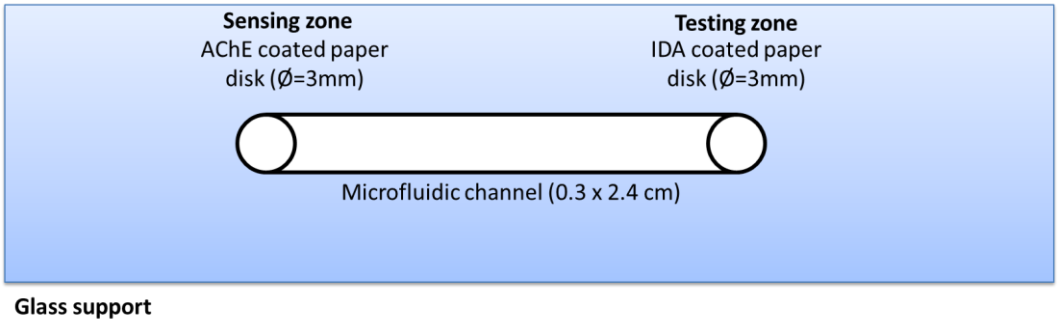

Figure 20. Schematic illustration of a **Device I** developed showing the arrangement and layout of paper disks with integrated buffer components for reagentless operation and microfluidic channel.

A second type of µPAD (**Device II**) was created using a process described in Figure 21. In contrast to **Device I,** the paper disks and channel were attached to the supports. Each µPAD had seven channels and corresponding disks. The process involved cutting reagent-coated paper disks and a microfluidic channel into individual strips, and then stacking them together using three different layers of double-sided adhesive tape, each designed for a specific purpose. The 1st one is the top layer and had 14 small wells (Ø=1.5 mm) to allow liquid to enter the device. The 2nd layer had 14 larger wells (Ø=3 mm) to hold the paper disks in place. The 3rd layer had 7 rectangular wells (0.5 x 2.5 cm) and was attached to a glass support. Paper disks were placed between the first and second layers, and flow channels were located between the second and third layers.

For both Devices, IDA coated paper disks and flow channel the membrane used was Whatman #4, while AChE coated paper the membrane used was Nylon Membrane.

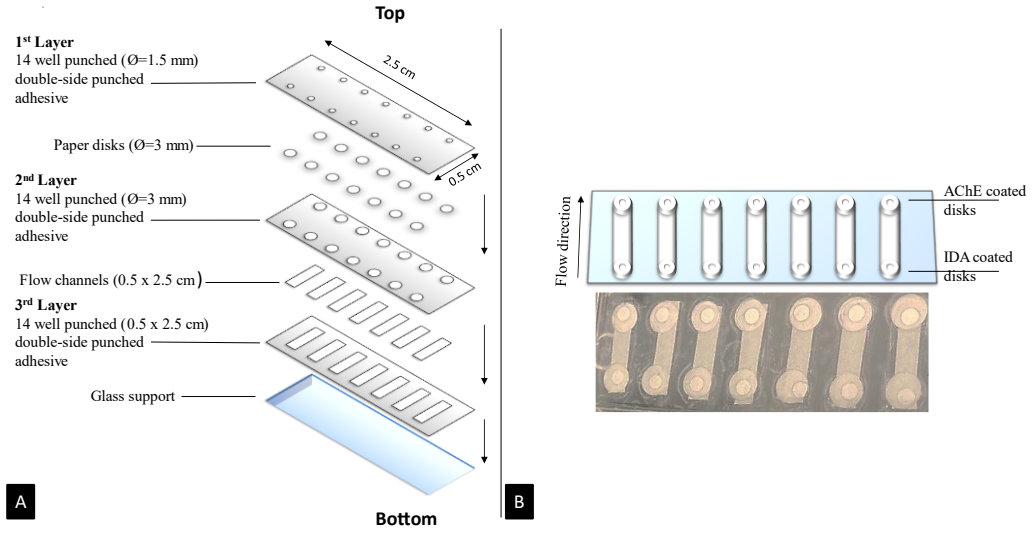

Figure 21. A) Schematic illustration of Device II showing the arrangement and layout of individual paper layers made of double-sided tape and paper disks with integrated buffer components for reagentless operation B) Virtual and real top view of Device II

In general, both Device I and Device II are based on the principle showed in Figure 22. To perform the assay, the first step involves adding a small amount of the sample solution, precisely 10 µL, into the well of the AChE coated disk. This is then followed by an incubation period of 20 min, which is considered the optimal time for the enzyme to be inhibited in case the pesticide is present in the solution. Once this step is complete, 10 µL of buffer solution is added to the IDA well, which helps to facilitate the movement of the chromogen to the sensing zone on the ACHE coated disk.

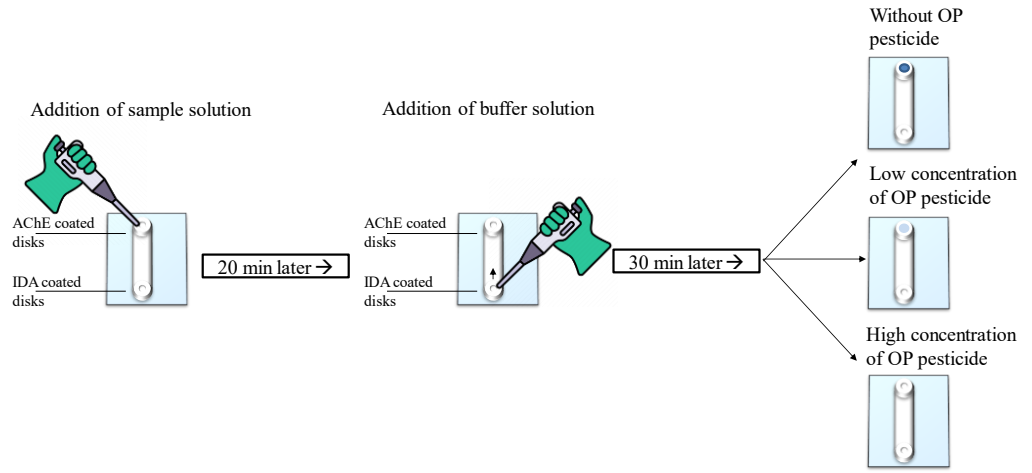

Figure 22. Illustration of the working mechanism of the µPADs created. Sample solution is pipetted on AChE coated disk. After 20 min, buffer solution is pipetted on IDA well.

The liquid addicted flows through the channel and reaches the AChE. Results are analysed after 30 min.

3.10 Optimizations of µPADs

Initially, Device I was used to conduct several experiments on the material and methods. The aim was to determine the effects of indoxyl acetate deposition on a paper disk. As a reference, a control was established by placing two reagent-coated paper disks in direct contact, without being separated by the channel. The first experiment investigated the ideal drying mode by pipetting 20 µL of indoxyl acetate onto the paper disks, which were then left to dry for 15 or 60 min at 35°C. The second experiment aimed to select the best material between Whatman #1, Whatman #4, and Nylon Membrane. The objective was to determine which material facilitated the most efficient transfer of chromogen from the paper disk to the enzyme site.

3.11 Test and validation of µPADs

Device II was tested. 10 µL of pesticides with 1µM and 1mM were dropped on each test and left to dry for 20 min. After that, 20µL of IDA were addicted. On each µPADs there were also a control where no pesticide was addicted.

Chapter 4: Results and Discussion

4.1 Spectrometer calibration

The acquired and analysed data of the first experiments taken to check if the spectrometer was calibrated were not consistent with what was expected in theory, it was assumed that the cause of this was due to poor pipetting skills on the part of the user. After various experiments and research to improve the performance required to achieve good pipetting accuracy, the results improved considerably. At this point, it was possible to assess the correct performance of the tool used, always assuming that a percentage of the errors were still due to the user[217]. In Figure 23 is shown the graph representing the reprocessing of the last experiment conducted with the aim of verifying the performance of the instrument used.

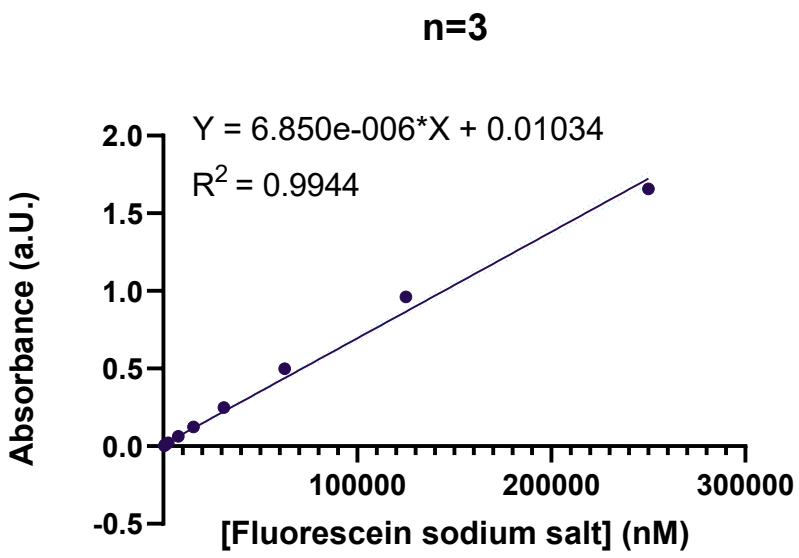

Figure 23. Fluorescence absorbance values (on the chordates) as a function of different concentration values (on the abscissae) ranging from 0 to 200 µM. The absorbance values are the result of the average of three equal concentrations and were backed by blank controls. The dashed line is the actual line passing through the various points obtained, without interpolation.

By Beer-Lambert law, absorbance must be proportional to concentration, according to the equation (3):

$$A = \varepsilon bc \qquad (3)$$

where ε is the molar absorption coefficient of the particular type of matter in the water sample, b is the optical path length of the water sample, and c is the concentration of matter in the water sample[218]. Hence, the graph representing the direct proportionality relationship between absorbance and concentration is a straight line. The reading of the graph representing the results is therefore a simple and fast way to have an overall view of the quality of the results achieved. Although in the Figure 23 the real curve and the curve obtained by linear interpolation do not coincide perfectly, the parameters expressing coefficient of determination R^2, which summarises in a single value how far the analysed quantity deviates on average from this line, is 0.9944 and standard error of the estimate $S_{y.z}$ is 0,03229. Since R^2 can take values ranging from 0 to 1, where 0 represents the total smoothness of the two lines and one the maximum correlation, and $S_{y.x}$ should have low values, with these values of the two parameters expressing the goodness-of-fit, it is possible to conclude that the correct functioning of the instrument is verified.

The results obtained in deciding which of the 3 different absorbance wavelengths in the literature (605, 620 and 650 nm)[134,214,215] should be used to analyse indoxyl acetate showed no significant differences (Figure 24). The wavelength of 650 nm was chosen for the subsequent analyses because the curve obtained for different concentrations of IDA, was the one with the steepest slope (confirmed quantitatively by the slope coefficient of the curve) and therefore with increasing absorbance values at the different concentrations.

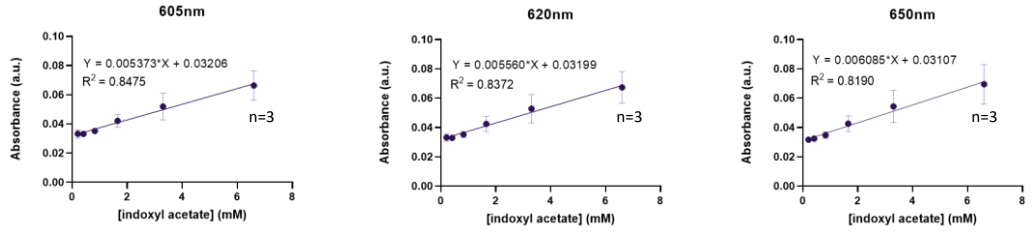

Figure 24. Comparison of the results obtained with different absorbance wavelength (605, 620, 650 nm). Concentration tested: 6.6, 3.3, 1.65, 0.82, 0.41, 0,21 mM. Results after 20 min from the change of pH from 7 to 10. All points are means ± s.d. of n=3 independent measurements for each concentration.

On the other hand, in order to understand which was the best volume to place in the 96-well plate, among the three volumes tested (50, 75 and 100 µL), the best curve obtained was the one in the case of 100 (Figure 25). It had the largest R-Squared value, so it was the most linear, and furthermore the absorbance values obtained were greater. In both cases, therefore, values of absorbance or volume were obtained which were high enough to be analysed.

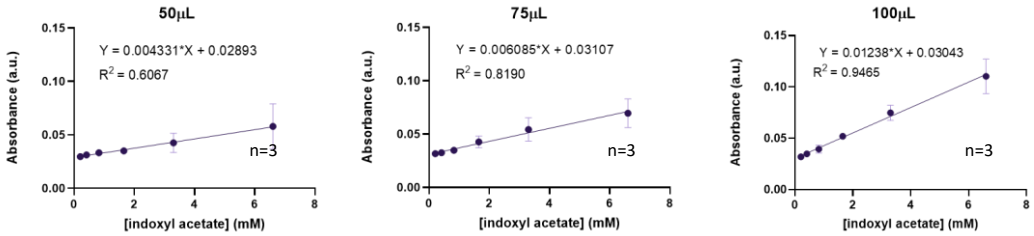

Figure 25. Comparison of the results obtained with different volumes in the 96-well plate. Concentration tested included 6.6, 3.3, 1.65, 0.825, 0.412 and 0.206 mM. Results after 20 min from the change of pH from 7 to 10. All points are means ± s.d. of n=3 independent measurements for each concentration.

Since in these two experiments, the curve in the range between 0 and 1 mM, was not linear, the LOD was calculated to determine the lowest concentration that the instrument could distinguish (Figure 26).

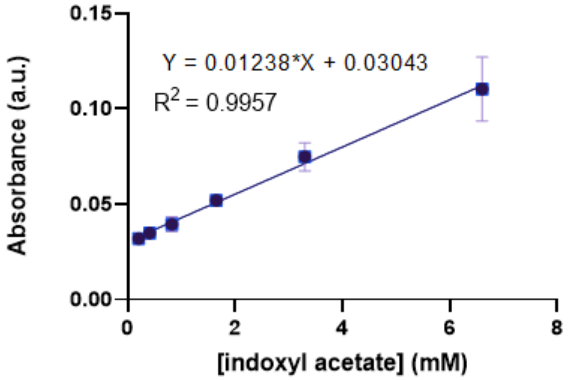

Figure 26. Curve obtained to calculate LOD. Concentration tested: 6.6, 3.3, 1.65. 0.825, 0.412, 0.206 mM. Results after 20 min from the change of pH from 7 to 10. All points are means ± s.d. of n=3 independent measurements for each concentration.

For the calculation of the LOD, the excel data analysis tool was used to extract the value of S.D. intercept and the value of Slope. Finally, through equation (2) the LOD has been calculated and resulted to be 0.88 mM.

4.2 Characterization and optimization of the chromogen

The study of the effects and control of certain external factors, such as temperature and pH, which can affect reactions between acetylcholinesterase and its inhibitors or the substrate chromogen, are important for the device to be developed and used correctly. According to studies on the influence of temperature on AChE activity, optimal temperatures range from 4° to 37° degrees[219–222]. Furthermore, the activity of AChE is also influenced by the pH dependence of the enzyme, with an optimum at pH above 7, whereas at pH values below 6 particularly the specific acetylcholinesterase is more or less inactive[223]. This chromogen was chosen because studies on visual acuity revealed that human visual cells are particularly sensitive to wavelengths that vary close to the blue-green spectrum[224]. Furthermore, it has been demonstrated that the indoxyl acetate is a good chromogenic substrate of AChE for the determination of the activity of the enzyme.[225] Indoxyl acetate was a useful chromogenic substrate of AChE for determining the activity of the enzyme, according to Villatte *et al.*[225] because they obstruct the enzyme's active site. The hydrolysis of the colorless (lavender) IDA can be catalyzed by AChE to produce hydroxyindole (indoxyl) and acetic acid in the presence of AChE. The hydroxyyindole is then quickly oxidized into the blue-green colored indogo dipolymer, as shown in the Figure 27.

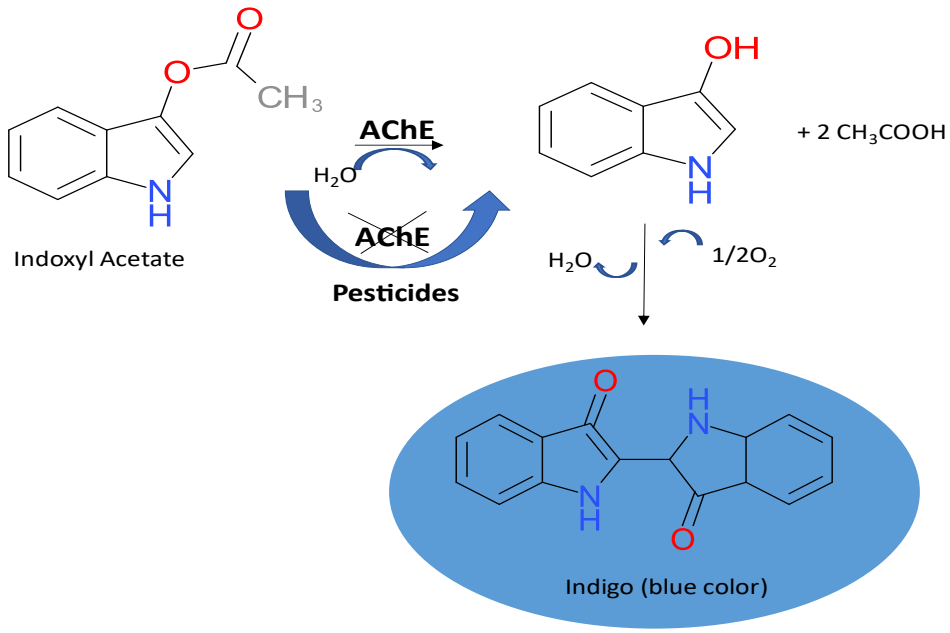

Figure 27. The hydrolysis mechanism of indoxyl acetate catalyzed by AChE

4.2.1 pH control

One of the factors that must be kept under control for the correct use of coloured substances used to detect the presence of the enzyme is the pH of the solution in which they are immersed. The colour change must only be related to the inhibition of the enzyme being controlled. The substances used in the absence of the enzyme must in fact be colourless substances, so it was checked whether and for what pH values they change colour. The pH values tested ranged from 3 to 12. Through this test, it was possible to verify that for values of pH above 10, the solution changed colour about 5 minutes after the pH change, as shown in Figure 28. From this experiment, knowing that optimal pH values for enzyme activity are around 7 and not below 6, it was deduced that the values of the solutions used to process enzyme and chromogen should be in the pH range of 6 to 9 to be sure of colour changes due only to the interaction between the reagents.

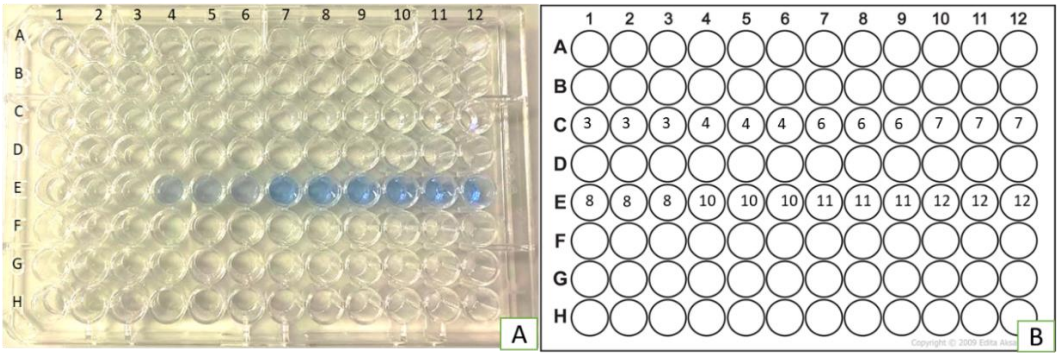

Figure 28. Pictures of the 96 well plate used to check the reaction and the stability of indoxyl acetate with different pH conditions. In the plates of the rows C10, C11, C12 there are 100µL of indoxyl diluted into Tris-HCl (pH 7.4). Every solution with the same pH has been released three times to make and average of the measurements taken. A) the photo was taken about 10 minutes after the pH of the main solution was changed B) reference image, in each plate in rows C and E the pH value of the various solutions in the 96-well plate present in images A and B is indicated.

The results (Figure 29) obtained by measuring the absorbance spectrum confirm what was expected through an initial qualitative analysis namely that for basic pH values, absorbance peaks around 670nm, that is near the wavelength used for measure IDA absorbance (605~650 nm).

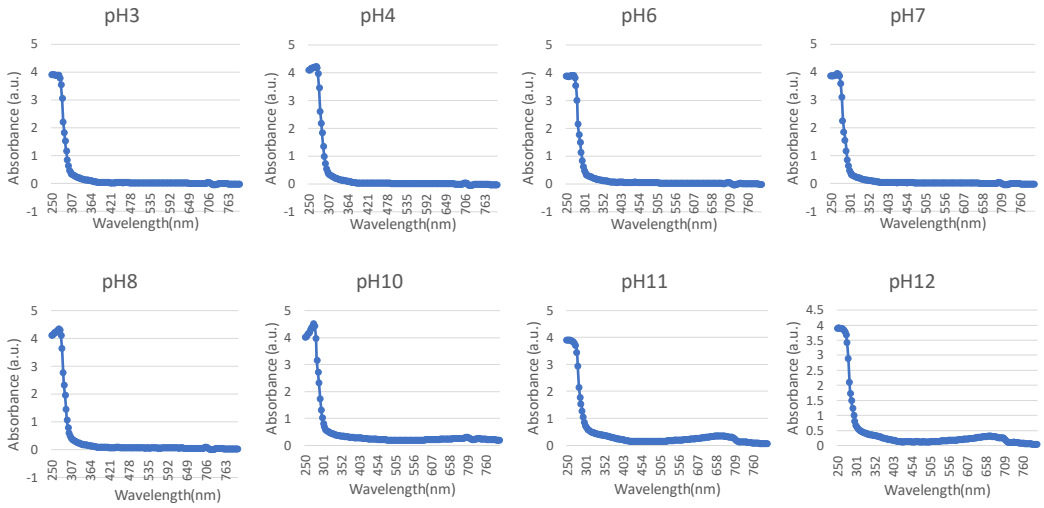

Figure 29. Absorbance Spectrum of indoxyl acetate (10mM) diluted in solution of Tris-HCl (20mM) for different pH. The different pH values below seven were obtained by adding different volumes of HCl. Values with a pH above seven, on the other hand, were obtained by adding NaOH. It can be verified that for pH values above 10, a more pronounced peak is present in the wavelength range from 605 to 706 nm than for pH values below 10. All points are means ± s.d. of n=3 independent measurements for each concentration measured 10 min after the pH adjustment.

4.2.2 External temperature influence on reaction

The results obtained for the three different temperatures (-4°, 24° ,37°) that determine a change in AChE activity, were very similar this means that chromogen does not significantly compromise the results for reaction at these three different temperatures (Figure 30). This confirm the fact that the final device can be used at room temperature.

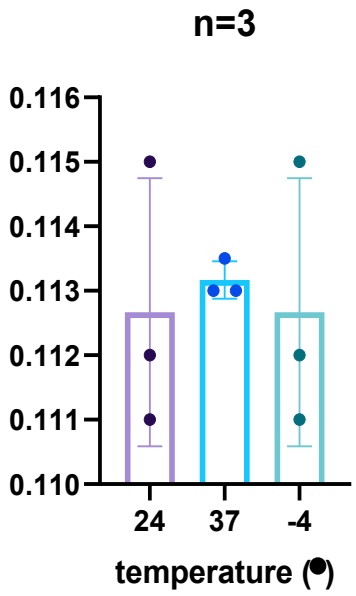

Figure 30. Comparison of the values of absorbance obtained for the hydrolysis of the chromogen IDA (16.6 mM) at different temperatures. Absorbance was measured after 20min. All points are means ± s.d. of n=3 independent measurements for each concentration.

After gaining information about the nature of the chromogen in relation to external agents, so that we know how to have reactions with the enzyme that are only due to their interaction, we move on to analysing the use of the chromogen with the enzyme.

4.2.3 Time of reaction of the hydrolysis mechanism

In order to be able to reliably quantify through absorbance measurement the amount of indoxyl produced as a result of the reaction between the enzyme and its substrate, the range of values the absorbance maintains was checked. From the graph in (Figure 31), it can be seen that from min 20 to min 40, the absorbance values are approximately constant. For this reason, the results were always evaluated at least 20 min after the substrate and enzyme came into contact.

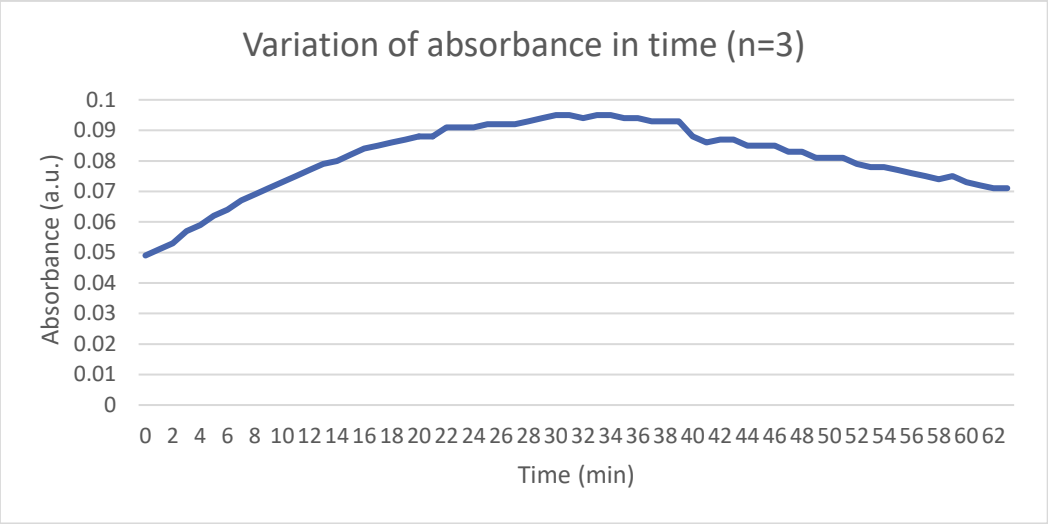

Figure 31. Measurement of the change of absorbance during the hydrolysis mechanism of IDA. Immediately after depositing 20 µL of AChE (800 U/mL) in the well containing 80 µL of 10 mM of indoxyl acetate in methanol, the value of absorbance were taking every 30 s for 60 min. All points are means ± s.d. of n=3 independent measurements for each concentration.

4.2.4 Results of the optimization of solutions for the assays using 96-well plate

The use of methanol, according to sources found in the literature, inhibits the activity of the enzyme[226]. At the same time, it has been used for in various colorimetric biosensors for the detection of organophosphate pesticides as they not only promote the dissolution of AChE inhibitors but also amplify the binding activity of the enzyme. For this reason, the difference in the colour change values of the reaction obtained with and without methanol for different concentrations of AChE was tested. The red and green in Figure 32 represent the data obtained when the chromogen was dissolved in methanol at a concentration of 90% (v/v) or less, respectively.

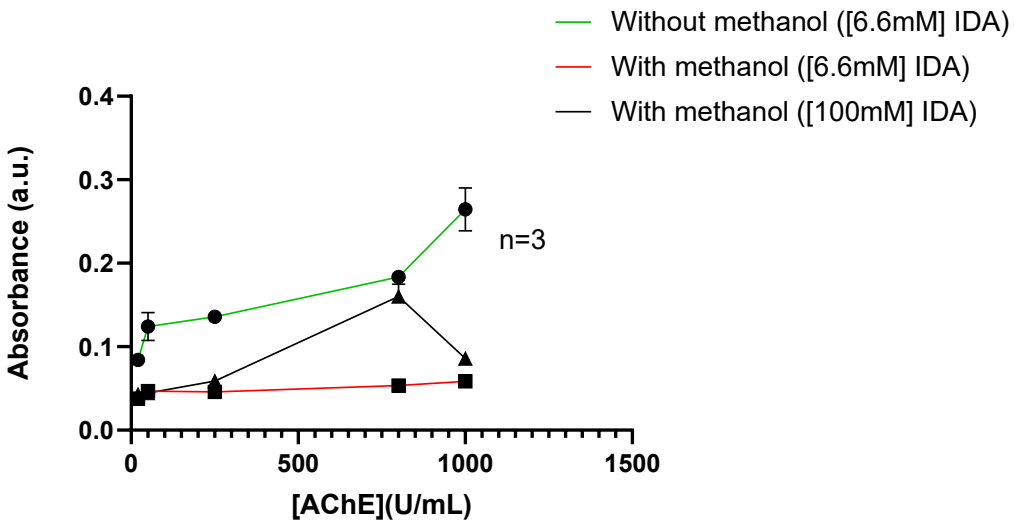

Figure 32. Comparison between the change color obtained using different percentage of methanol in the solvent made of Tris-HCl (20 mM, pH 7.4). Red line and green line indicate results using chromogen solutions with final IDA concentration of 6.6 mM, with 90% and 0% of methanol respectively. Black line indicates the values of color change obtained using higher concentration of IDA (100 mM) dissolved in Tris-HCl with 90% (v/v) of methanol. Volume of IDA addicted (80 µL) was 4 time the volume of AChE solution pipette. Absorbance was measured after 20 min. All points are means ± s.d. of n=3 independent measurements for each concentration. All points are means ± s.d. of n=3 independent measurements for each concentration.

From this comparison, it was possible to deduce that methanol does indeed reduce the activity of the enzyme (the green curve stays below the red). For this reason, the experiment with methanol was repeated using a higher IDA concentration (black curve Figure 32). In order not to reduce the activity of the enzyme too much, however, a methanol concentration of 5% was preferred. By using Tris-HCl with 5% (v/v) methanol as the chromogen solvent, the results obtained were satisfactory (Figure 33). In the graph on the left, the colour change for different concentrations of AChE for IDA values of 10mM is shown. From these results, it was possible to deduce that from 250 U/mL color change is visible at naked eyes and that the ideal minimum concentration of AChE should be 500 U/mL. Subsequently, different concentrations of IDA were tested to find which was the optimal minimum at the chosen AChE value. From concentrations of 1.65 mM color change was is visible, but 6.6 mM is a chromogen concentration that results in a good compromise both qualitatively (visible) and quantitatively.

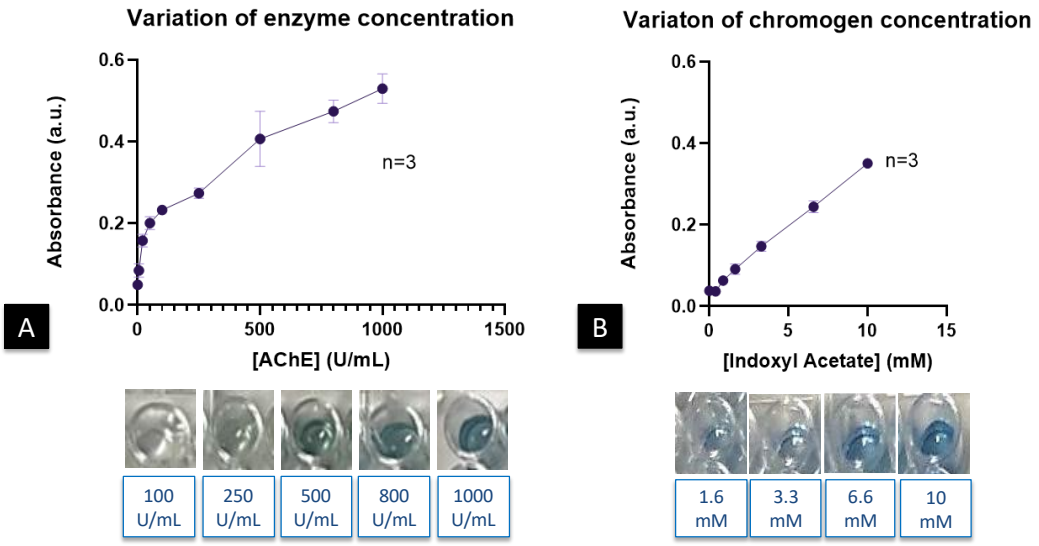

Figure 33. (A) Optimization of AChE concentration. For IDA concentration of 10mM, different concentrations of AChE diluted in DBPS were tried (1,000, 800, 500, 250, 100, 50, 20, 5, 0 U/mL). (B) Optimization of IDA concentration diluted in Tris-HCl with 5% (v/v) methanol (10, 6.6, 3.3, 1.65, 0.875, 0.412, 0 mM), with the minimum ideal concentration of AChE (500 U/mL). (A,B) Volume of IDA addicted (80 µL) was 4 time the volume of AChE solution pipette (20µL). Results after 30 min the addiction of the chromogen. The photos below the graphs, taken after 30 min the addiction of the chromogen, show results corresponding to the concentrations (only the most representative ones, to have an indicative reference). All points are means ± s.d. of n=3 independent measurements for each concentration.

4.3 Optimization of the visual screening cards

4.3.1 Comparison between various immobilization conditions and optimization

The most popular method among the various ones used in literature is cross-linking, whereas physical adsorption is the one that is simplest to use. Furthermore, studies sponsored by Guo *et al.*[215], which were crucial for the overall development of these test cards, have demonstrated certain advantages of using bi-functional cross-linkers such glutaraldehyde (GA) and BSA as protein stabilisers. Because of its chemically active characteristics, GA would not only react with the amino groups of the enzyme molecules to form the cross-linked structure but would also oxidise the nitrogen compounds on the neutral nylon membrane surface into a polymerized substance, changing the background colour from white to yellow. The BSA adsorbed on the membrane surface was thought to have been easily extracted, leading to the white crystalline particles. Therefore,

physical adsorption was chosen for this project in order to have a consistent colour development in addition to reducing the time and complexity of device construction. Enzyme activity was significantly impacted by the environment. The results for ideal immobilisation determined by experimenting with enzyme solution (volume and concentration), immobilization temperature and drying mode. The data obtained by immobilising 5 different volumes on a support are shown in Figure 34, where it is evident both visually and semi-quantitatively that the best volume is 5 µL when the volume is extended throughout the entire surface.

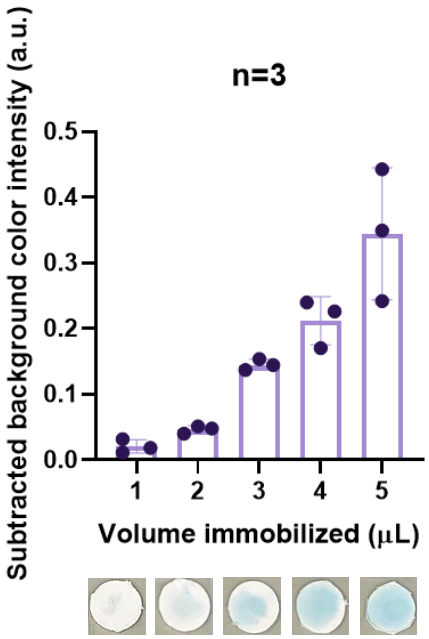

Figure 34. Differences of the volume of the enzyme used to immobilize it. The paper disks with diameter of 6 mm. AChE 1000 U/mL indoxyl acetate 10mM (highest and highest). Volume of IDA addicted was 4 time the volume of AChE solution pipette. Photos taken after 20 min. All points are means ± s.d. of n=3 independent measurements for each concentration.

In order to immobilise the enzyme, based on those already established and documented in literature, four different temperatures were tested using two different drying modes (DM) (Figure 35). In general, it is possible to see that the method that leads to the best results is immobilising the enzyme at a temperature of 4° for 30 min and laying it out for at least 2 hours at the same temperature.

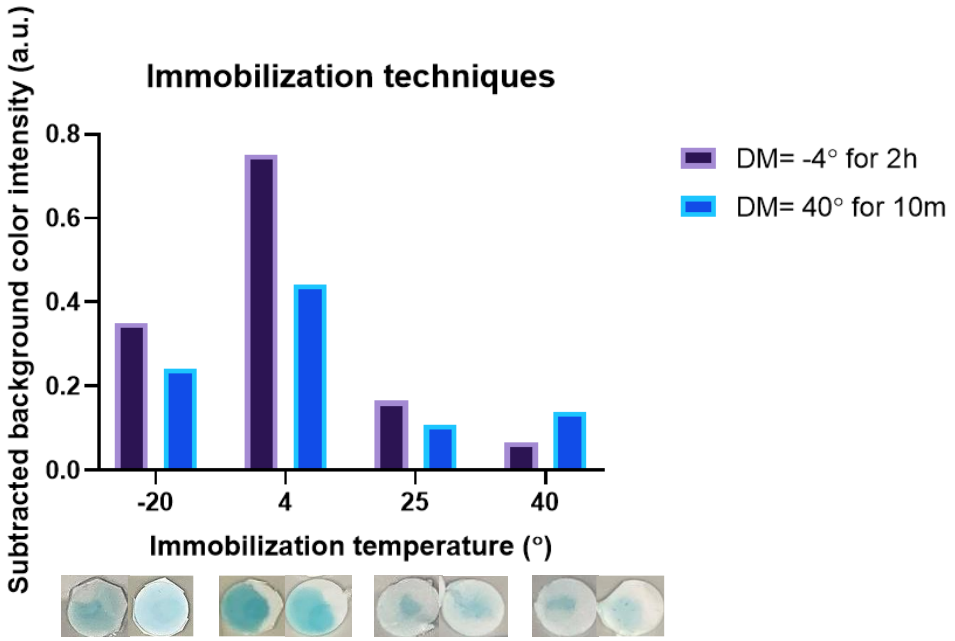

Figure 35. Immobilization techniques. In the graph are shown the different color intensity for different temperature used for immobilizing the enzyme for 30 min. The paper disks with diameter of 8 mm. Violet and blue columns represents the data obtained for the two different drying mode (DM) tried. AChE 1000 U/mL indoxyl acetate 10mM (highest and highest). Volume of IDA (20 µL) addicted was 4 time the volume of AChE solution pipetted (5 µl). Photos taken after 20 min. All points are means ± s.d. of n=3 independent measurements for each concentration.

This drying mode's disadvantage is an excessive time expense. The drying mode that allows for a good compromise between drying time cost and performance quality may be the one that calls for a 2-min vacuum. as demonstrated by results by Guo *et al.* [215]. Without a suitable instrument to produce the vacuum, it was tried to reduce the drying time to 4° from 2 h to 1 h. The findings have demonstrated that drying times at this temperature cannot be reduced.

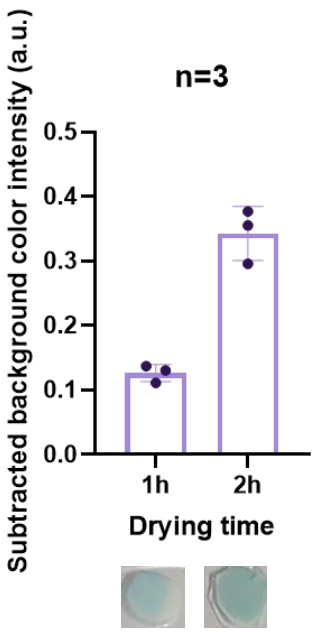

Figure 36. Drying mode optimization. The paper disks with diameter of 6 mm were dried at 4° for different time. AChE 1000 U/mL indoxyl acetate 10mM (highest and highest). Volume of IDA addicted (20 µL) was 4 time the volume of AChE solution pipetted . Photos taken after 20 min. All points are means ± s.d. of n=3 independent measurements for each concentration**.**

In order to optimise the quality and quantity of immobilised enzyme on paper, the efficiency and usefulness of using a blocking and washing solution after immobilising the chosen enzyme (30 min at 4°), before drying the enzyme (2h at 4°), was evaluated. The graph and pictures in the Figure 37 show that there are no advantages but disadvantages in using this intermediate step. The reason why it was tried is because the results obtained by Apilux *et al.*[227] showed that it improved optimisation. Probably the reason why the desired results were not obtained in this case is that the solutions were created with similar solvents and reagents for the function but different ones.

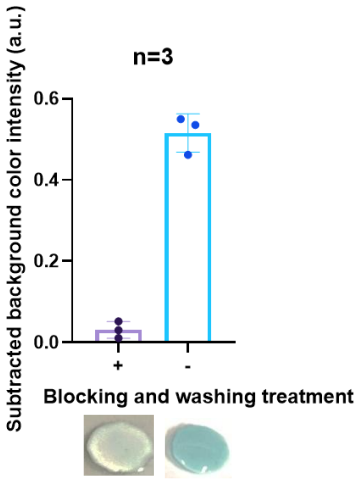

Figure 37. Treatment with/without blocking and washing solution. The paper disks with diameter of 6 mm were with AChE 1000 U/mL and IDA 10 mM deposited. Volume of IDA (20 µL) added was 4 time the volume of AChE solution pipetted (5 µL). Photos taken after 20 min. All points are means ± s.d. of n=3 independent measurements for each concentration.

4.3.2 Estimated enzyme immobilized on the paper support

A stable biocatalyst produced via immobilisation should have the fewest structural and functional distortions possible. There are, however, few instances when enzyme activity is unaffected or even enhanced by immobilisation[228], and many cases where it does. In every instance, it is crucial to assess the enzyme's activity upon immobilisation and to establish the precise quantity of active sites that are still present. The absence of precise spectroscopic tests due to the presence of solid support is one of the main issues encountered while analysing the activity of immobilised enzymes. Since the enzyme is mounted on a solid surface and consequently unavailable to traditional biochemical procedures, that in this case is the spectrometer, determining active site concentrations is another frequent issue. The enzyme content of the solution before and after immobilisation has historically been used to estimate the amount of immobilised enzyme on the support [229–231]. *Chapter 3.7.2*, details the method I used to calculate this quantity approximately. The graph in Figure 38A shows results obtained applying this method. The blue line fits absorbance values measured in a solution with a free enzyme for increasing IDA concentrations while the black line the absorbance

values of the solution where there was the paper with immobilized enzyme for the same IDA concentration.

The results obtained by applying formula (2) and shown in Figure 38B indicate a direct correlation between the amount of immobilised enzyme measurable and the amount of chromogen used. However, this method has a drawback: it only confirms that the enzyme was immobilised because the absorbance values depend on indoxyl acetate molecules bound to the enzyme. Consequently, determining the real active site concentration using this indirect method is unlikely.

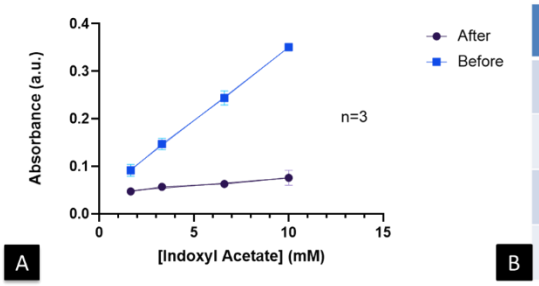

B

IDA concentration (mM)	EI(%)
10	78.327
6.6	74.180
3.3	61.224
1.65	48.540

Figure 38. Comparison of free and immobilised enzyme A) The graph shows the absorbance values of 100µL solutions (80 µL of AChE [500 U/mL] and 20 µL of indoxyl acetate (from 1.65 to 10 mM) in a 96-well plate. The blue curve represents the values of solutions containing free enzyme in the solution (blue curve, before immobilisation). The black curve represents the solutions in which the enzyme media had been immersed (following immobilisation). B) The table represents the correlation between the chromogen concentration (IDA) and the EI% calculated. Each measurement was repeated 3 times independently.

As a result, an assay is necessary to establish the concentration of the immobilised active sites or, better yet, the total number of active sites on the support.

4.3.3 Comparison of quantitative, semi-quantitative, and qualitative data

The study compared quantitative measurements obtained with a spectrometer to semi-qualitative and quantitative measurements using ImageJ. The change in color resulting from the reaction of chromogen with free enzyme was clearly discernible and visible for enzyme concentrations between 250 and 800 U/mL and for chromogen concentrations between 1.66 and 6.6 mM, as discussed in *chapter 4.2.4* (see Figure 39 (A-B)). These concentrations were selected to test the color change on paper disks, and the results were reliable, as the trend of color intensity values in relation to enzyme or chromogen concentrations matched the expected

values. However, there was a difference in the quality of the two measurement methods. In the quantitative case, the absorbance value for 500 U/mL AChE (Figure 39A) was similar to the value assumed for 10 mM IDA (Figure 39B) . This was expected since both measurements were taken in a solution containing 500 U/mL AChE and 10 mM IDA. In contrast, in the semi-quantitative case (Figure 40 (A-B)), the values were not comparable, and this difference was also noticeable visually. Therefore, it was concluded that the problem was due to the amount of enzyme immobilized on the medium.

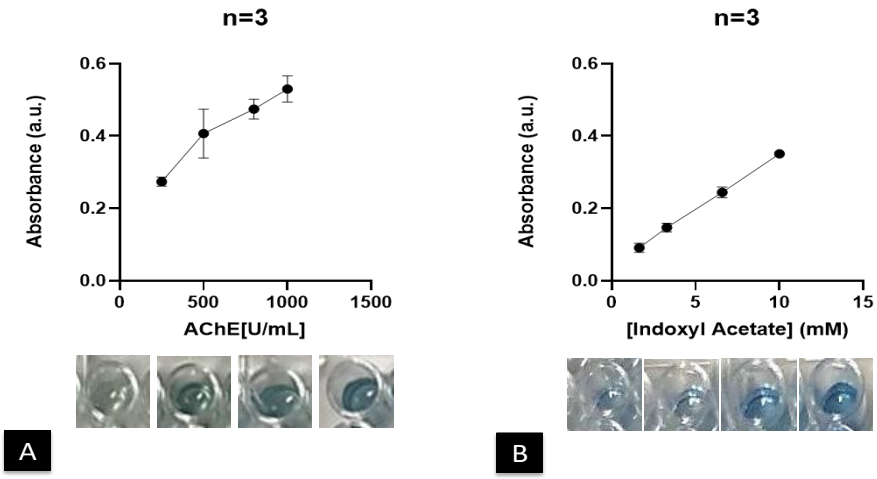

Figure 39. (A) Result of absorbance measured with spectrometer of 96-well plates containing 80 µL of different AChE concentration diluted with DPBS (1000 800 500 250 U/mL) and 20 µL of IDA. (B) IDA concentration diluted in Tris-HCl with 5% (v/v) methanol (10 6.6 3.3 1.65 mM), with the minimum ideal concentration of AChE (500 U/mL) immobilized on paper. Volume of IDA addicted (20 µL) was 4 time the volume of AChE immobilized on paper (5 µL). The pictures below the graph were taken and analyzed after 30 min the addiction of chromogen All points are means ± s.d. of n=3 independent measurements for each concentration.

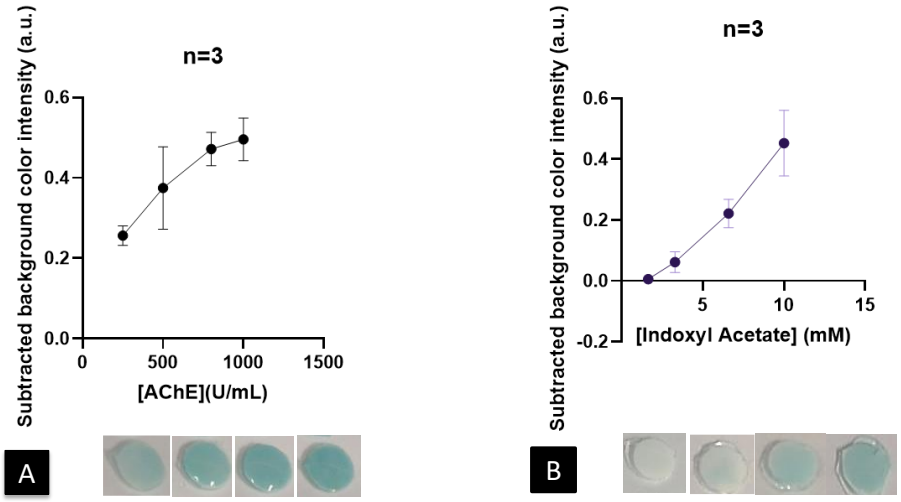

Figure 40. (A) Different AChE concentration diluted with DPBS (1000 800 500 250 U/mL) immobilized on paper, 20 µL of IDA [10 mM] were pipetted. (B) IDA concentration diluted in Tris-HCl with 5% (v/v) methanol (10 6.6 3.3 1.65 mM), with the minimum ideal concentration of AChE (500 U/mL) immobilized on paper. Volume of IDA addicted (20 µL) was 4 time the volume of AChE immobilized on paper (5 µL). The pictures below the graph were taken and analyzed after 30 min the addiction of chromogen. All point s are means ± s.d. of n=3 independent measurements for each concentration.

In any case, again, AChE values of 500 U/mL and indoxyl acetate 6.6 mM seem to be a good compromise for sufficiently intense colour with minimal quantities. These enzyme and chromogen values are those used for the next experiments.

4.4 Test results of pesticide inhibition on paper-based assay

The initial test with pesticides aimed to determine if the color change correlated with the pesticide concentrations ranging from high (1 mM) to low (1 µM) in the solution. However, the findings were unsatisfactory as the paper assays (Figure 41) did not clearly indicate which paper disk was impounded with the highest malathion concentration, except for the last two higher concentrations (100 µL and 1 mM), which differences were distinguishable qualitatively and semi-quantitatively. To improve the test results, various parameters have been periodically changed, including the time of inhibition, concentrations, and the percentage of methanol used in the solvents for pesticide dilution.

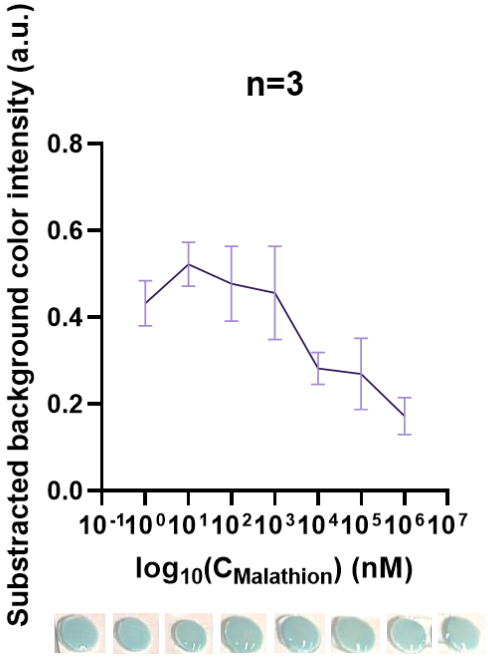

Figure 41. Dilution of 1:10 of malathion from 1 mM to 1 nM. Inhibition time: 20 min. Volume of IDA [6.6 mM] addicted (20 µL) was 4 time the volume of AChE [500 U/mL] immobilized on paper (5 µL). The pictures below the graph were taken and analyzed after 30 min the addiction of chromogen. All points are means ± s.d. of n=3 independent measurements for each concentration

To assess the effect of inhibition time on the results, a range of inhibition times (0 to 20 min) were tested for relatively high malathion concentrations (100 µM). However, the results were not very accurate, as increasing the inhibition time was expected to reduce the intensity of the color due to inhibition (as shown Figure 42). Several factors, including the accuracy of pipetting the pesticide and reagent, which depend on the operator, contributed to the lack of accuracy. The small area of the paper disk also posed a challenge, as adding the remaining 20 µL of chromogen too soon after depositing the first 10 µL of pesticide resulted in excess liquid accumulating outside the test area, as seen in the 10 and 20 min results. Therefore, it was determined that a minimum of 20 minutes should pass after depositing the first 10 µL of pesticide before adding the remaining 20 µL of chromogen to avoid this issue. To increase inhibition, longer inhibition times of 30 and 40 minutes were also tested. However, after 30 minutes, a drastic decrease in color intensity was observed. Although maximum inhibition was reached after 40 minutes, an optimal inhibition time of 30 minutes was chosen to provide a good compromise between efficiency and time cost.

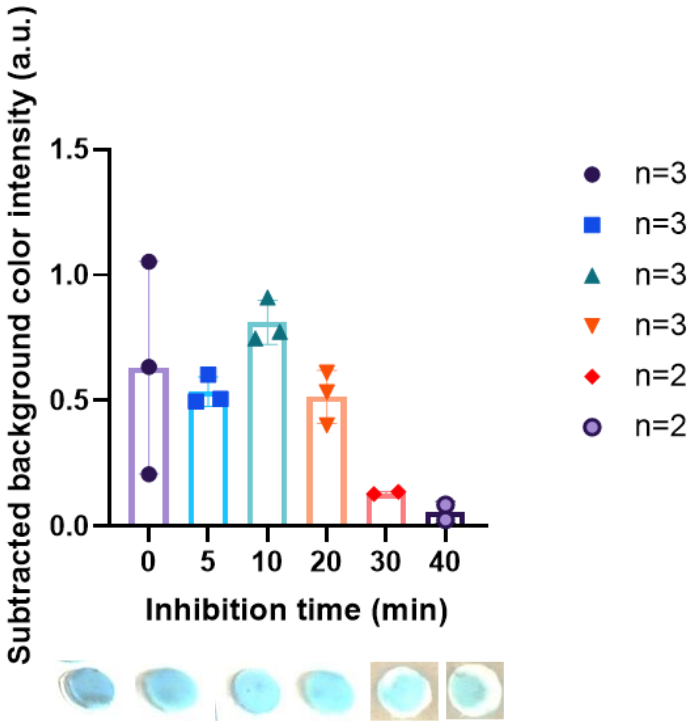

Figure 42. Different inhibition time for 100µM of malathion. Volume of IDA [6.6 mM] addicted (20 µL) was 4 time the volume of AChE [500 U/mL] immobilized on paper (5 µL). The pictures below the graph were taken and analyzed after more than 30 min the addiction of chromogen. All points are means ± s.d. of n=3 independent measurements for each concentration

At this point it was examined whether using sufficiently high inhibition time determined (30 min), the colour change was proportional to the pesticide concentration. In this case, higher concentration values of 20 mM and 1 mM were also tried to have more inhibition. The trend in the graph (Figure 43) confirms that with a min inhibition time the results appear to be better.

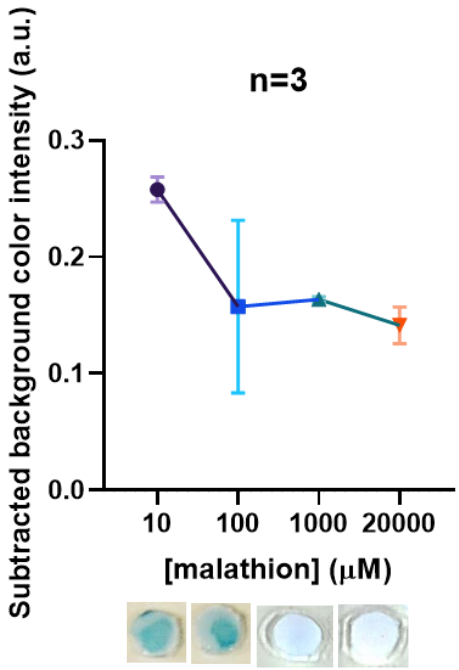

Figure 43. Different concentrations of 10 µL malathion (diluted in Tris-HCl with 5% (v/v) % methanol, inhibition time: 30 min. Volume of IDA [6.6 mM] addicted (20 µL) was 4 time the volume of AChE [500 U/mL] immobilized on paper (5 µL). The pictures below the graph were taken and analysed after 30 min the addiction of chromogen. All points are means ± s.d. of n=3 independent measurements for each concentration

Despite this, the concentrations for which there is a clear inhibition remain too high. According to the data in the literature[203], for values of 100 µM, the enzyme's activity should be completely inhibited, whereas in this case for values of 1000 µL (i.e. an order of magnitude more), the intensity of the colour shows that the reaction between the enzyme and the chromogen substrate still takes place. For this reason, solutions containing different percentages of methanol were tried to increase the binding affinity between the pesticide and the enzyme (Figure 44). For this reason, solutions containing different percentages of methanol were tried to increase the binding affinity between the pesticide and the enzyme. As the graph and the images correlated to the data point interpolated in the curve, the higher was the percentage of methanol, the higher the enzyme was inhibited. In order to ensure that the cause of the inhibition was the methanol and not the pesticide, a minimum effective amount of methanol to be used in pesticide solvents was chosen, namely 10%.

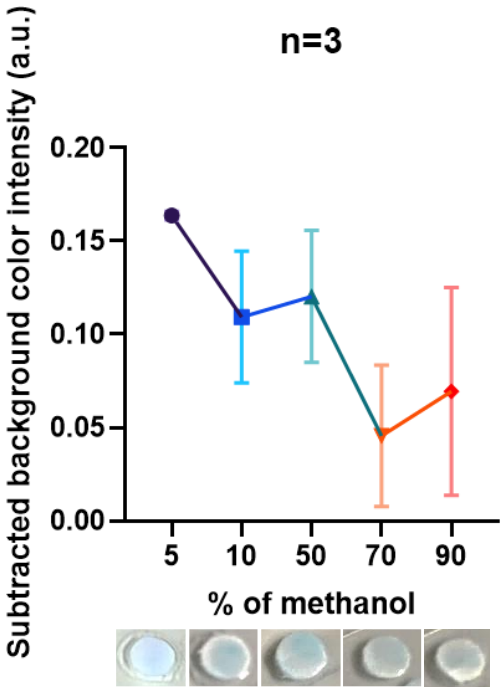

Figure 44. Different concentration of methanol in Tris-HCl (malathion solvent). 10 µL of malathion [1mM], inhibition time: 20 min. Volume of IDA [6.6 mM] addicted (20 µL) was 4 time the volume of AChE [500 U/mL] immobilized on paper (5 µL). The pictures below the graph were taken and analysed after 30 min the addiction of chromogen. All points are means ± s.d. of n=3 independent measurements for each concentration

4.4.1 Visual screen cards validation parameters

To ensure that the biosensor meets the requirements for its intended use, its performance characteristics were evaluated. The following are the key parameters that need to be evaluated during the validation process:

1. Stability: The stability of the biosensor is evaluated by testing the sensor's response over a period of time under various storage conditions. The stability test is important to ensure that the biosensor maintains its performance over time.
2. Linearity: The linearity of the biosensor refers to the relationship between the biosensor response and the concentration of the analyte being measured. Linearity testing is conducted to ensure that the biosensor responds proportionally to changes in analyte concentration. For this performance, various concentrations of the pesticides were tested on paper disks.

3. Precision: Precision refers to the reproducibility of the biosensor measurements. Precision testing is conducted by measuring the same sample multiple times to evaluate the variability in the measurements. In this case, measurements were repeated three times.
4. Detection limit: The detection limit of the biosensor refers to the lowest concentration of the analyte that can be detected with a specified level of confidence. Detection limit testing is conducted to determine the minimum detectable concentration of the analyte. In this thesis, it is determined by the IC_{50} (see *chapter 4.4.1 Visual screen cards validation parameters*)
5. Accuracy: Accuracy refers to the closeness of the measured value to the true value. Accuracy testing is conducted by comparing the biosensor measurements to a known reference value. The known reference in this case were results obtained for the same concentration of pesticides and the IC_{50} found in studies about AChE inhibition-based assays already in literature
6. Selectivity: Selectivity refers to the ability of the biosensor to detect only the target analyte and not interfere with other substances in the sample. Selectivity testing is conducted to ensure that the biosensor is specific to the target analyte.
7. Sensitivity: Sensitivity refers to the biosensor's ability to detect small changes in analyte concentration. Sensitivity testing is conducted to determine the biosensor's limit of detection and to optimize the biosensor's performance.
8. Robustness: Robustness refers to the ability of the biosensor to maintain its performance under varying experimental conditions. Robustness testing is conducted to ensure that the biosensor can withstand minor variations in experimental conditions without affecting its performance.

Paper disks with immobilized enzyme were stored at -20°C for more than two weeks without losing their functionality and work principle, this means that have a good stability.

To measure the performance of final multiple screen papers, optimized solution of chromogen, enzyme, and pesticides on paper disks were used. However, some

problems with the measurement method used for dichlorvos were found. The method involved measuring the average pixel intensity of the sensing area was not always accurate because pixel intensity of blanks (or completely inhibited) is not always the same. In the other cases, this method was successful and was proportional with the colour intensity visible to the naked eye, as there was never too low a colour intensity that was indistinguishable. This anomaly was confirmed by *Sicard et al.*[204]. This confirms that once again, the semi-quantitative method of measurement is not accurate as it is subject to the light to which the object in the photo is exposed. The reason of this variation can be also found in the batches of test disks, in fact the control without pesticide were not also the same. To address partially this issue, the method proposed by Sicard *et al*. [204]was tried. It consists in measuring the intensity for the three different RGB color channels. The pesticide images the pesticide images are split into separate RGB channels and the maximum color intensity of the sensing area on the red channel image is measured. This method proved to be more reliable than the previous method, as a measure of the maximal color intensity in the red channel, as a channel transition of blue to white is produced by an increase in the red and green channels. Correspondingly, as a pixel changes from blue to white, the red component increases. Therefore, a measure of the maximal color intensity in the red channel is a direct measure of the presence of dye. It was found that the green channel was less representative of the change in device-determined color intensity than the red channel. This is hypothesized to be due to the indigo having a higher green component than red component. Values obtained measuring pixel intensity with red RGB channel were compared to the mean of RGB channels, and the red RGB channel measurements showed better results (Figure 45). However, it's important to note that this method is also semi-quantitative and still does not solve the problems caused by light exposure and batches of the test disks. Moreover, the batches of test disks cause increase the inaccuracy, in fact the control without pesticide were not always the same.

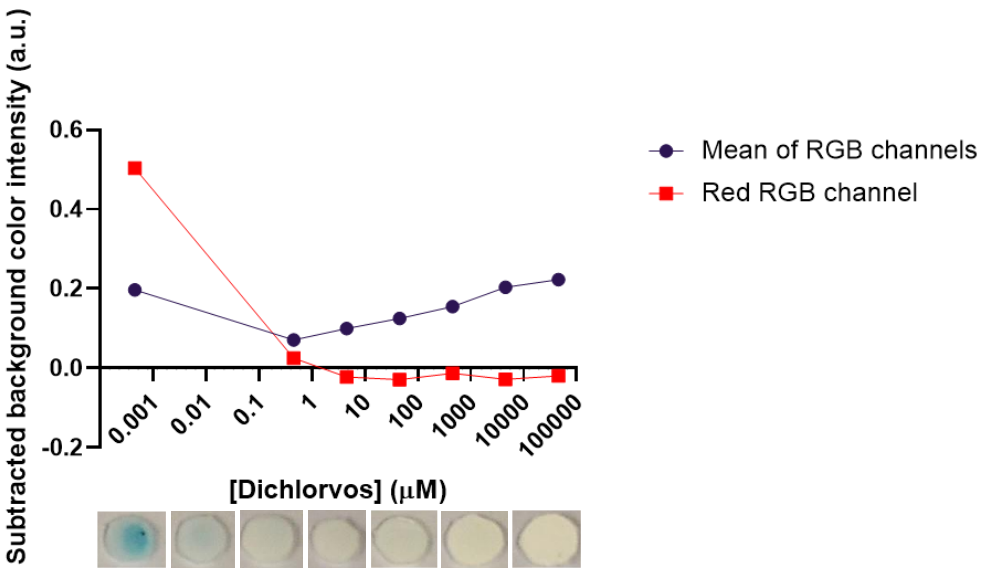

Figure 45. Differences between measure intensity from RED RGB channel vs measuring intensity as a mean of RGB channels (red, blue, green). Images and the graph are related to paper disks where 10 µL of dichlorvos in different concentrations were pipped. After 20 min, 20 µL of chromogen were addicted. Images were taken after 30 min from the addiction of chromogen.

The trend of the dose response curves obtained with the modified MATLAB function, were compared to the one obtained from the studies used as referment [202,215] for the thesis is shown in Figure 46. It is possible to see that the three curves obtained with three pesticides are not comparable with the ideal one, excepting for the one of dichlorvos that is the more similar. This means that the accuracy of the screening test cards card is very low. Moreover, the trend highlights the low linearity and sensitivity of the screening test cards. One of main reasons that caused these low performance parameters is for sure due the poor precision and robustness of these optical biosensors. In many cases, measurements repeated three times independently give different results (Figure 47). The images show that the color is not consistent throughout the sensing region, which can result in increased errors for analysis tools such as ImageJ.

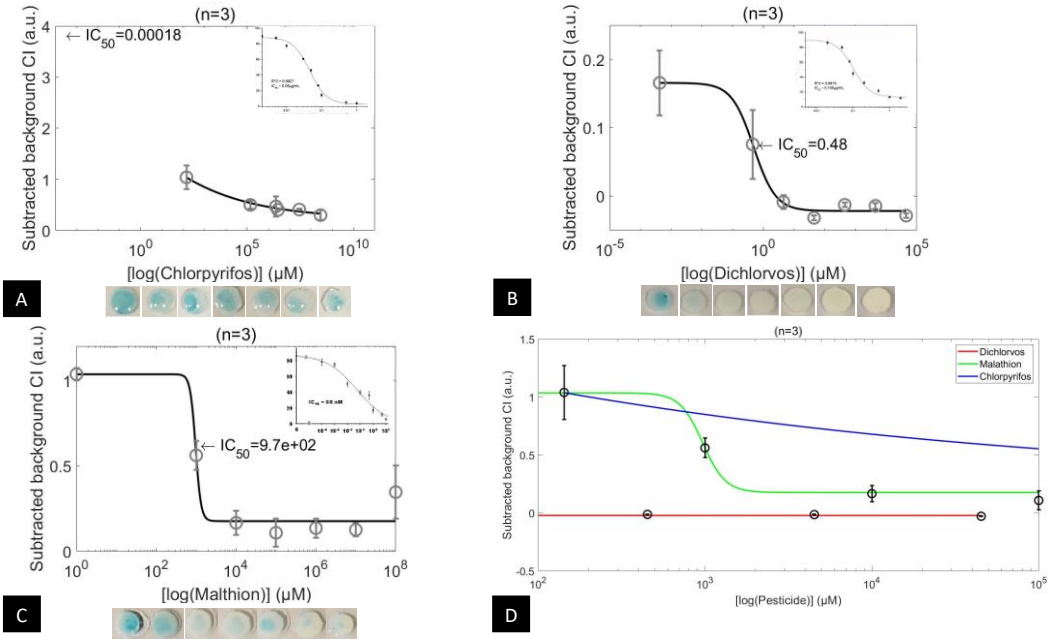

Figure 46. A-C) IC_{50} calculated using dose response curve fitted to the Hill equation with MATLAB. Images and the graph are related to paper disks where 10 µL of pesticides in different concentrations were pipped. After 20 min, 20 µL of chromogen were addicted. Images were taken after 30 min from the addiction of chromogen. On the right corner are shown the ideal curves obtained from Hossain *et al*.[215] for malathion and from Guo *et al*.[215] for chlorpyrifos and dichlorvos. D) Concentrations in range 10^2-10^5 µM. All points are means ± s.d. of n=3 independent measurements for each concentration. CI=color intensity.

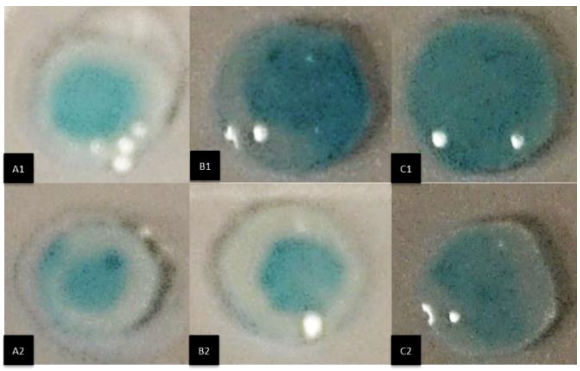

Figure 47. Three independent measurements on paper disks (A, B,C). A1, B1 and C1 are controls without pesticide, while A2, B2 and C2 are the correspondent batches inhibited by the same concentration of the pesticide (1µM of chlorpyrifos).

The IC_{50}, or LOD in this thesis, estimated for Chloryrifos, Dichlorvos and Malathion were respectively 0.18 nM, 480nM and 9.7 mM. It is important to highlight that these values were obtained using range of concentration that must be optimized. In order to improve and make the data obtained more meaningful in fact, the concentration ranges of the pesticides tested should be different. For

Dichlorvos and Malathion, much lower concentrations should be tested (at least two orders of magnitude lower) to start from higher intensity of color intensity, while for Chloryrifos much higher concentration should be investigated to achieve complete inhibition and a correct IC_{50} value. Another possible optimization to have a higher sensitivity could sample preparation using solvent extraction and/or pre-concentration methods can be performed. The paper-based sensor, combined with the wet test showed better results [215].In any case, if one assumes that the dose response curves are acceptable, the following observations can be made. For comparison purposes, in Figure 46D the concentration ranges between 10^2 and 10^5 μM can be observed. First, it is evident that every pesticide has a different inhibitory power (as expected). In particular, for chlorpyrifos, the blue intensity is very high, whereas that of malathion is less intense. Dichlorvos seems to develop the lowest blue intensity from very low concentrations. This means that paper disks are very selective to dichlorvos from very low concentrations. Secondly, the presence of high levels of either pesticide (10 mM) leads to complete inhibition of AChE and a lack of color. Finally, the robustness of this screening card is poor since its performance is highly dependent on the way the solutions are deposited: pipetting by the operator must be slow and inaccurate, the contact between the pipe tip and the drop being deposited must remain constant and superficial.

To get an idea of the reliability and to quantify qualitatively the accuracy of the data obtained, the IC_{50} values, which in this case concur with the LOD values, were compared with those found in the literature. Table 2 shows that the difference between the values obtained and those found in the literature is very high, except for the Dichlorvos.

Table 2. Comparison between IC50 values[2]

Pesticide	**IC_{50} valued (nM)**	**IC_{50} in literature (nM)**	**Reference**
Chlorpyrifos	0.18	140	Guo *et al*.[215]

[2] Comparison is only significant as the solutions and overall design of the paper test disks is not the same as those compared, found in the literature.

Dichlorvos	480	488	Guo *et al.*[215]
Malathion	9.7e+05	50-53	Hossain *et al.*[200] Sicard *et al.*[202,204]

4.5 Proof of concept: paper disks integrated into a microfluidic device

To enhance the reliability of the visual screening cards, they were incorporated into a novel microfluidic platform. As there were no previous references to the conceptual designs to the best of my knowledge, it was impossible to rely on existing literature results. The goal was to develop a user-friendly device that required only one operator action: adding the pesticide to be tested. Both Device I and Device II featured two disks containing the necessary reagents, along with a mixing channel that combined them as the liquid flowed through. Device I was instrumental in providing a preliminary assessment of how the system worked, and it also helped us optimize the solutions and the microfluidic fabrication process. Device II, on the other hand, had seven fixed-paper channels that allowed for multiple tests, including controls.

Device I was utilized to test two different drying times (15 and 60 min) for the IDA-coated paper. After 15 min, the papers were still wet, while after 1 hour, the paper was finally dried. Figure 48 shows that better outcomes are possible when the IDA-coated paper is still wet. However, this presents a disadvantage since the goal was to create a user-friendly device that only required the addition of the pesticide. If the paper on which the chromogen is deposited must be wet, a stable device that can be used after creation is not possible and the device must be used immediately. Despite this limitation, the results obtained with the wet IDA paper led to significantly better outcomes, so this technique was ultimately chosen.

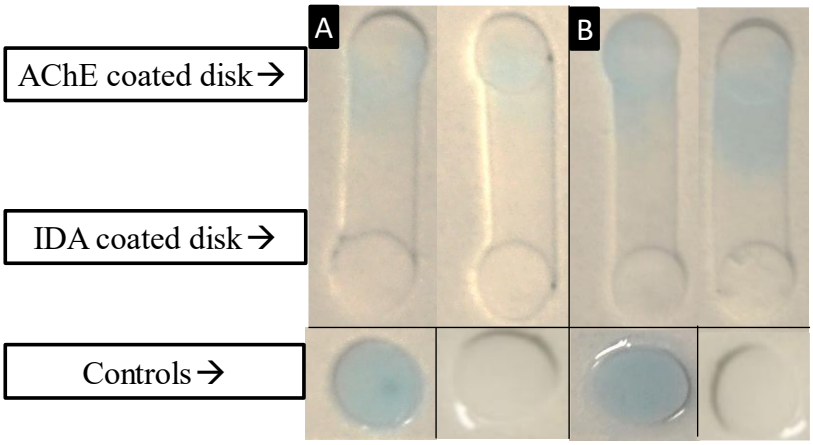

Figure 48. A) Two samples of Device I made with IDA coated disk dried. B) Two samples of Device I made with IDA coated disk wet. In both cases, 10µL of Tris HCl with 10% (v/v) of methanol was pipetted on IDA coated disk to make liquid flow. Controls include the case were IDA working solution was directly addicted to enzyme substrate and the blank control (no chromogen addiction). Photos were taken after 30 min from the addiction.

In order to ensure optimal device performance, it is crucial to carefully select the appropriate paper with properties tailored to its intended function. As shown in Figure 49, papers with specific properties were utilized for this purpose. In the case of AChE coated paper, it was necessary to utilize a membrane similar to the one previously studied by Guo[215] *et al.* for the same application. However, instead of using a positively charged Hybon N+ membrane as in Guo *et al*.'s study, a Nylon Membrane was used. Both membranes are composed of nylon and have high tensile strength and nucleic acid binding capacity, making them ideal for applications requiring high sensitivity and reproving capabilities. It is worth noting that due to its high protein binding capacity, nylon requires extensive blocking prior to detection with antibodies to prevent high background levels.

In contrast, no research references were available for IDA coated paper as to the best of our knowledge, no similar device had been previously developed. To determine the optimal paper for IDA coating, in addiction to nylon membrane, two types of papers commonly utilized in dipstick or lateral flow-based biosensors, Whatman #4[209] and Whatman #1[202], were tested. Results demonstrated that Whatman #4 paper facilitated the movement of IDA from the coating to the enzyme zone, possibly due to its rapid flow characteristics.

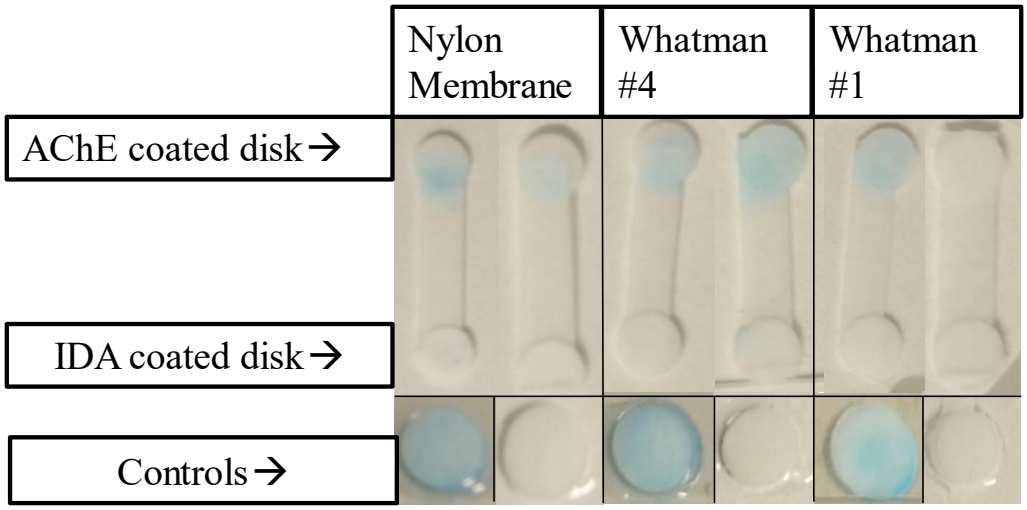

Figure 49. Comparison between different kind of paper used for IDA coated disk (experiments were repeated two times). In both cases, 10µL of Tris HCl with 10% (v/v) of methanol was pipetted on IDA coated disk to make liquid flow. Controls include the case were IDA working solution was directly addicted to enzyme substrate and the blank control (no chromogen addiction). Photos were taken after 30 min from the addiction.

4.5.1 Validation of µPADs and future optimizations

The final experiment aimed to validate the feasibility of the proposed concept for future studies. Initially, a control test was conducted to verify if the mechanism still functioned when all components were assembled. However, the first attempt failed as the addition of 10 µL of Tris-Buffer on IDA coated paper did not elicit any response after 30 minutes. To address this issue, 20 µL of IDA were directly added twice (at 10 minutes interval) onto the enzyme zone to assess whether the enzyme was immobilized correctly. As a result, the sensing zone began to exhibit an increasing intensity of blue color after only 5 minutes. This confirmed that the integration was not successful (Figure 50). To demonstrate the proof of concept, data obtained by adding 40 µL are presented in Figure 51.

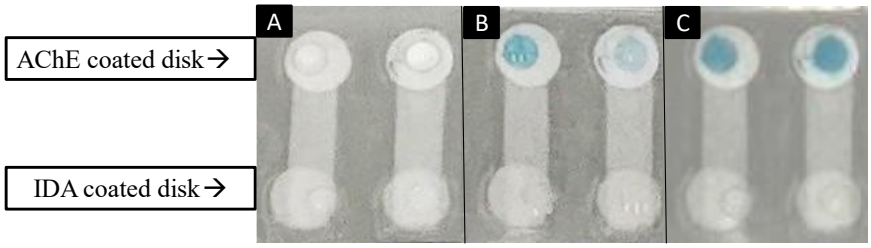

Figure 50. Device II tested in different ways. A) Results after 30 min from the addiction of 10 µL of Tris-HCl with 10% (v/v) on IDA coated disk. B) Results after 10 min from the addiction of 20 µL of IDA working solution with 10% (v/v) on AChE coated disk. C) Results after 10 min from the addiction of other 20 µL of IDA working solution with 10% (v/v) methanol on AChE coated disk.

In order to provide a proof of concept, we tested three pesticides at two different concentrations: one concentration was 1mM, which almost completely inhibited the AChE enzyme (chapter 4.4.1). However, since the sensitivity of the visual screening cards was not high enough, we also tested a lower concentration of the pesticides (1µM), which was three orders of magnitude lower. This additional test was conducted both for comparison purposes and to determine if the screening cards could detect such a low concentration of the pesticides.

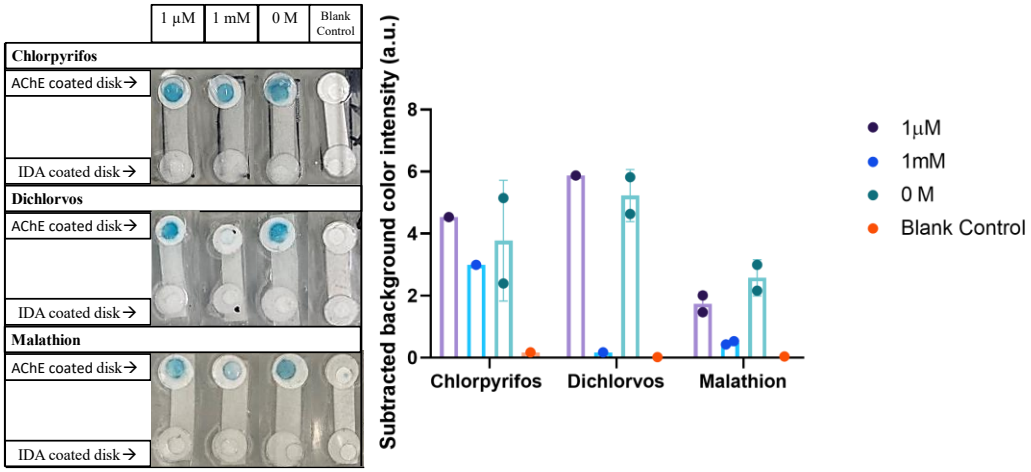

Figure 51. Device II tested with 10µL different pesticides for concentrations of 1m,1µM and no concentration. Blank control referrers to the microfluidic system featured by AChE coated paper-disk and a blank paper disk. Photos were taken after 30 min from the addiction of the chromogen IDA (which was pipetted on AChE coated disk after pesticide was addicted on the same disk)

The obtained results were in line with those from the visual screening cards (see *chapter 4.4.1).* This is because the inhibition mechanism was the same - by adding chromogen directly on the immobilized enzyme site. Dichlorvos was found to be the most potent among the three pesticides tested, indicating that the device exhibits higher selectivity towards it. Conversely, chlorpyrifos exhibited the least inhibitory effect, suggesting that the device's selectivity against it may be lower.

In order to further enhance the stability of the IDA coated disk, future optimizations can be explored. One potential approach is to increase the concentration of IDA in the coating to achieve a higher color intensity, which may improve the device's overall stability. Additionally, incorporating sol-gel technology may also be a viable option. Sol-gel is a technique that involves the use of a chemical solution to form a solid material, which can be used to deposit chromogen on the paper substrate. Many dipsticks and reagentless lateral flow bioactive papers that have used sol-gel to deposit chromogen have succeeded in creating devices that could be stored for long periods without significant loss of performance[202,204,232].

Another promising approach is to take inspiration from the work of Ua *et al*.[209], who developed a 3D device with appropriate channel length and wax barriers that facilitated flow. This device only required the addition of the test solution for

analysis and demonstrated excellent stability over time. By employing a similar design approach, it may be possible to further optimize the stability of the IDA coated disk and increase its utility for long-term storage.

Chapter 5: Conclusion and future developments

Low-cost sensors have the potential to greatly improve global public health, particularly in the field of point-of-care (POC) diagnostics. In recent years, paper-based microfluidic analytical devices (μPADs) have been developed for environmental and medical POC diagnostics, such as diagnosing liver function or blood group and detecting a range of biomedical analytes. However, one area where μPAD test technology is lacking is in the development of simple, quantitative on-site analysis methods that can be performed at low cost by untrained personnel. The development of a comprehensive water monitoring platform using μPADs to detect contaminants in water and provide on-site quantification and reporting could greatly improve the health of people worldwide. Currently, highly expensive and specialized analytical methods are used, which rely on liquid chromatography coupled with mass spectrometry. Although water monitoring sensors have been developed to detect certain pesticides, a need still exists for simple, quantitative on-site analysis methods that are low cost and can be performed by untrained personnel.

In this thesis, paper-based colorimetric assays have been developed for detecting pesticide residues, although they require improvement. A visual screening card was created for enzyme immobilization and required the addition of the sample to be analysed followed by the addition of the chromogen after an incubation period. The pesticide residues can be observed with the naked eye or with an image processing program thanks to the color change produced by the reaction between AChE and indoxyl acetate. While the performance of the biosensor was not optimal, it showed satisfactory performance and has the potential to be a simple and rapid screening method for pesticide detection with minor optimizations. In summary, the biosensor was validated to ensure that its stability, linearity, precision, limit of detection, accuracy, sensitivity, selectivity, and robustness met the intended use requirements. However, the performance of the assay was found

to be suboptimal compared to similar devices in the literature, except for Dichlorvos which was found to be comparable. Minor optimizations could lead to better results in a simple way. To increase the sensitivity of the device in detecting pesticide residues, sample preparation using solvent extraction and/or pre-concentration methods can be performed. The paper-based sensor, combined with the wet test, could provide a cost-effective screening tool for pesticide residues in food and the environment with minimal reagent consumption and simple operation by untrained individuals. Furthermore, the protocols presented in this study aim to improve the sensitivity of paper-based devices for measuring other assays.

To improve the robustness of the visual screening cards, two new μPADs were created to integrate them into a microfluidic system. These devices had reagents already deposited on two discs, separated by a paper channel, making it easy for the operator to add pesticide to the enzyme well and neutral liquid to the chromogen well. So, in contrast to the visual screening cards, they involved only the addition of the sample and the application of a buffer solution after an incubation period. However, the hydrolysis mechanism was only successful when the microfluidic system was not enclosed by hydrophobic barriers. When the system was enclosed, the liquid could not display any color after the usual analysis time of 30 min. To solve this problem, sol-gel solutions could be used to better immobilize the IDA. A 3D μPAD device could also be created, similar to the 'walk away' device devised by Ua *et al.* [209]. This device requires only the addition of a sample solution and allows long incubation periods before image scanning for signal acquisition. The flow rate is controlled by changing the lengths and widths of fluid paper channels modelled with wax barriers. This system effectively combines the two-step analysis procedure commonly required for pesticide detection with paper-based devices into one complete device, requiring only the application of the sample liquid, without the need for external reagents, manual device reversal, or paper valve changes.

In conclusion, over the past decade, there has been significant research aimed at developing and advancing paper-based analytical devices, resulting in a current

state of the art. Initially, paper was chosen as a substrate for developing such devices due to its wide availability and potential for use in disease diagnosis and water screening in areas with limited resources. The World Health Organization (WHO) has established the 'ASSURED' criteria to guide the development of low-cost diagnostics for developing regions, which has helped researchers identify areas of focus and commercialization pathways. The paper-based analytical platform is well-suited for meeting these criteria due to its accessibility, portability, and availability.

References

1. Wang, B. *et al.* Acetylcholinesterase electrochemical biosensors with graphene-transition metal carbides nanocomposites modified for detection of organophosphate pesticides. (2020) doi:10.1371/journal.pone.0231981.

2. Qian, S. & Lin, H. Colorimetric sensor array for detection and identification of organophosphorus and carbamate pesticides. *Anal Chem* **87**, 5395–5400 (2015).

3. Aragay, G., Pino, F. & Merkoçi, A. Nanomaterials for sensing and destroying pesticides. *Chem Rev* **112**, 5317–5338 (2012).

4. Boulanouar, S., Combès, A., Mezzache, S. & Pichon, V. Synthesis and application of molecularly imprinted silica for the selective extraction of some polar organophosphorus pesticides from almond oil. *Anal Chim Acta* **1018**, 35–44 (2018).

5. Dhull, V., Gahlaut, A., Dilbaghi, N. & Hooda, V. Acetylcholinesterase biosensors for electrochemical detection of organophosphorus compounds: A review. *Biochem Res Int* **2013**, (2013).

6. Trojanowicz, M. Determination of pesticides using electrochemical biosensors. *Electroanalysis* **14**, 1311–1328 (2002).

7. Barr, D. B. & Needham, L. L. Analytical methods for biological monitoring of exposure to pesticides: A review. *J Chromatogr B Analyt Technol Biomed Life Sci* **778**, 5–29 (2002).

8. Panuwet, P. *et al.* Agricultural pesticide management in Thailand: Status and population health risk. *Environ Sci Policy* **17**, 72–81 (2012).

9. Laschi, S., Ogończyk, D., Palchetti, I. & Mascini, M. Evaluation of pesticide-induced acetylcholinesterase inhibition by means of disposable carbon-modified electrochemical biosensors. *Enzyme Microb Technol* **40**, 485–489 (2007).

10. Trojanowicz, M. Determination of pesticides using electrochemical enzymatic biosensors. *Electroanalysis* **14**, 1311–1328 (2002).

11. Townson, H. Public health impact of pesticides used in agriculture. *Transactions of the Royal Society of Tropical Medicine and Hygiene* vol. 86 350 Preprint at https://doi.org/10.1016/0035-9203(92)90345-D (1992).

12. Pundir, C. S. & Chauhan, N. Acetylcholinesterase inhibition-based biosensors for pesticide determination: A review. *Anal Biochem* **429**, 19–31 (2012).

13. Nouanthavong, S., Nacapricha, D., Henry, C. S. & Sameenoi, Y. Pesticide analysis using nanoceria-coated paper-based devices as a detection platform. *Analyst* **141**, 1837–1846 (2016).

14. Shah, M. M. *et al.* Colorimetric Detection of Organophosphate Pesticides Based on Acetylcholinesterase and Cysteamine Capped Gold Nanoparticles as Nanozyme. (2021) doi:10.3390/s21238050.

15. Goldfrank, L. R. 110. Insecticides Organic Phosphorus Compounds and Carbamates. 2016 (2016).

16. Gunnell, D., Eddleston, M., Phillips, M. R. & Konradsen, F. The global distribution of fatal pesticide self-poisoning: Systematic review. *BMC Public Health* **7**, 1–15 (2007).

17. Gunnell, D. J. & Eddleston, M. Suicide by intentional ingestion of pesticides: A continuing tragedy in developing countries. *Int J Epidemiol* **32**, 902–909 (2003).

18. Eddleston, M. Patterns and problems of deliberate self-poisoning in the developing world. *QJM* **93**, 715–731 (2000).

19. King, A. M. & Aaron, C. K. Organophosphate and Carbamate Poisoning. *Emerg Med Clin North Am* **33**, 133–151 (2015).

20. Maddy, K. T., Edmiston, S. & Richmond, D. Illness, injuries, and deaths from pesticide exposures in California 1949-1988. *Rev Environ Contam Toxicol* **114**, 57–123 (1990).

21. Wesseling, C., McConnell, R., Partanen, T. & Hogstedt, C. Agricultural pesticide use in developing countries: Health effects and research needs. *International Journal of Health Services* **27**, 273–308 (1997).

22. Solé, S., Merkoçi, A. & Alegret, S. Determination of toxic substances based on enzyme inhibition. Part I. Electrochemical biosensors for the determination of pesticides using batch procedures. *Crit Rev Anal Chem* **33**, 89–126 (2003).

23. Hernández, F., Sancho, J. v., Pozo, O., Lara, A. & Pitarch, E. Rapid direct determination of pesticides and metabolites in environmental water samples at sub-μg/l level by on-line solid-phase extraction-liquid chromatography - Electrospray tandem mass spectrometry. *J Chromatogr A* **939**, 1–11 (2001).

24. van der Hoff, G. R. & van Zoonen, P. Trace analysis of pesticides by gas chromatography. *J Chromatogr A* **843**, 301–322 (1999).

25. Hua, Q. T. Development of Portable Analytical Devices for Organophosphate Pesticide Detection. (2019).

26. Hu, H. & Yang, L. Development of enzymatic electrochemical biosensors for organophosphorus pesticide detection. *J Environ Sci Health B* **56**, 168–180 (2020).

27. Taylor, P. Chapter 10 . Anticholinesterase Agents. *Goodman & Gilman's: The Pharmacological Basis of Therapeutics, 12e* 1–22 (2014).

28. Gupta, R. C. Classification and Uses of Organophosphates and Carbamates. in *Toxicology of Organophosphate and Carbamate Compounds* 5–24 (Elsevier Inc., 2005). doi:10.1016/B978-012088523-7/50003-X.

29. Colovic, M. B., Krstic, D. Z., Lazarevic-Pasti, T. D., Bondzic, A. M. & Vasic, V. M. Acetylcholinesterase Inhibitors: Pharmacology and Toxicology. *Curr Neuropharmacol* **11**, 315–335 (2013).

30. Spradling, K. D. & Dillman, J. F. *The Molecular Toxicology of Chemical Warfare Nerve Agents*. *Advances in Molecular Toxicology* vol. 5 (2011).

31. Bajgar, A. J. British journal of industrial medicine. *Public Health* **57**, 63–64 (1943).

32. de Araujo Furtado, M., Rossetti, F., Chanda, S. & Yourick, D. Exposure to nerve agents: From status epilepticus to neuroinflammation, brain damage, neurogenesis and epilepsy. *Neurotoxicology* **33**, 1476–1490 (2012).

33. Pohanka, M. Electrochemical biosensors based on acetylcholinesterase and butyrylcholinesterase. A review. *Int J Electrochem Sci* **11**, 7440–7452 (2016).

34. Attack, S. on 640 Victims of the Tokyo Subway Sarin Attack. (1996).

35. Roberts, D. M. & Aaron, C. K. Managing acute organophosphorus pesticide poisoning. *Br Med J* **334**, 629–634 (2007).

36. Zhang, J. *et al.* Detection of organophosphorus pesticides using potentiometric enzymatic membrane biosensor based on methylcellulose immobilization. *Analytical Sciences* **25**, 511–515 (2009).

37. Vreuls, J. J. *et al.* Automated on-line gel permeation chromatography-gas chromatography for the determination of organophosphorus pesticides in olive oil. *J Chromatogr A* **750**, 275–286 (1996).

38. Chapalamadugu, S. & Chaudhry, G. R. Microbiological and biotechnological aspects of metabolism of carbamates and organophosphates. *Crit Rev Biotechnol* **12**, 357–389 (1992).

39. Ellman, G. L., Courtney, K. D., Andres, V. & Featherstone, R. M. A new and rapid colorimetric determination of acetylcholinesterase activity. *Biochem Pharmacol* **7**, 88–95 (1961).

40. Long, Q., Li, H., Zhang, Y. & Yao, S. Upconversion nanoparticle-based fluorescence resonance energy transfer assay for organophosphorus pesticides. *Biosens Bioelectron* **68**, 168–174 (2015).

41. Mulchandani, A., Chen, W., Mulchandani, P., Wang, J. & Rogers, K. R. Biosensors for direct determination of organophosphate pesticides. *Biosens Bioelectron* **16**, 225–230 (2001).

42. Yi, Y. *et al.* A label-free silicon quantum dots-based photoluminescence sensor for ultrasensitive detection of pesticides. *Anal Chem* **85**, 11464–11470 (2013).

43. Centers for Disease Control and Prevention. CDC Estimates of Foodborne Illness in the United States. *CDC 2011 Estimates* **68**, 3–4 (2011).

44. Gharagozloo, M. *et al.* CLINICAL STUDY Immune-mediated cochleovestibular disease. *Bratislavsk?? lek??rske listy* **116**, 296–301 (2015).

45. Pohanka, M. Cholinesterases, a target of pharmacology and toxicology. *Biomedical Papers* **155**, 219–230 (2011).

46. Pohanka, M. Inhibitors of Acetylcholinesterase and Butyrylcholinesterase Meet Immunity. 9809–9825 (2014) doi:10.3390/ijms15069809.

47. Pohanka, M. Alpha7 nicotinic acetylcholine receptor is a target in pharmacology and toxicology. *Int J Mol Sci* **13**, 2219–2238 (2012).

48. Lin, G., Chen, G. H. & Ho, H. C. Conformationally restricted carbamate inhibitors of horse serum butyrylcholinesterase. *Bioorg Med Chem Lett* **8**, 2747–2750 (1998).

49. Grossberg, G. T. Cholinesterase inhibitors for the treatment of Alzheimer's disease: Getting on and staying on. *Curr Ther Res Clin Exp* **64**, 216–235 (2003).

50. Coban, A., Carr, R. L., Chambers, H. W., Willeford, K. O. & Chambers, J. E. Comparison of inhibition kinetics of several organophosphates, including some nerve agent surrogates, using human erythrocyte and rat and mouse brain acetylcholinesterase. *Toxicol Lett* **248**, 39–45 (2016).

51. Brun, S., Cabanis, J. C. & Mestres, J. P. Analytical chemistry. *Experientia* **42**, 893–904 (1986).

52. Patocka, J., Kuca, K. & Jun, D. Acetylcholinesterase and butyrylcholinesterase--important enzymes of human body. *Acta medica (Hradec Králové) / Universitas Carolina, Facultas Medica Hradec Králové* **47**, 215–228 (2004).

53. Eddleston, M., Buckley, N. A., Eyer, P. & Dawson, A. H. Management of acute organophosphorus pesticide poisoning. *The Lancet* **371**, 597–607 (2008).

54. Costa, L. G. Current issues in organophosphate toxicology. *Clinica Chimica Acta* **366**, 1–13 (2006).

55. Olovi, M. B., Krsti, D. Z., Lazarevi-Pati, T. D., Bondi, A. M. & Vasi, V. M. Acetylcholinesterase Inhibitors: Pharmacology and Toxicology.

56. Jang, Y. J., Kim, K., Tsay, O. G., Atwood, D. A. & Churchill, D. G. Destruction and detection of chemical warfare agents. *Chem Rev* **115**, PR1–PR76 (2015).

57. Fernández-Ramos, M. D., Ogunneye, A. L., Barbarinde, N. A. A., Erenas, M. M. & Capitán-Vallvey, L. F. Bioactive microfluidic paper device for pesticide determination in waters. *Talanta* **218**, 121108 (2020).

58. Hara, T. O. & Singh, B. Electrochemical Biosensors for Detection of Pesticides and Heavy Metal Toxicants in Water: Recent Trends and Progress. *ACS Environmental Science and Technology Water* **1**, 462–478 (2021).

59. Russo, M. V., Campanella, L. & Avino, P. Determination of organophosphorus pesticide residues in human tissues by capillary gas chromatography-negative

chemical ionization mass spectrometry analysis. *J Chromatogr B Analyt Technol Biomed Life Sci* **780**, 431–441 (2002).

60. Pérez-Ruiz, T., Martínez-Lozano, C., Tomás, V. & Martín, J. High-performance liquid chromatographic assay of phosphate and organophosphorus pesticides using a post-column photochemical reaction and fluorimetric detection. *Anal Chim Acta* **540**, 383–391 (2005).

61. Fillion, J., Sauvé, F. & Selwyn, J. Multiresidue method for the determination of residues of 251 pesticides in fruits and vegetables by gas chromatography/ mass spectrometry and liquid chromatography with fluorescence detection. *J AOAC Int* **83**, 698–713 (2000).

62. Kochman, M., Gordin, A., Goldshlag, P., Lehotay, S. J. & Amirav, A. Fast, high-sensitivity, multipesticide analysis of complex mixtures with supersonic gas chromatography–mass spectrometry. *J Chromatogr A* **974**, 185–212 (2002).

63. Jeannot, R., Sabik, H., Sauvard, E. & Genin, E. Application of liquid chromatography with mass spectrometry combined with photodiode array detection and tandem mass spectrometry for monitoring pesticides in surface waters. *J Chromatogr A* **879**, 51–71 (2000).

64. Peng, L., Zhu, J., Yang, B., Hao, H. & Lou, S. A green photocatalytic-biosensor for colorimetric detection of pesticide (carbaryl) based on inhibition of acetylcholinesterase. *Talanta* **246**, 123525 (2022).

65. Hu, T. *et al.* Visual detection of mixed organophosphorous pesticide using QD-AChE aerogel based microfluidic arrays sensor. *Biosens Bioelectron* **136**, 112–117 (2019).

66. Sgobbi, L. F. & Machado, S. A. S. Functionalized polyacrylamide as an acetylcholinesterase-inspired biomimetic device for electrochemical sensing of organophosphorus pesticides. *Biosens Bioelectron* **100**, 290–297 (2018).

67. Ivanov, A., Davletshina, R., Sharafieva, I. & Evtugyn, G. Electrochemical biosensor based on polyelectrolyte complexes for the determination of reversible inhibitors of acetylcholinesterase. *Talanta* **194**, 723–730 (2019).

68. Li, Y., Bai, H., Li, C. & Shi, G. Colorimetric assays for acetylcholinesterase activity and inhibitor screening based on the disassembly-assembly of a water-soluble polythiophene derivative. *ACS Appl Mater Interfaces* **3**, 1306–1310 (2011).

69. Birman, S. Determination of acetylcholinesterase activity by a new chemiluminescence assay with the natural substrate. *Biochemical Journal* **225**, 825–828 (1985).

70. Andreani, A. *et al.* Chemiluminescent high-throughput microassay applied to imidazo[2,1-b]thiazole derivatives as potential acetylcholinesterase and butyrylcholinesterase inhibitors. *Eur J Med Chem* **43**, 657–661 (2008).

71. Li, Y. *et al.* Metal coordination polymer induced perylene probe excimer fluorescence and its application in acetylcholinesterase sensing and alpha-fetoprotein immunoassay. *Analyst* **144**, 2034–2041 (2019).

72. Xu, X. *et al.* A ratiometric fluorescence probe based on carbon dots for discriminative and highly sensitive detection of acetylcholinesterase and butyrylcholinesterase in human whole blood. *Biosens Bioelectron* **131**, 232–236 (2019).

73. Guo, J., Wu, S., Wang, Y. & Zhao, M. A label-free fluorescence biosensor based on a bifunctional MIL-101(Fe) nanozyme for sensitive detection of choline and acetylcholine at nanomolar level. *Sens Actuators B Chem* **312**, 128021 (2020).

74. Marston, A., Kissling, J. & Hostettmann, K. A rapid TLC bioautographic method for the detection of acetylcholinesterase and butyrylcholinesterase inhibitors in plants. *Phytochemical Analysis* **13**, 51 (2002).

75. Zhongduo, Y. *et al.* Modified TLC bioautographic method for screening acetylcholinesterase inhibitors from plant extracts. *J Sep Sci* **32**, 3257–3259 (2009).

76. Yang, G. di *et al.* Determination of organophosphorus pesticides by capillary electrophoresis-inductively coupled plasma mass spectrometry with collective sample-introduction technique. *Electrophoresis* **30**, 1718–1723 (2009).

77. Liu, D. *et al.* Acetylcholinesterase-catalyzed hydrolysis allows ultrasensitive detection of pathogens with the naked eye. *Angewandte Chemie - International Edition* **52**, 14065–14069 (2013).

78. Taylor, P. Anticholinesterase Agents. in *Goodman & Gilman's: The Pharmacological Basis of Therapeutics, 13e* (eds. Brunton, L. L., Hilal-Dandan, R. & Knollmann, B. C.) (McGraw-Hill Education, 2017).

79. Song, Y. *et al.* A novel biosensor based on acetylecholinesterase/prussian blue–chitosan modified electrode for detection of carbaryl pesticides. *Electrochim Acta* **56**, 7267–7271 (2011).

80. Liu, G. & Lin, Y. Electrochemical Sensor for Organophosphate Pesticides and Nerve Agents Using Zirconia Nanoparticles as Selective Sorbents phosphoric group , nitroaromatic OPs strongly bind to the. *Anal Chem* **77**, 5894–5901 (2005).

81. Zacco, E., Pividori, M. I., Alegret, S., Galve, R. & Marco, M. Electrochemical Magnetoimmunosensing Strategy for the Detection of Pesticides Residues. *Comprehensive Analytical Chemistry* **78**, 1780–1788 (2006).

82. Grieshaber, D., MacKenzie, R., Vörös, J. & Reimhult, E. Electrochemical biosensors - Sensor principles and architectures. *Sensors* **8**, 1400–1458 (2008).

83. Thvenot, D. R., Toth, K., Durst, R. A. & Wilson, G. S. Electrochemical biosensors: Recommended definitions and classification (Technical Report). *Pure and Applied Chemistry* **71**, 2333–2348 (1999).

84. Justino, C. I. L., Duarte, A. C. & Rocha-Santos, T. A. P. Recent progress in biosensors for environmental monitoring: A review. *Sensors (Switzerland)* **17**, (2017).

85. Ruan, C., Zeng, K., Varghese, O. K. & Grimes, C. A. A magnetoelastic bioaffinity-based sensor for avidin. *Biosens Bioelectron* **19**, 1695–1701 (2004).

86. Long, F., Zhu, A. & Shi, H. Recent advances in optical biosensors for environmental monitoring and early warning. *Sensors (Switzerland)* **13**, 13928–13948 (2013).

87. Cai, H. *et al.* SAW based mass-loading biosensor for DNA detection. *2013 IEEE International Conference of Electron Devices and Solid-State Circuits, EDSSC 2013* 4–5 (2013) doi:10.1109/EDSSC.2013.6628122.

88. Luka, G. *et al.* Microfluidics integrated biosensors: A leading technology towards lab-on-A-chip and sensing applications. *Sensors (Switzerland)* **15**, 30011–30031 (2015).

89. Zhang, S. X. *et al.* Polyacrylic acid-coated cerium oxide nanoparticles: An oxidase mimic applied for colorimetric assay to organophosphorus pesticides. *Biosens Bioelectron* **85**, 457–463 (2016).

90. Cheng, A. K. H., Ge, B. & Yu, H. Z. Aptamer-based biosensors for label-free voltammetric detection of lysozyme. *Anal Chem* **79**, 5158–5164 (2007).

91. Mohanty, S. P. Biosensors : A Tutorial Review Biosensors : A Tutorial Review. *IEEE Potentials* **25**, 35–40 (2015).

92. Justino, C. I. L., Freitas, A. C., Pereira, R., Duarte, A. C. & Rocha Santos, T. A. P. Recent developments in recognition elements for chemical sensors and biosensors. *TrAC Trends in Analytical Chemistry* **68**, 2–17 (2015).

93. Singh, M., Kathuroju, P. K. & Jampana, N. Polypyrrole based amperometric glucose biosensors. *Sens Actuators B Chem* **143**, 430–443 (2009).

94. Kissinger, P. T. Biosensors - A perspective. *Biosens Bioelectron* **20**, 2512–2516 (2005).

95. Datta, S., Christena, L. R. & Rajaram, Y. R. S. Enzyme immobilization: an overview on techniques and support materials. *3 Biotech* **3**, 1–9 (2013).

96. Santano, E., del Carmen Pinto, M. & Macías, P. Xenobiotic oxidation by hydroperoxidase activity of lipoxygenase immobilized by adsorption on controlled pore glass. *Enzyme Microb Technol* **30**, 639–646 (2002).

97. Arduini, F., Guidone, S., Amine, A., Palleschi, G. & Moscone, D. Acetylcholinesterase biosensor based on self-assembled monolayer-modified gold-screen printed electrodes for organophosphorus insecticide detection. *Sens Actuators B Chem* **179**, 201–208 (2013).

98. Guo, L. *et al.* Colorimetric biosensor for the assay of paraoxon in environmental water samples based on the iodine-starch color reaction. *Anal Chim Acta* **967**, 59–63 (2017).

99. Zhang, W., Asiri, A. M., Liu, D., Du, D. & Lin, Y. Nanomaterial-based biosensors for environmental and biological monitoring of organophosphorus pesticides and nerve agents. *TrAC - Trends in Analytical Chemistry* **54**, 1–10 (2014).

100. Maduraiveeran, G. & Jin, W. Nanomaterials based electrochemical sensor and biosensor platforms for environmental applications. *Trends in Environmental Analytical Chemistry* **13**, 10–23 (2017).

101. Zhao, Y., Zhang, W., Lin, Y. & Du, D. The vital function of Fe3O4@Au nanocomposites for hydrolase biosensor design and its application in detection of methyl parathion. *Nanoscale* **5**, 1121–1126 (2013).

102. Lang, Q., Han, L., Hou, C., Wang, F. & Liu, A. A sensitive acetylcholinesterase biosensor based on gold nanorods modified electrode for detection of organophosphate pesticide. *Talanta* **156–157**, 34–41 (2016).

103. Rakow, N. A. & Suslick, K. S. A Colorimetric Sensor Array For Odour Visualization. **406**, 2–5 (2000).

104. Sun, J. *et al.* Trends in Analytical Chemistry Colorimetric sensor array based on gold nanoparticles : Design principles and recent advances. *Trends in Analytical Chemistry* **122**, 115754 (2020).

105. Liu, D. M., Xu, B. & Dong, C. Recent advances in colorimetric strategies for acetylcholinesterase assay and their applications. *TrAC Trends in Analytical Chemistry* **142**, 116320 (2021).

106. Oujji, N. ben. Acetylcholinesterase Immobilized on Magnetic Beads for Pesticides Detection: Application to Olive Oil Analysis. 7893–7904 (2012) doi:10.3390/s120607893.

107. Meng, X., Schultz, C. W., Cui, C., Li, X. & Yu, H. Ac ce p te us t. *Sens Actuators B Chem* (2015) doi:10.1016/j.snb.2015.04.011.

108. Yanjie, L. I. *et al.* Detection of Organophosphorus Pesticides with Colorimetry and Computer Image Analysis. **32**, (2016).

109. Badawy, M. E. I. & El-Aswad, A. F. Bioactive paper sensor based on the acetylcholinesterase for the rapid detection of organophosphate and carbamate pesticides. *Int J Anal Chem* **2014**, (2014).

110. Fuyal, M. & Giri, B. A Combined System of Paper Device and Portable Spectrometer for the Detection of Pesticide Residues. (2020).

111. Oujji, N. ben *et al.* SC. *Food Control* (2014) doi:10.1016/j.foodcont.2014.05.006.

112. Ingkaninan, K., Temkitthawon, P., Chuenchom, K., Yuyaem, T. & Thongnoi, W. Screening for acetylcholinesterase inhibitory activity in plants used in Thai traditional rejuvenating and neurotonic remedies. **89**, 261–264 (2003).

113. Cacciotti, I., Pallotto, F. & Scognamiglio, V. Jo ur l P re of. *Materials Science & Engineering C* 110744 (2020) doi:10.1016/j.msec.2020.110744.

114. Kostelnik, A., Cegan, A. & Pohanka, M. Acetylcholinesterase inhibitors assay using colorimetric pH sensitive strips and image analysis by a smartphone. *Int J Anal Chem* **2017**, (2017).

115. Wong, F. C. M., Ahmad, M., Heng, L. Y. & Peng, L. B. An optical biosensor for dichlovos using stacked sol-gel films containing acetylcholinesterase and a lipophilic chromoionophore. *Talanta* **69**, 888–893 (2006).

116. Pohanka, M. *et al.* Colorimetric dipstick for assay of organophosphate pesticides and nerve agents represented by paraoxon, sarin and VX. *Talanta* **81**, 621–624 (2010).

117. Xue, W. X., Zhang, D. Q., Zhang, G. X. & Zhu, D. ben. Colorimetric detection of glucose and an assay for acetylcholinesterase with amine-terminated polydiacetylene vesicles. *Chinese Science Bulletin* **56**, 1877–1883 (2011).

118. Liu, D. M., Xu, B. & Dong, C. Recent advances in colorimetric strategies for acetylcholinesterase assay and their applications. *TrAC - Trends in Analytical Chemistry* **142**, 116320 (2021).

119. Lin, T. *et al.* A sensitive colorimetric assay for cholesterol based on the peroxidase-like activity of MoS2 nanosheets. *Microchimica Acta* **184**, 1233–1237 (2017).

120. Chen, H. *et al.* Colorimetric assay of copper ions based on the inhibition of peroxidase-like activity of MoS2 nanosheets. *Spectrochim Acta A Mol Biomol Spectrosc* **185**, 271–275 (2017).

121. Ni, P. *et al.* Colorimetric determination of the activity of acetylcholinesterase and its inhibitors by exploiting the iodide-catalyzed oxidation of 3,3′,5,5′-tetramethylbenzidine by hydrogen peroxide. *Microchimica Acta* **183**, 2589–2595 (2016).

122. Liang, X. & Han, L. White Peroxidase-Mimicking Nanozymes: Colorimetric Pesticide Assay without Interferences of O2 and Color. *Adv Funct Mater* **30**, 1–10 (2020).

123. Sun, Y., Tan, H. & Li, Y. A colorimetric assay for acetylcholinesterase activity and inhibitor screening based on the thiocholine–induced inhibition of the oxidative power of MnO2 nanosheets on 3,3′,5,5′–tetramethylbenzidine. *Microchimica Acta* **185**, 4–11 (2018).

124. Jin, R. *et al.* Sensitive colorimetric sensor for point-of-care detection of acetylcholinesterase using cobalt oxyhydroxide nanoflakes. *J Mater Chem B* **7**, 1230–1237 (2019).

125. Bagheri, N., Khataee, A., Hassanzadeh, J. & Habibi, B. Sensitive biosensing of organophosphate pesticides using enzyme mimics of magnetic ZIF-8. *Spectrochim Acta A Mol Biomol Spectrosc* **209**, 118–125 (2019).

126. Li, Z. *et al.* Colorimetric assay for acetylcholinesterase and inhibitor screening based on the Ag [I] ion-3,3′,5,5′-tetramethylbenzidine (TMB). *Sens Actuators B Chem* **226**, 104–109 (2016).

127. Pavlov, V., Xiao, Y. & Willner, I. inhibition of the acetycholine esterase-stimulated growth of Au nanoparticles.pdf. 1–5 (2005).

128. Nanda Kumar, D., Satija, J., Chandrasekaran, N. & Mukherjee, A. Acetylcholinesterase-based inhibition screening through in situ synthesis of gold nanoparticles: Application for detection of nerve agent simulant. *J Mol Liq* **249**, 623–628 (2018).

129. Qing, Z. *et al.* Thiol-suppressed I2-etching of AuNRs: acetylcholinesterase-mediated colorimetric detection of organophosphorus pesticides. *Microchimica Acta* **187**, (2020).

130. Bala, R., Sharma, R. K. & Wangoo, N. Highly sensitive colorimetric detection of ethyl parathion using gold nanoprobes. *Sens Actuators B Chem* **210**, 425–430 (2015).

131. Satnami, M. L. *et al.* Gold nanoprobe for inhibition and reactivation of acetylcholinesterase: An application to detection of organophosphorus pesticides. *Sens Actuators B Chem* **267**, 155–164 (2018).

132. Wu, S. *et al.* Gold nanoparticles dissolution based colorimetric method for highly sensitive detection of organophosphate pesticides. *Sens Actuators B Chem* **238**, 427–433 (2017).

133. Kramer, D. N. & Gamson, R. M. Colorimetric Determination of Acetylcholinesterase Activity. *Anal Chem* **30**, 251–254 (1958).

134. Wu, Y., Sun, Y., Xiao, F., Wu, Z. & Yu, R. Sensitive inkjet printing paper-based colormetric strips for acetylcholinesterase inhibitors with indoxyl acetate substrate. *Talanta* **162**, 174–179 (2017).

135. Pohanka, M. & Vlcek, V. Preparation and performance of a colorimetric biosensor using acetylcholinesterase and indoxylacetate for assay of nerve agents and drugs. *Interdiscip Toxicol* **7**, 215–218 (2014).

136. No, H. Y., Kim, Y. A., Lee, Y. T. & Lee, H. S. Cholinesterase-based dipstick assay for the detection of organophosphate and carbamate pesticides. *Anal Chim Acta* **594**, 37–43 (2007).

137. Sackmann, E. K., Fulton, A. L. & Beebe, D. J. The present and future role of microfluidics in biomedical research. *Nature* **507**, 181–189 (2014).

138. Haeberle, S. & Zengerle, R. Microfluidic platforms for lab-on-a-chip applications. *Lab Chip* **7**, 1094–1110 (2007).

139. Xia, Y. & Whitesides, G. M. Soft lithography. *Angewandte Chemie - International Edition* **37**, 550–575 (1998).

140. Brouzes, E. *et al.* Cytotoxicity Screen. *Proc Natl Acad Sci U S A* **106**, 14195–200 (2009).

141. Pol, R., Céspedes, F., Gabriel, D. & Baeza, M. Microfluidic lab-on-a-chip platforms for environmental monitoring. *TrAC - Trends in Analytical Chemistry* **95**, 62–68 (2017).

142. Go´mez, R. *et al.* Microfluidic biochip for impedance spectroscopy of biological species. *Biomed Microdevices* **3**, 201–209 (2001).

143. Fernández-la-Villa, A., Pozo-Ayuso, D. F. & Castaño-Álvarez, M. Microfluidics and electrochemistry: an emerging tandem for next-generation analytical microsystems. *Curr Opin Electrochem* **15**, 175–185 (2019).

144. Wongkaew, N., Simsek, M., Griesche, C. & Baeumner, A. J. Functional Nanomaterials and Nanostructures Enhancing Electrochemical Biosensors and Lab-on-a-Chip Performances: Recent Progress, Applications, and Future Perspective. *Chem Rev* **119**, 120–194 (2019).

145. Maguire, I., O'Kennedy, R., Ducrée, J. & Regan, F. A review of centrifugal microfluidics in environmental monitoring. *Analytical Methods* **10**, 1497–1515 (2018).

146. Samiei, E., Tabrizian, M. & Hoorfar, M. A review of digital microfluidics as portable platforms for lab-on a-chip applications. *Lab Chip* **16**, 2376–2396 (2016).

147. Auroux, P. A., Iossifidis, D., Reyes, D. R. & Manz, A. Micro total analysis systems. 2. Analytical standard operations and applications. *Anal Chem* **74**, 2637–2652 (2002).

148. Snyder, W., Bilbro, G., Han, Y. S., Whitaker, R. & Pizer, S. Miniaturized Total Chemical Analysis Systems: a Novel Concept for Chemical Sensing. *IEEE Trans Pattern Anal Mach Intell* **17**, 620–624 (1995).

149. Stone, H. A. & Kim, S. Microfluidics: Basic issues, applications, and challenges. *AIChE Journal* **47**, 1250–1254 (2001).

150. Anwar, K., Han, T., Yu, S. & Kim, S. M. An integrated micro-nanofluidic system for sample preparation and preconcentration of proteins. *14th International Conference on Miniaturized Systems for Chemistry and Life Sciences 2010, MicroTAS 2010* **1**, 443–445 (2010).

151. Liu, K. K. *et al.* Microfluidic systems for biosensing. *Sensors* **10**, 6623–6661 (2010).

152. Kudr, J., Zitka, O., Klimanek, M., Vrba, R. & Adam, V. Microfluidic electrochemical devices for pollution analysis–A review. *Sens Actuators B Chem* **246**, 578–590 (2017).

153. Havelaar, A. H. *et al.* World Health Organization Global Estimates and Regional Comparisons of the Burden of Foodborne Disease in 2010. *PLoS Med* **12**, 1–23 (2015).

154. Wang, Q., Yang, Q. & Wu, W. Graphene-Based Steganographic Aptasensor for Information Computing and Monitoring Toxins of Biofilm in Food. *Front Microbiol* **10**, (2020).

155. Wang, Y. & Duncan, T. v. Nanoscale sensors for assuring the safety of food products. *Curr Opin Biotechnol* **44**, 74–86 (2017).

156. Wu, W. *et al.* Research advances of DNA aptasensors for foodborne pathogen detection. *Crit Rev Food Sci Nutr* **60**, 2353–2368 (2020).

157. Valencia, P. M., Farokhzad, O. C., Karnik, R. & Langer, R. Microfluidic technologies for accelerating the clinical translation of nanoparticles. *Nat Nanotechnol* **7**, 623–629 (2012).

158. Sun, J., Xianyu, Y. & Jiang, X. Point-of-care biochemical assays using gold nanoparticle-implemented microfluidics. *Chem Soc Rev* **43**, 6239–6253 (2014).

159. Wang, M. *et al.* Microfluidic Paper-Based Analytical Devices for the Determination of Food Contaminants: Developments and Applications. *J Agric Food Chem* **70**, 8188–8206 (2022).

160. Cate, D. M., Adkins, J. A., Mettakoonpitak, J. & Henry, C. S. Recent developments in paper-based microfluidic devices. *Anal Chem* **87**, 19–41 (2015).

161. Morbioli, G. G., Mazzu-Nascimento, T., Stockton, A. M. & Carrilho, E. Technical aspects and challenges of colorimetric detection with microfluidic paper-based analytical devices (μPADs) - A review. *Anal Chim Acta* **970**, 1–22 (2017).

162. Yetisen, A. K., Akram, M. S. & Lowe, C. R. Paper-based microfluidic point-of-care diagnostic devices. *Lab Chip* **13**, 2210–2251 (2013).

163. Yang, Y. *et al.* Paper-Based Microfluidic Devices: Emerging Themes and Applications. *Anal Chem* **89**, 71–91 (2017).

164. Lim, H., Jafry, A. T. & Lee, J. Fabrication, flow control, and applications of microfluidic paper-based analytical devices. *Molecules* **24**, 1–32 (2019).

165. Lisowski, P. & Zarzycki, P. K. Microfluidic paper-based analytical devices (μPADs) and micro total analysis systems (μTAS): Development, applications and future trends. *Chromatographia* **76**, 1201–1214 (2013).

166. Mao, K. *et al.* Paper-based microfluidics for rapid diagnostics and drug delivery. *Journal of Controlled Release* **322**, 187–199 (2020).

167. Nilghaz, A., Guan, L., Tan, W. & Shen, W. Advances of Paper-Based Microfluidics for Diagnostics - The Original Motivation and Current Status. *ACS Sens* **1**, 1382–1393 (2016).

168. Jang, I., Carraõ, D. B., Menger, R. F., Moraes De Oliveira, A. R. & Henry, C. S. Pump-Free Microfluidic Rapid Mixer Combined with a Paper-Based Channel. *ACS Sens* **5**, 2230–2238 (2020).

169. Almeida, M. I. G. S., Jayawardane, B. M., Kolev, S. D. & McKelvie, I. D. Developments of microfluidic paper-based analytical devices (μPADs) for water analysis: A review. *Talanta* **177**, 176–190 (2018).

170. Martinez, A. W., Phillips, S. T., Butte, M. J. & Whitesides, G. M. Patterned paper as a platform for inexpensive, low-volume, portable bioassays. *Angewandte Chemie - International Edition* **46**, 1318–1320 (2007).

171. Busa, L. S. A. *et al.* Advances in microfluidic paper-based analytical devices for food and water analysis. *Micromachines (Basel)* **7**, (2016).

172. Dungchai, W., Chailapakul, O. & Henry, C. S. A low-cost, simple, and rapid fabrication method for paper-based microfluidics using wax screen-printing. *Analyst* **136**, 77–82 (2011).

173. Nargang, T. M. *et al.* Photolithographic structuring of soft, extremely foldable and autoclavable hydrophobic barriers in paper. *Analytical Methods* **10**, 4028–4035 (2018).

174. Suresh, V., Qunya, O., Kanta, B. L., Yuh, L. Y. & Chong, K. S. L. Non-invasive paper-based microfluidic device for ultra-low detection of urea through enzyme catalysis. *R Soc Open Sci* **5**, (2018).

175. Shibata, H., Hiruta, Y. & Citterio, D. Fully inkjet-printed distance-based paper microfluidic devices for colorimetric calcium determination using ion-selective optodes. *Analyst* **144**, 1178–1186 (2019).

176. Wang, J. *et al.* Hydrophobic sol-gel channel patterning strategies for paper-based microfluidics. *Lab Chip* **14**, 691–695 (2014).

177. Yamada, K., Henares, T. G., Suzuki, K. & Citterio, D. Paper-based inkjet-printed microfluidic analytical devices. *Angewandte Chemie - International Edition* **54**, 5294–5310 (2015).

178. Huang, G. W., Li, N., Xiao, H. M., Feng, Q. P. & Fu, S. Y. A paper-based touch sensor with an embedded micro-probe array fabricated by double-sided laser printing. *Nanoscale* **9**, 9598–9605 (2017).

179. Lamas-Ardisana, P. J., Martínez-Paredes, G., Añorga, L. & Grande, H. J. Glucose biosensor based on disposable electrochemical paper-based transducers fully fabricated by screen-printing. *Biosens Bioelectron* **109**, 8–12 (2018).

180. Kao, P. K. & Hsu, C. C. Battery-operated, portable, and flexible air microplasma generation device for fabrication of microfluidic paper-based analytical devices on demand. *Anal Chem* **86**, 8757–8762 (2014).

181. Mani, N. K., Prabhu, A., Biswas, S. K. & Chakraborty, S. Fabricating Paper Based Devices Using Correction Pens. *Sci Rep* **9**, 1–8 (2019).

182. Nie, J. *et al.* Low-Cost Fabrication of Paper-Based Micro fl uidic Devices by One- Step Plotting. (2012).

183. Cao, R., Zhang, X., Tan, W. & Shen, W. Precipitation assay meets low wettability on paper: a simple approach for fabricating patterned paper sensors. *Cellulose* **25**, 583–592 (2018).

184. Dornelas, K. L., Dossi, N. & Piccin, E. A simple method for patterning poly(dimethylsiloxane) barriers in paper using contact-printing with low-cost rubber stamps. *Anal Chim Acta* **858**, 82–90 (2015).

185. Glavan, A. C. *et al.* Omniphobic “rF paper” produced by silanization of paper with fluoroalkyltrichlorosilanes. *Adv Funct Mater* **24**, 60–70 (2014).

186. Cai, L. *et al.* A simple paper-based sensor fabricated by selective wet etching of silanized filter paper using a paper mask. *Biomicrofluidics* **8**, (2014).

187. Cardoso, T. M. G. *et al.* Versatile fabrication of paper-based microfluidic devices with high chemical resistance using scholar glue and magnetic masks. *Anal Chim Acta* **974**, 63–68 (2017).

188. Jiang, Y., Hao, Z., He, Q. & Chen, H. A simple method for fabrication of microfluidic paper-based analytical devices and on-device fluid control with a portable corona generator. *RSC Adv* **6**, 2888–2894 (2016).

189. Nie, J. *et al.* One-step patterning of hollow microstructures in paper by laser cutting to create microfluidic analytical devices. *Analyst* **138**, 671–676 (2013).

190. Sadri, B., Goswami, D. & Martinez, R. v. Rapid fabrication of epidermal paper-based electronic devices using razor printing. *Micromachines (Basel)* **9**, 1–14 (2018).

191. Jiang, X. *et al.* A three-dimensional paper-based isoelectric focusing device for direct analysis of proteins in physiological samples. *Anal Chem* **93**, 3959–3967 (2021).

192. Thuo, M. M. *et al.* Fabrication of low-cost paper-based microfluidic devices by embossing or cut-and-stack methods. *Chemistry of Materials* **26**, 4230–4237 (2014).

193. Theillet, G. *et al.* Laser-cut paper-based device for the detection of dengue non-structural NS1 protein and specific IgM in human samples. *Arch Virol* **163**, 1757–1767 (2018).

194. Adkins, J. A. *et al.* Colorimetric and Electrochemical Bacteria Detection Using Printed Paper- and Transparency-Based Analytic Devices. (2017) doi:10.1021/acs.analchem.6b05009.

195. Pena-pereira, F., Velázquez, A., Lavilla, I. & Bendicho, C. A paper-based colorimetric assay with non-instrumental detection for determination of boron in water samples. *Talanta* **208**, 120365 (2020).

196. Guo, X. *et al.* Signal-Enhanced Detection of Multiplexed Cardiac Biomarkers by a Paper-Based Fluorogenic Immunodevice Integrated with Zinc Oxide Nanowires. (2019) doi:10.1021/acs.analchem.9b02557.

197. Hassanzadeh, J., Lawati, H. A. J. al & Lawati, I. al. Metal − Organic Framework Loaded by Rhodamine B As a Novel Chemiluminescence System for the Paper-Based Analytical Devices and Its Application for Total Phenolic Content Determination in Food Samples. (2019) doi:10.1021/acs.analchem.9b01862.

198. Ma, Y. *et al.* Rapid and sensitive on-site detection of pesticide residues in fruits and vegetables using screen-printed paper-based SERS swabs. *Analytical Methods* **10**, 4655–4664 (2018).

199. Dai, G., Hu, J., Zhao, X. & Wang, P. A colorimetric paper sensor for lactate assay using a cellulose-Binding recombinant enzyme. *Sens Actuators B Chem* **238**, 138–144 (2017).

200. Boonsri, M., Vongnam, K., Namuangruk, S., Sukwattanasinitt, M. & Rashatasakhon, P. Pyrenyl benzimidazole-isoquinolinones: Aggregation-induced emission enhancement property and application as TNT fluorescent sensor. *Sens Actuators B Chem* **248**, 665–672 (2017).

201. Zakir Hossain, S. M. *et al.* Development of a bioactive paper sensor for detection of neurotoxins using piezoelectric inkjet printing of sol-gel-derived bioinks. *Anal Chem* **81**, 5474–5483 (2009).

202. Hossain, S. M. Z., Luckham, R. E., McFadden, M. J. & Brennan, J. D. Reagentless bidirectional lateral flow bioactive paper sensors for detection of pesticides in beverage and food samples. *International Pest Control* **51**, 296–304 (2009).

203. Jahanshahi-Anbuhi, S. *et al.* Creating fast flow channels in paper fluidic devices to control timing of sequential reactions. *Lab Chip* **12**, 5079–5085 (2012).

204. Sicard, C. *et al.* Tools for water quality monitoring and mapping using paper-based sensors and cell phones. *Water Res* **70**, 360–369 (2015).

205. Fu, E. & Downs, C. Progress in the development and integration of fluid flow control tools in paper microfluidics. *Lab on a Chip* vol. 17 614–628 Preprint at https://doi.org/10.1039/c6lc01451h (2017).

206. Lutz, B. *et al.* Dissolvable fluidic time delays for programming multi-step assays in instrument-free paper diagnostics. *Lab Chip* **13**, 2840–2847 (2013).

207. Jang, I. & Song, S. Facile and precise flow control for a paper-based microfluidic device through varying paper permeability. *Lab Chip* **15**, 3405–3412 (2015).

208. Park, J. & Park, J. K. Pressed region integrated 3D paper-based microfluidic device that enables vertical flow multistep assays for the detection of C-reactive protein based on programmed reagent loading. *Sens Actuators B Chem* **246**, 1049–1055 (2017).

209. Ua, Q. T. H., Hibata, H. S., Iruta, Y. H. & Itterio, D. C. Flow control based 3D microPADs for OPs detection. **35**, 393–399 (2019).

210. Fennouh, S., Casimiri, V. & Burstein, C. Increased paraoxon detection with solvents using acetylcholinesterase inactivation measured with a choline oxidase biosensor. *Biosens Bioelectron* **12**, 97–104 (1997).

211. Arduini, F. *et al.* Enzymatic spectrophotometric method for aflatoxin B detection based on acetylcholinesterase inhibition. *Anal Chem* **79**, 3409–3415 (2007).

212. Zhang, C. & Malhotra, S. v. Increased paraoxon detection by acetylcholinesterase inactivation with ionic liquid additives. *Talanta* **67**, 560–563 (2005).

213. Nagaya, T., Nakamura, Y. A., Choyke, P. L. & Kobayashi, H. *Current and new fluorescent probes for fluorescence-guided surgery*. *Strategies for Curative Fluorescence-Guided Surgery of Cancer* (INC, 2020). doi:10.1016/B978-0-12-812576-2.00006-9.

214. Valek, T., Kostelnik, A., Valkova, P. & Pohanka, M. Indoxyl Acetate as a Substrate for Analysis of Lipase Activity. *Int J Anal Chem* **2019**, (2019).

215. Guo, X., Zhang, X., Cai, Q., Shen, T. & Zhu, S. Developing a novel sensitive visual screening card for rapid detection of pesticide residues in food. *Food Control* **30**, 15–23 (2013).

216. Sengoku, T., Morita, K., Sakuma, S., Motoyama, Y. & Goto, T. *Possible inhibitory mechanism of FK506 (tacrolimus hydrate) ointment for atopic dermatitis based on animal models*. *European Journal of Pharmacology* vol. 379 (1999).

217. This, R. & Online, A. READ THIS ARTICLE ONLINE A Guide to Proper Pipetting. (2018).

218. Clark, J. The Beer-Lambert Law The Absorbance of a Solution The Beer-Lambert Law. *Chemistry LibreTexts* 1–4 (2015).

219. Pfeifer, S., Schiedek, D. & Dippner, J. W. Effect of temperature and salinity on acetylcholinesterase activity, a common pollution biomarker, in Mytilus sp. from the south-western Baltic Sea. *J Exp Mar Biol Ecol* **320**, 93–103 (2005).

220. Acta, B. THERMAL INACTIVATION OF THE MOLECULAR FORMS OF ACETYLCHOLINESTERASE AND BUTYRYLCHOLINESTERASE. **742**, 509–516 (1983).

221. Vidal, C. J., Chai, M. S. Y. & Plummer, D. T. The effect of temperature on the activity of acetylcholinesterase preparations from rat brain. *Neurochem Int* **11**, 135–141 (1987).

222. Asisdiq, I., Sudding & Side, S. Effects of Incubating Temperature on Inhibitions of Acetylcholinesterase Activity by Dichlorvos in Three Parasitoids and Their Host Insects. *Pendidikan Kimia PPs UNM* **1**, 91–99 (2017).

223. Wessler, I., Michel-Schmidt, R. & Kirkpatrick, C. J. PH-dependent hydrolysis of acetylcholine: Consequences for non-neuronal acetylcholine. *Int Immunopharmacol* **29**, 27–30 (2015).

224. R.W.G. Hunt. *The Reproduction of Colour*. *The Bloomsbury Handbook of the Anthropology of Sound* (2020). doi:10.5040/9781501335402.ch-029.

225. Villatte, F., Bachman, T. T., Hussein, A. S. & Schmid, R. D. Acetylcholinesterase assay for rapid expression screening in liquid and solid media. *Biotechniques* **30**, 81–86 (2001).

226. Gholamhoseinian, A., Moradi, M. N. & Sharifi-far, F. Screening the methanol extracts of some Iranian plants for acetylcholinesterase inhibitory activity. *Res Pharm Sci* **4**, 105–112 (2009).

227. Apilux, A., Isarankura-Na-Ayudhya, C., Tantimongcolwat, T. & Prachayasittikul, V. PAPER-BASED ACETYLCHOLINESTERASE INHIBITION ASSAY COMBINING A WET SYSTEM FOR ORGANOPHOSPHATE AND CARBAMATE PESTICIDES DETECTION. *EXCLI J* **14**, 307–319 (2015).

228. Rodrigues, R. C., Ortiz, C., Berenguer-Murcia, Á., Torres, R. & Fernández-Lafuente, R. Modifying enzyme activity and selectivity by immobilization. *Chem Soc Rev* **42**, 6290–6307 (2013).

229. Gashtasbi, F., Ahmadian, G. & Noghabi, K. A. New insights into the effectiveness of alpha-amylase enzyme presentation on the Bacillus subtilis spore surface by adsorption and covalent immobilization. *Enzyme Microb Technol* **64–65**, 17–23 (2014).

230. Leão-Silva, A. C., Naves, A. F., Pereira, E. M. A., Petri, D. F. S. & Carmona-Ribeiro, A. M. Assembly of horseradish peroxidase within supported cationic bilayers. *Biotechnol Prog* **27**, 1433–1441 (2011).

231. Aybastier, Ö., Şahin, S., Işik, E. & Demir, C. Determination of total phenolic content in Prunella L. by horseradish peroxidase immobilized onto chitosan beads. *Analytical Methods* **3**, 2289–2297 (2011).

232. Luckham, R. E. & Brennan, J. D. Bioactive paper dipstick sensors for acetylcholinesterase inhibitors based on sol-gel/enzyme/gold nanoparticle composites. *Analyst* **135**, 2028–2035 (2010).

Appendix A

```
function
[hillCoeffic50]=doseresponsebyme(dose,response,coorx,titlestr,nsamples)
% DOSERESPONSE     Computes the Hill Coefficient and IC50 of a
% dose/response relationship given two vectors describing the doses and
% responses. A semilog graph is plotted illustrating the relationship,
upon
% which the man and standard error of the response to each dose level is
% plotted along with the fitted Hill Equation sigmoid. The EC50 is also
% labelled. Requires nlinfit from statistics toolbox.
%   Example
%       d=[3.75 3.75 3.75 3.75 3.75 7.5 7.5 7.5 7.5 15 15 15 15 15 60 60
60 60]
%       r=[107 91 99 124 100 96 92 133 119 84 66 86 106 91 52 37 10 69]
%       [hill ec50]=doseResponse(d,r,[pesticide],pesticide,3)
%
%   Inputs
%       Two vectors of the same length, the first containing the dose
and
%       the second the response. If doses of 0 are contained in the
data,
%       these are used as control values and the data are normalised by
%       their mean value.
%          dose = concentration of the enzyme
%          response = color intesity measured with ImageJ
%          coorx= name of the xlabel
%          titlestr= title of the graph
%          nsamples= number of samples analysed
%   Notes
%       This function was written to rapidly produce simple
dose/response curves
%       and IC50s for publication.
%deal with 0 dosage by using it to normalise the results.
normalised=0;
if (sum(dose(:)==0)>0)
    %compute mean control response
    controlResponse=mean(response(dose==0));
    %remove controls from dose/response curve
    response=response(dose~=0)/controlResponse;
    dose=dose(dose~=0);
    normalised=1;
end
%hill equation sigmoid
sigmoid=@(beta,x)beta(1)+(beta(2)-beta(1))./(1+(x/beta(3)).^beta(4));
%calculate some rough guesses for initial parameters
minResponse=min(response);
maxResponse=max(response);
midResponse=mean([minResponse maxResponse]);
minDose=min(dose);
maxDose=max(dose);
%fit the curve and compute the values
[coeffs,r,J]=nlinfit(dose,response,sigmoid,[minResponse maxResponse
midResponse 1]);
ic50=coeffs(3);
hillCoeff=coeffs(4);
```

```
%plot the fitted sigmoid
xpoints=logspace(log10(minDose),log10(maxDose),1000);
semilogx(xpoints,sigmoid(coeffs,xpoints),'Color',[0 0 0],'LineWidth',2)
hold on
%notate the EC50
text(ic50,mean([coeffs(1) coeffs(2)]),[' \leftarrow '
sprintf('IC_{50}=%0.2g',ic50)],'FontSize',16);
%plot mean response for each dose with standard error
doses=unique(dose);
meanResponse=zeros(1,length(doses));
stdErrResponse=zeros(1,length(doses));
for i=1:length(doses)
    responses=response(dose==doses(i));
    meanResponse(i)=mean(responses);
    stdErrResponse(i)=std(responses)/sqrt(length(responses));
    %stdErrResponse(i)=std(responses);
end
errorbar(doses,meanResponse,stdErrResponse,'o','Color',[0.5 0.5
0.5],'LineWidth',2,'MarkerSize',12)
%label axes
xlabel(coorx,'FontSize',16);
if normalised
    ylabel('Normalised Response','FontSize',16);
else
    ylabel('Subtracted background CI (a.u.)','FontSize',16);
end
set(gca,'FontSize',16);
title(titlestr)
subtitle(nsamples)
hold off;
```

Appendix B

```
close all
clear all
clc
%testA
dD =[0.000425 0.452 4.52 45.2 452 4520 45200 0.000425 0.452 4.52 45.2
452 4520 45200 0.000425 0.452 4.52 45.2 452 4520 45200];
rD =[0.213098523 0.12617854 0.001616653 -0.027821141 -0.00925852 -
0.010134259 -0.031525561 0.213098523 0.12617854 0.001616653 -0.027821141
-0.00925852 -0.010134259 -0.031525561 0.070683346 -0.025089634 -
0.028767607 -0.039478479 -0.019615336 -0.022465117 -0.022338547];
[hill ic50]=doseresponsebyme(dD,rD,'[log(Dichlorvos)]
(µM)','Dichlorvos','(n=3)')
figure()
dM = [1 1000 10000 100000 1000000 10000000 100000000 1 1000 10000 100000
1000000 10000000 100000000 1 1000 10000 100000 1000000 10000000
100000000];
rM = [0.994131895 0.730257089 0.031006502 0.260449818 0.10236214
0.121484889 0.364677538 1.105870219 0.464504953 0.259016338 -0.018109637
0.060105806 0.196937075 0.605726761 1.007059955 0.489942529 0.210313584
0.083416023 0.245184899 0.060006902 0.068579984];
[hill ic50]=doseresponsebyme(dM,rM,'[log(Malthion)]
(µM)','Malathion','(n=3)')
figure()
dC = [143 143000 2280000 285000 2850000 28500000 285000000 143 143000
2280000 285000 2850000 28500000 285000000 143 143000 2280000 285000
2850000 28500000 285000000];
rC = [0.574398 0.357564 0.326682 0.527776 0.404685 0.385293 0.156
1.254005 0.516324 0.217416 NaN 0.388101 0.438704 0.257002 1.291369248
0.629415305 0.867198489 0.545247943 0.418815316 0.407111315
0.488229618];
[hill ic50]=doseresponsebyme(dC,rC,'[log(Chlorpyrifos)]
(µM)','Chlorpyrifos','(n=3)')
```